JOURNAL
OF
GEOMAGNETISM
AND
GEOELECTRICITY

VOL. VII NOS. 1–2

SOCIETY
OF
TERRESTRIAL MAGNETISM AND ELECTRICITY
OF
JAPAN

JUNE 1955
KYOTO

JOURNAL
OF
GEOMAGNETISM
AND
GEOELECTRICITY

VOL. VII NOS. 1–2

SOCIETY
OF
TERRESTRIAL MAGNETISM AND ELECTRICITY
OF
JAPAN

JUNE 1955
KYOTO

JOURNAL OF GEOMAGNETISM AND GEOELECTRICITY

The fields of interest of this quarterly journal are as follows:

Terrestrial Magnetism	Aurora and Night Airglow
Atmospheric Electricity	The Ozone Layer
The Ionosphere	Physical States of the Upper Atmosphere
Radio Wave Propagation	Solar Phenomena relating to the Above Subjects
Cosmic Rays	Electricity within the Earth

The text should be written in English, German or French. The price is set as 1 dollar per number. We hope to exchange this Journal with periodical publications of any kind in the field of natural science.

The Editors

JOURNAL
OF
GEOMAGNETISM
AND
GEOELECTRICITY

VOL. VII NOS. 1-3

SOCIETY
OF
TERRESTRIAL MAGNETISM AND ELECTRICITY
OF
JAPAN

KYOTO

JOURNAL OF GEOMAGNETISM AND GEOELECTRICITY

EDITORIAL OFFICE: Society of Terrestrial Magnetism and Electricity of Japan, Geophysical Institute, Kyoto University, Kyoto, Japan

The fields of interest of this quarterly Journal are as follows:

Terrestrial Magnetism	Aurora and Night Airglow
Atmospheric Electricity	The Ozone Layer
The Ionosphere	Physical States of the Upper Atmosphere
Radio Wave Propagation	Solar Phenomena relating to the Above Subjects
Cosmic Rays	Electricity within the Earth

The text should be written in English, German or French. The price is set as 1 dollar per number. We hope to exchange this Journal with periodical publications of any kind in the field of natural science.

The Editors

JOURNAL OF GEOMAGNETISM AND GEOELECTRICITY

The fields of interest of this quarterly journal are as follows:

Terrestrial Magnetism	Aurora and Night Airglow
Atmospheric Electricity	The Ozone Layer
The Ionosphere	Physical States of the Upper Atmosphere
Radio Wave Propagation	Solar Phenomena relating to the Above Subjects
Cosmic Rays	Electricity within the Earth

The text should be written in English, German or French. The price is set as 1 dollar per number. We hope to exchange this journal with periodical publications of any kind in the field of natural science.

The Editors

may be called the variability of cosmic-ray intensity (abbrev. *V-I*). Since magnetic horizontal component is thought to be closely connected to the change in intensity of cosmic rays, the same procedure mentioned above was applied on it (*V-H*). For the variability of cosmic ray intensity, the [illegible] the period 1936 through 1946 were used, and for the magnetic variability, Kakioka Magnetic Observatory data in Japan were used. Kakioka is situated at comparatively magnetically less disturbed latitude, and hence the day-to-day variation of the horizontal component is thought to indicate the field having the close relation to cosmic-ray variation.

Making use of the variability one can disregard the variation in periods longer than [illegible] increases [illegible] Such distortion is named "variability" [illegible] statistical [illegible]

The frequency distribution of variability for both cosmic rays and horizontal component deviate from the normal distribution toward negative, and this character is nearly the same amount for two cases throughout one sunspot cycle from 1936 to 1946.

2. The maximum value of monthly variability delays from the [illegible] of sunspot maximum. Since the circumstance is nearly similar to that of horizontal component, it may be said that a large number of the cosmic-ray disturbance observed at the sunspot maximum time is due to the phenomena related to the magnetic disturbances.

Though there are several evidences which indicate the close relation between cosmic-ray and geomagnetic variability, apparent difference is seen at the period of sunspot minimum. It suggests that there is some kind of magnetic disturbance which is independent of cosmic-ray variation.

1. Introduction

It has been well known that the intensity of cosmic rays changes at the time of magnetic storm [1], and that the intensity itself shows the 27-day recurrence during several intervals as was established by Monk and Compton [2]. While magnetic activity also shows the 27-day variation, the problem still remains what relationship does exist between these two kinds of variations [3]. Recently, Meyer and Simpson [4] have reported that the amplitude of the cosmic-ray 27-day intensity variation from 1936 to 1952 is closely related to the eleven year cycle in general solar activity. Similar problems have been studied by the present authors from somewhat different point of view. The results are presented in this paper and possible interpretations are considered.

The authors aimed not only at the cosmic-ray 27-day variation, but also at any disturbance having period of several days, hence we carried on the difference of the daily values from the 27-day running average intensity. This measure

Eleven Year Variation of Cosmic-Ray Disturbance and Its Relation to Solar and Geomagnetic Activities

By Yukio MIYAZAKI and Masami WADA
Scientific Research Institute

Abstract

The daily mean intensity of cosmic rays and geomagnetic horizontal component are measured from the 27-day running average values, and this measure of disturbance is named "variability." The frequency distribution of variability for both cosmic rays and horizontal component deviate from the normal distribution toward negative, and this character is nearly the same amount for two cases throughout one sunspot cycle from 1936 to 1945.

The maximum value of cosmic-ray variability delays from the sunspot maximum. Since the circumstance is nearly similar to that of horizontal component, it may be said that a large number of the cosmic-ray disturbance observed at the sunspot maximum time is due to the phenomena related to the magnetic disturbances.

Though there are several evidences which indicate the close relation between cosmic-ray and geomagnetic variability, apparent difference is seen at the period of sunspot minimum. It suggests that there is some kind of magnetic disturbance which is independent of cosmic-ray variation.

1. Introduction

It has been well known that the intensity of cosmic rays changes at the time of magnetic storm [1], and that the intensity itself shows the 27-day recurrence during several intervals as was established by Monk and Compton [2]. While magnetic activity also shows the 27-day variation, the problem still remains what relationship does exist between these two kinds of variations [3]. Recently, Meyer and Simpson [4] have reported that the amplitude of the cosmic-ray 27-day intensity variation from 1936 to 1953 is closely related to the eleven year cycle in general solar activity. Similar problems have been studied by the present authors from somewhat different point of view. The results are presented in this paper and possible interpretations are considered.

The authors aimed not only at the cosmic-ray 27-day variation, but also at any disturbance having period of several days, hence, we carried on the difference of the daily average from the 27-day running average intensity. This measure

may be called the variability of cosmic-ray intensity (abbrev. V-I). Since magnetic horizontal component is thought to be closely connected to the change in intensity of cosmic rays, the same procedure mentioned above was applied on it (V-H). For the variability of cosmic-ray intensity, the Forbush ion chamber data for the period 1936 through 1946 at Huancayo (0.6° south geomagnetic latitude) [5] were analysed, and for the magnetic variability, Kakioka Magnetic Observatory data in Japan were used. Kakioka (26.0° north geomag. lat.) is situated at comparatively magnetically less disturbed latitude than the polar region and hence the day-to-day variation of the horizontal component is thought to indicate the field having the close relation to cosmic-ray variation.

Making use of the variability one can disregard the variation in periods longer than 27 days. However, because of the 27-day running average, apparent increases of the intensity are seen before and after the actual severe decreases. Such distortion restricts the method of analysis. Therefore, we applied some statistical treatments on the variabilities.

The character figure of dark Hα- flocculi which was used in the analysis of M-region by Waldmeier [6], as well as relative sunspot-numbers for the year 1936 through 1946 were used as the measure of the solar activity.

2. The frequency distributions of variabilities

The V-I and V-H histograms are shown in Fig. 1. We can easily notice that

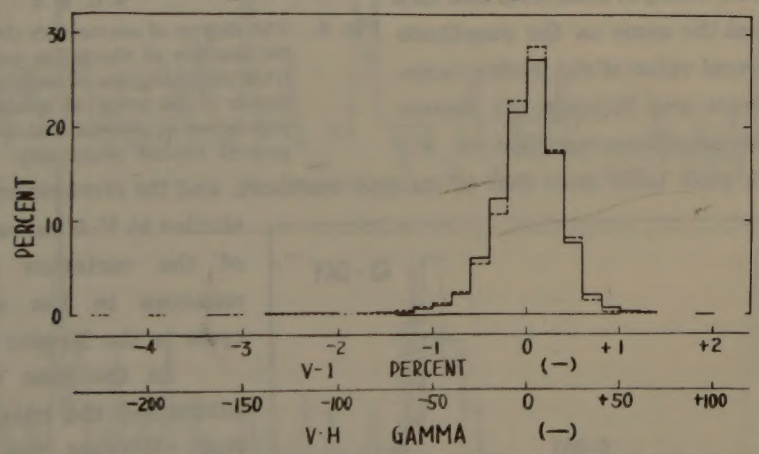

Fig. 1. Histograms of the cosmic-ray (full line) and geomgnetic (broken line) variabilities summarized for years from 1936 to 1945. Nnmber of samples is 3400.

they display the same distribution. Fig. 2 is the quantitative representation of these distributions for each year. The lower part of Fig. 2 is the degree of asymmetry which is the cubic root of g_1-statistics [7] derived from the third moment around the mean value. If the distribution is normal, this value comes to zero, and owing to the finite number of samples, 95 percent of observed points would fall in the hatched region in the figure. The degree of sharpness, which is the quadruple root of the absolute value of g_2-statistics derived from the fourth moment around the mean value, is plotted in the upper part of Fig. 2. The hatched region has the

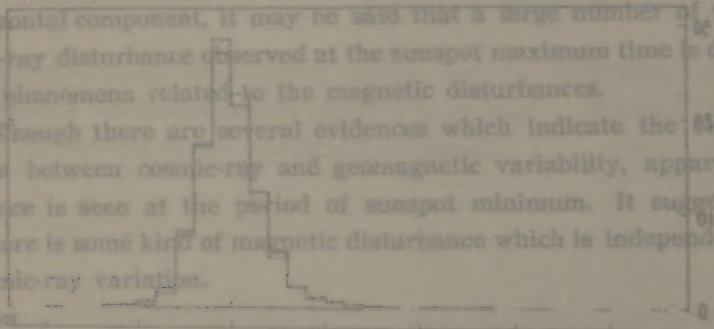

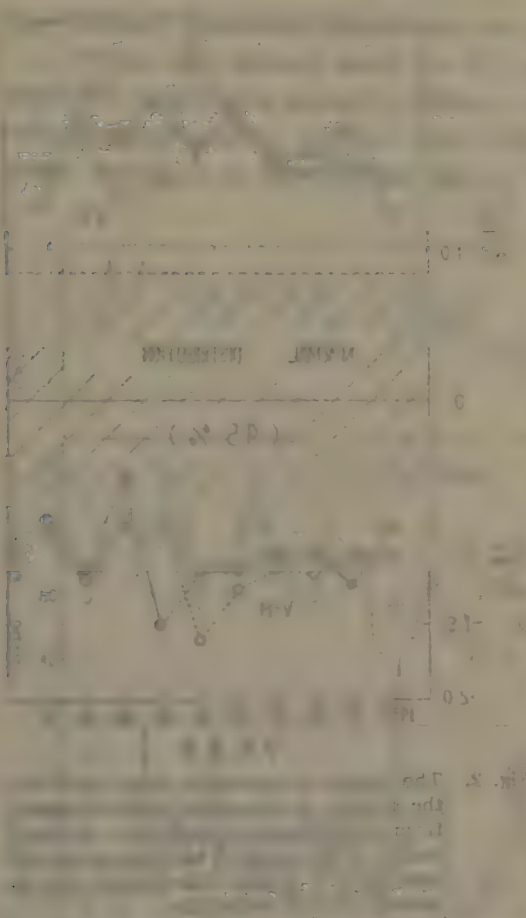

same meaning as above. Fig. 2 indicates that the distribution of V-I and V-H in each year is not normal, but is largely deviated towards negative value. No regard was taken of the differene among years, because the scattering of value may be of little meaning.

The frequency distribution of cosmic-ray variability at the international quiet or disturbed days are shown in Fig. 3. It is seen that the large deviation towards negative is mainly due to the magnetic storm effect.

The standard deviation of each year is shown in Fig. 4 together with the annual mean of sunspot-numbers, in which the scale values are normalized by the mean of the whole period. From this, one may find that V-I runs almost parallel with sunspot-numbers, and this result is just the same as the amplitude of semi-annual value of the 27-day variation by Meyer and Simpson [4]. Nevertheless, the maximum position of V-I appeares a year later than that of sunspot-numbers, and the circumstance is nearly similar to V-H curve. The range of the variation of sunspot-numbers in the eleven year cycle is the largest of three.

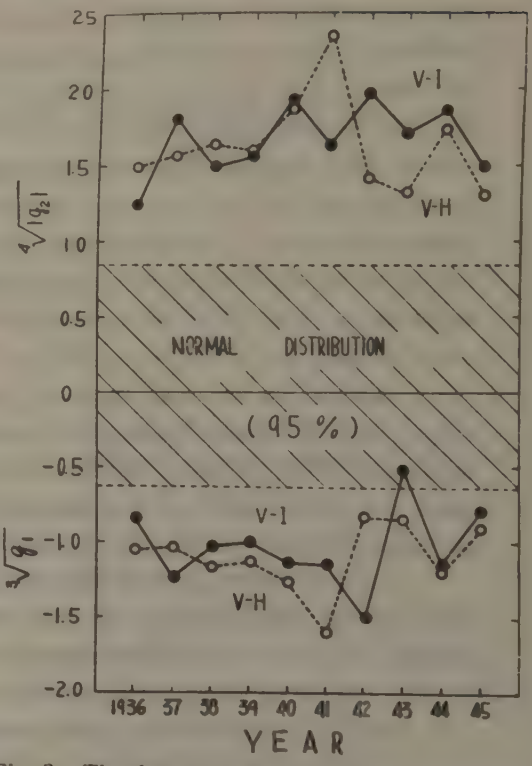

Fig. 2. The degree of asymmetry (lower part) and the degreee of sharpness (upper) obtained from the histogram of each year. Hatched region is the error of sampling from the population of normal distribution with 95 percent fiducial probability.

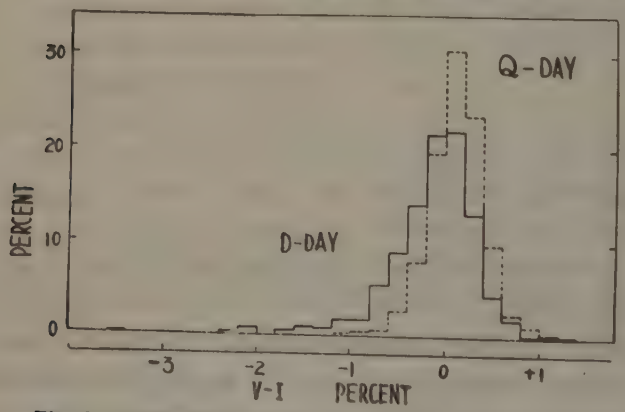

Fig. 3. Histograms of the cosmic-ray variability corresponding to the international quiet (broken line) and disturbed (full line) days. Number of samples is 550.

In the case of V-I, we subtracted the natural fluctuation. Without this correction, the results are almost the same.

3. The 27-day mean deviations of the variabilities

The mean deviation which is 0.8 of the standard deviation in the case of normal distribution is obtained by averaging the absolute value of variability for the Bartels' 27-day solar rotation period. They are plotted in Fig. 5 together with the 27-day average of sunspot-numbers and the monthly value of dark $H\alpha$-flocculi character figures from Mt. Wilson Observatory

reported in "Terrestrial Magnetism and Atmospheric Electricity."

There are several peaks in V-I and V-H curves. V-I peaks gradually decrease towards the sunspot minimum, while those of V-H do not show any change with sunspot-numbers but the peak widths gradually become wider. In spite of these difference in the form of peaks, V-I and V-H peaks almost coincide with

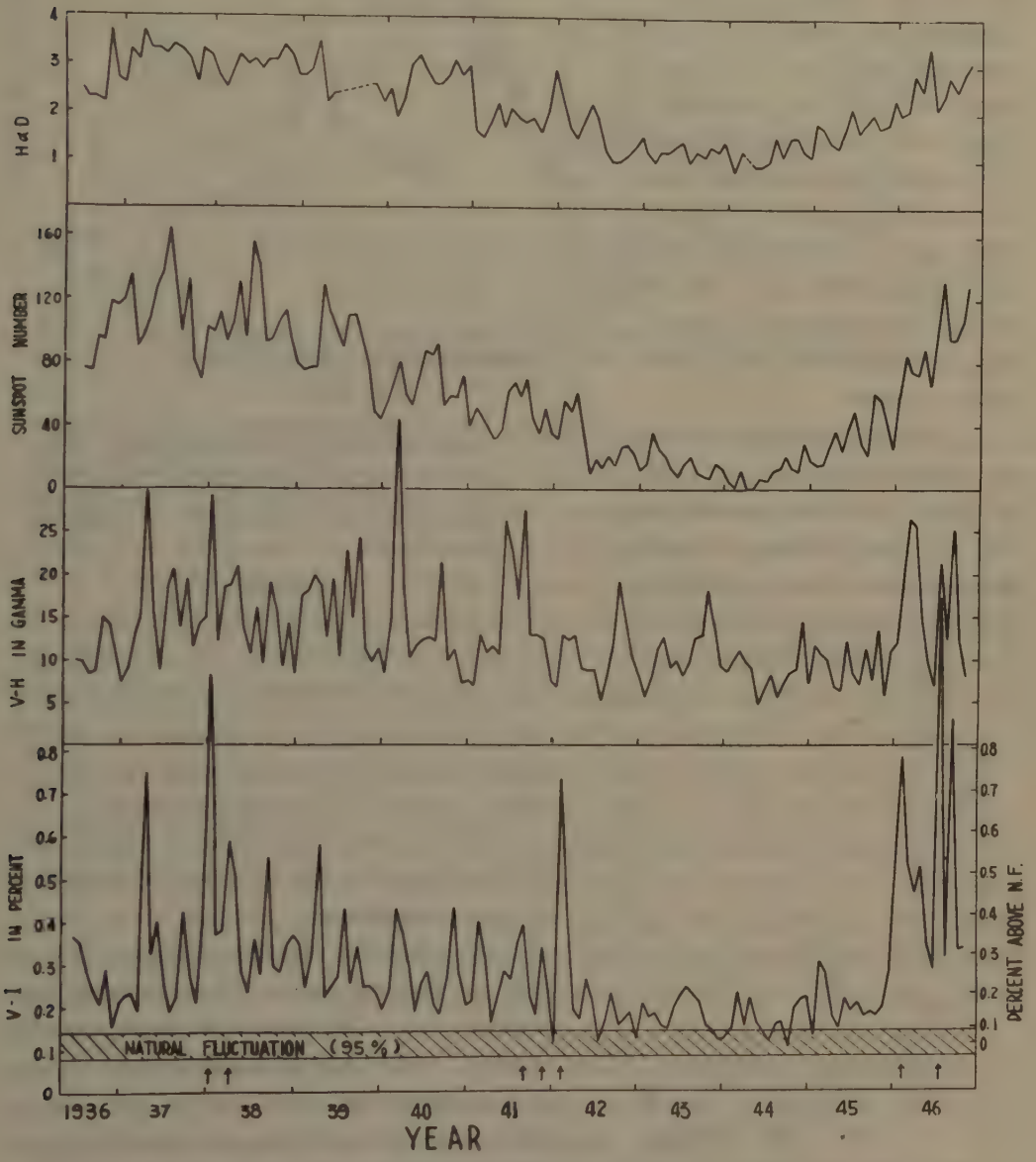

Fig. 5. 27-day mean deviations of the variabilities for cosmic rays (V-I) and geomagnetic horizontal component (V-H), 27-day averages of sunspot-numbers (Zürich) and monthly values of dark Hα-flocculi character figures (Mt. Wilson), 1936-1946.

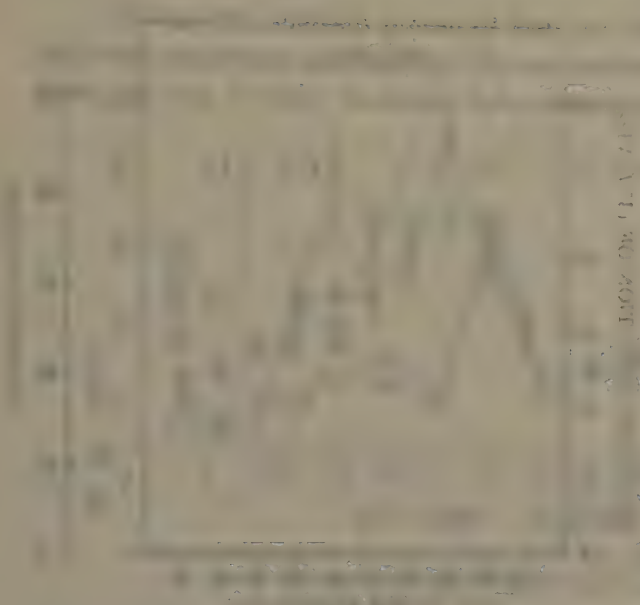

each other, i.e., from 1936 through 1945, 16 peaks coincide out of 35 during 120 solar rotations. Now, 120 rotations were divided into three parts according to the grade of sunspot-numbers: (a) period of sunspot maximum, (b) period of decrease, and (c) period of minimum. The results are shown in Table I in which the product of I and H means the number of coincident peaks between V-I and V-H, while that of I and H means the number of V-I peaks not accompanied by V-H peaks and vise versa.

The probability of having no relation between V-I and V-H is 8% in the case of (a) and 0.4% in (b), hence, we may conclude that there exist the relation between V-I and V-H.

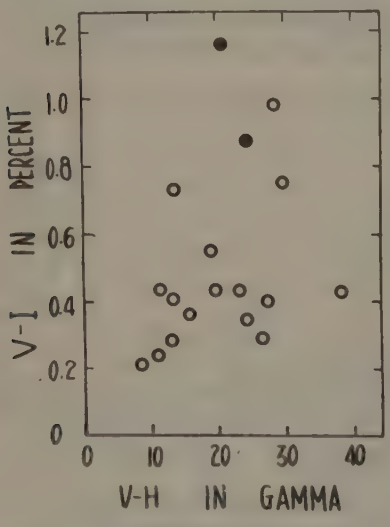

Fig. 6.
Relation between the peaks (in Fig. 5) of 27-day mean deviation of cosmic-ray and geomagnetic variabilities. White circles are those in the period from 1936 to 1945, and black circles are in 1946.

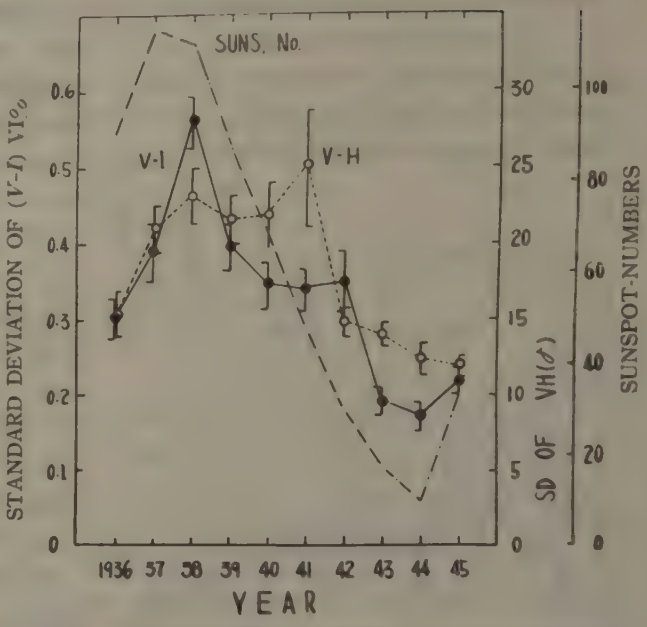

Fig. 4. The standard deviations of the cosmic-ray (black circle) and geomagnetic (white circle) variabilities and sunspot-numbers in each year for 1936 through 1945. The ordinate scale values are normalized by mean of whole period.

Table I

	(a)			(b)			(c)		
	H	$\bar{H}$	sum	H	$\bar{H}$	sum	H	$\bar{H}$	sum
I	6	6	12	8	3	11	2	10	12
$\bar{I}$	6	22	28	6	23	29	7	21	28
sum	12	28	40	14	26	40	9	31	40

On the contrary, the relation in the cese of (c) is not significant.

Fig. 6 is the relations between V-I and V-H of coupled peaks. There seems little evidence that V-I and V-H are in simple relation. This scattered quantitative relation is the cause of the fact that the significant level of (a) in Table I is not so much higher than that of (b), but lower. There are frequent occurrence of disturbances in the period of (a), and they overlap with each other in the 27-day period which make the time of peak rather obscure.

Though the analyses presented here are unpreferable methods for the study of 27-day recurrence phenomenon, we can derive the following informations from them. In Fig. 7 which is drawn by superposing the peaks in Fig. 5 for *V-I* and

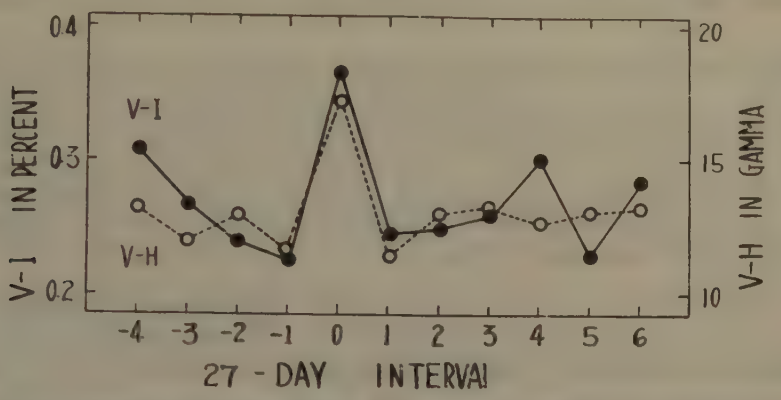

Fig. 7. Superposed average curves of 27-day mean deviations of cosmic-ray and geomagnetic variabilities. 35 peaks in Fig. 5 (all in 1936–1945) are taken as original days.

V-H, respectively, a peak appears only at the original point, and no decay curve is seen. It may be said that the amplitude of recurrence phenomenon is small when it appears again, so that they cannot be discriminated from the background phenomena which may be the after effect of disturbances of such kind.

However, broad peaks of *V-H* curve at the time of sunspot decrease in Fig. 5 are seemed to be the appearance of 27-day recurrence of magnetic activity called as M-region [8]. Meanwhile, *V-I* peaks are not clear at that time and moreover, they drop to the order of the natural fluctuation at the time of sunspot minimum. From these facts, we may conclude that the fractions which still remain in *V-H* at sunspot minimum are not effective to the cosmic-ray disturbances.

Meyer and Simpson [4] delated Forbush type variation from their study on the amplitude of 27-day variation. The periods which were delated from are shown in Fig. 5 by arrows. There might still exist some large peaks in their study, and their result may be somewhat ambiguous in this respect. We do not commit ourselves to the problem of 27-day variation, because the 27-day variation of cosmic-ray intensity and the Forbush type magnetic storm effect have not yet been clearly distinguished from each other.

One may notice that there is difference in background lines between *V-I* and *V-H* in Fig. 5. Namely, eleven year variation is more remarkable in *V-I* than *V-H*. However, we shall study about it in next paper.

Character figure of dark Hα-flocculi shows clear eleven year variation, but it does not reach to zero at the sunspot minimum period. This is because we choose character figure instead of the area. If one takes area, such deviation above zero may be vanished [9]. Restricting the curves in Fig. 5, we can not expect for different effect from different measures of solar activity.

4. Discussion and summary

The variations of the disturbances of cosmic rays and geomagnetism in the sunspot cycle have been examined above. Here we intend to summarize the known facts, and to discuss by what degree these facts might be established or not.

Cosmic-ray intensity variation has been observed at the time of magnetic storm. This effect is also recognized by the peak coincidence of V-I and V-H, and at the same time, by the fact that the frequency distributions of the variabilities of them show almost the same character. In spite of this, any simple quantitative relation have not been found from coincident peaks, and it is the already known fact for the case of individual storms [1].

The difference in V-I and V-H at the time of sunspot minimum suggests that at least two types of magnetic disturbances exist. Recently, Kitamura [10] reported that remarkable decrease of cosmic-ray intensity was observed at the time of SC storm, but there was little effect at non-SC storm, even if the disturbance index was large. Meanwhile, Newton and Milson [11] have studied the relation between sunspot-numbers and the occurrence frequency of SC and non-SC storms, and concluded that SC storm has closer relation to sunspot-numbers than non-SC storm, and the latter has stonger tendency of 27-day recurrence than the former. These results do not seem to contradict with the fact that the occurrence of cosmic-ray disturbance is almost parallel to the sunspot-numbers.

On the other hand, the strong evidence of 27-day recurrence tendency of cosmic-ray intensity which was established by Monk and Compton [2] is not agreeable with the phenomena mentioned above. We wonder whether this phenomenon is due to SC storm or non-SC storm effect, and whether it is independent of magnetic disturbance or not.

Finally, we may summarize the resluts of the analyses as follows:

(1) The frequency distributions of deviated values in daily mean cosmic-ray and geomagnetic intensities are of the same character as seen in Figs. 1 and 2.

(2) The eleven year cycle variations are seen in the disturbances of cosmic rays and magnetic force, and the phases nearly coincide with each other.

(3) However, the times of their maxima are not identical with the sunspot maximum, but shift several years. In view of this fact, disturbance of cosmic-ray intensity relates closer to geomagnetic activity than sunspot-numbers.

(4) Magnetic disturbance does not become small at the time of sunspot minimum, but cosmic-ray disturbance becomes very small even to the amount of natural fluctuation. This fact suggests that the cosmic-ray variation relates more simply to solar activity than geomagnetic disturbance does.

(5) Further, it may be considered that the magnetic disturbance is caused by other component which is quite independent of cosmic-ray disturbance at the time of sunspot minimum.

In conclusion, the authors would like to express their thanks to Drs. S.E.

Forbush and I. Lange for the publication of cosmic-ray data on which the present research was performed.

References

[1] General review: H. Elliot, Progress in Cosmic Ray Physics edited by J.G. Wilson, North-Holland Pub. Co., 1952, p. 492.
[2] A.T. Monk and A.H. Compton, Rev. Mod. Phys., **11**, 173 (1939).
[3] J.A. Simpson, Phys. Rev., **94**, 426 (1954).
[4] P. Meyer and J.A. Simpson, Phys. Rev., **96**, 1085 (1954).
[5] I. Lange and S.E. Forbush, Cosmic Ray Results from Huancayo Observatory, Carnegie Inst. Pub. 175, Vol. 14 (1948).
[6] M. Waldmeier, Terr. Mag., **51**, 537 (1946).
[7] R.A. Fisher, Statistical Methods for Research Workers, Oliver and Boyd., 1950, p. 75.
[8] J. Bartels, Terr. Mag., **37**, 1 (1932).
[9] G. Righni and G. Godoli, J. Geophys. Res., **55**, 415 (1950).
[10] M. Kitamura, Rep. Ionosphere Res. Japan, 8, 145 (1954).
[11] H.W. Newton and A.S. Milson, J. Geophys. Res., **59** 203 (1954).

Magnetic Interaction between Ferromagnetic Materials Contained in Rocks*

By Seiya UYEDA
Geophysical Institute, Tokyo University

Abstract

The detailed mechanism of the self-reversal of thermo-remanent magnetism of rocks was studied. The ferromagnetic mineral grains responsible for this phenomenon were determined as $A'B$-grains, which consist of two constituents, A' and B. The magnetic and crystallographic examinations of Haruna rocks showed that the constituent with higher Curie point, in the two-constituent model, should be estimated to be a solid solution between ilmenite and hematite, and not the Ti-poor titanomagnetite as was estimated to be in the previous studies. In other words, the magnetic interaction causing the self-reversal of thermo-remanent magnetism is between two ilmenite-hematite solid solutions with different Curie points. Electron-microscopic observations showed that the constituent with higher Curie point is intergrown into the constituent with lower Curie point as fine lamellae. The observed configurations of these two constituents indicated that the phenomenon of reverse thermo-remanent magnetism could be explained theoretically, provided that the grains as fine as the observed lamellae have very strong thermo-remanence.

Similar examinations were conducted on ferromagnetic minerals of several other rocks with the same mineral assemblage as the Haruna ferromagnetic minerals. The results of these examinations indicated that there exist, in natural ferromagnetic minerals, various degrees of magnetic interaction which are governed by their state of co-existence.

§ 1. Introduction

In the previous papers [1], [2], [3], written jointly by Nagata, Akimoto and this author, the discovery of the self-reversal phenomenon of thermo-remanent magnetism of igneous rocks as well as the tentative results of the study on its mechanism were reported. In outline summary those results were as follows: the

* Contribution from Division of Geomagnetism and Geoelectricity, Geophysical Institute, Tokyo University. Series II, No. 54.

ferromagnetic minerals contained in a dacitic pumice of Mt. Haruna and in a dacitic pitchstone of Mt. Asio mainly consist of two phases. One is a titanomagnetite phase, called *A*, and the other is a phase of ferromagnetic solid solutions of ilmenite and hematite, called *B*. Their Curie points are respectively about 500 C and 230 C. In the process of a weak field-cooling from a temperature above the Curie point of *B*, the thermo-remanent magnetism of *B* is produced in the direction just opposite to that of the external magnetic field, due to a magnetic interaction with the magnetization of *A*, which has been magnetized in the direction of the external field while the temperature of the specimen was still above the Curie point of *B*.

Although the composition of the ferromagnetic minerals is the same for both the Haruna and the Asio rocks, there is an important difference in their characteristics: i.e. while the total thermo-remanent magnetism of the Haruna rock is reversed, the Asio rock shows the reversed magnetization only in some cases of partial thermo-remanent magnetism. This difference, though essential from the geophysical point of view, was interpreted to have been caused merely by the fact that the amount of reversely oriented magnetization of *B* in the Asio rock was not large enough to overcome the normal magnetization of *A* at the room temperature in the total thermo-remanent magnetism.

To clarify the actual mechanism of the above mentioned interaction, some detailed study was made on the various magnetic behaviours of *individual single grains* of ferromagnetic minerals in these rocks. According to that study, the reverse thermo-remanent magnetism takes place within almost all the individual grains containing *B*, while the grains containing only *A* have the normal characteristics of thermo-remanence alone. This fact suggests that the mechanism of reverse thermo-remanent magnetism in the present cases is somewhat different from Néel's original model [4].

Since the discovery of this peculiar phenomenon, many scientists in palaeomagnetism examined the possibility of the occurence of similar phenomenon on a large number of the naturally reversely magnetized rocks, in an attempt to explain their reverse natural remanent magnetism [5], [6], [7], [8], 9], [10]. But in most of these tests, the results were reported to be negative. These negative results have promoted the wider acceptance of the hypothesis that the earth's magnetic field was reversed at the times of formation of these rocks. However, in a few cases among them, it was reported that the magnetic interaction between two different constituents should not be overlooked. For instance, Balsley and Buddington [11] have shown that the reverse natural remanent magnetization of the rocks in Adirondack, U.S.A. would be explained by the two-constituent mechanism; Graham [12] also mentioned the possibility of some cases where the magnetic interaction may play an important role in magnetization of rocks; Saito [13] discovered recently another example of partial self-reversal of thermo-remanent magnetism in an iron sand at the Sokota-mines, Japan, which is quite similar to the Asio case.

minerals contained in a dacitic pumice of Mt. Iwaona and in a
itchstone of Mt. Aso mainly consist of two phases. One is a titanomagnetite
point of B.
from the respective point of view [illegible] does instead merely
of the [illegible] already [illegible] at the
[illegible] of thermo-remanent [illegible] has suggested [illegible] mechanism of

As can be expected, magnetic interaction seems to exist always when magnetically different phases are intimately intergrown, whatever the phases of the concerned ferromagnetic minerals may be. In the present paper, special attention is given to the study of the general nature of the magnetic interaction acting in rocks containing the *ferromagnetic solid solutions of ilmenite and hematite*, together with the titanomagnetite phase, placing special emphasis on the Haruna-type self-reversal.

Abbreviations of technical terms used in this paper are as follows:

TRM.....thermo-remanent magnetism,
RTRM .....reverse thermo-remanent magnetism,
H_{ex}.....externally applied magnetic field,
H_d .....demagnetizing field,
Ti-Mt .....titanomagnetite,
Il-Ht .....ilmenite-hematite.

§ 2. Nature of Grains Responsible for Production of Reverse Thermo-remanent Magnetism

As was stated in the Introduction, the self-reversal of TRM of the Haruna type was found in a dacitic pumice of Mt. Haruna, a pitchstone of Mt. Asio and an iron sand of the Sokota-mines. Since the experiments [3], [13] revealed that their self-reversal mechanism must be quite similar, the Haruna rock will mainly be discussed in this paper.

During the study of RTRM characteristics of *single grains* [3-2], the peculiar fact was noticed that intense RTRM can take place even in the a*B*-grain, where the presence of Ti-poor Ti-Mt phase was hardly detectable by thermo-magnetic analysis. As long as the two-constituent mechanism theory is accepted, this fact may force one to choose one or the other of the following two possibilities: (i) the Ti-poor Ti-Mt phase playing an essential role in RTRM can be assumed to be so scarce that it is less than the limit of detectability by the thermo-magnetic study, say 1%, or (ii) the effective *A*-constituent in the two-constituent model is not Ti-poor Ti-Mt but some other phase that has a $J_s(T)$-curve hardly distinguishable from that of *B* when they are mixed. At the stage of the previous study, it was more natural to assume the first proposition. However, a number of later experimental results have made the second proposition more plausible.

Fig. 1, a is a photomicrograph of the polished surface of a grain showing a distinct stepwise character in the $J_s(T)$-curve. In this figure, the fact that coarse masses of *A* and *B* are attached to each other can be observed. A simple calculation can show that such a state of coarse co-existence has little relevance in explaining the appearance of RTRM. On the other hand, on the surface of the grain of which the $J_s(T)$-curve showed only the Il-Ht type curve, no Ti-Mt phase was observed (Fig. 1, b). Both of these grains have the RTRM characteristics.

It may be concluded, from these observations, that the presence of the *A* phase attached to the *B* phase in the *AB*-grains is not the nessesary condition for the appearance of RTRM and that therefore this case could be excluded from

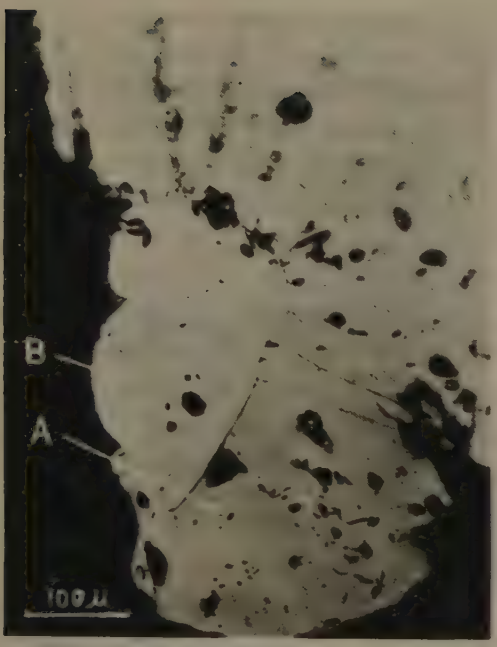

Fig. 1, a. Photomicrograph of an *AB*-grain, showing coexistence of *A*- and *B*-phases in coarse masses. Reflected light.

Fig. 1, b. Photomicrograph of an a*B*-grain, showing no existence of *A*-phase in visible size. Reflected light.

the study of its mechanism.

In order to exclude the trivial *A* phase, a chemical method was used together with thermo-magnetic separation. Since HCl effectively dissolves Ti-Mt but not ferromagnetic Il-Ht, thermo-magnetic separation at about 250 C and boiling in HCl for 5 hours of the whole specimen of the Haruna ferromagnetic minerals were alternately repeated for the elimination of the Ti-Mt phase. The non-existence of Ti-Mt phase in the grains thus extracted was ascertained by the fact that they gave no tinge of Fe^{+++}-ions to HCl. From 206 gr. of the original ferromagnetic grains, 7.26 gr. of such grains was obtained by the above method. Therefore, the ratio of the latter to the former 0.035 may be regarded as giving the approximate value of the concentration of grains responsible for the RTRM in the original ferromagnetic minerals in Haruna rock. In Fig. 2, the full curve shows the mode of the development of the total TRM of the grains thus obtained, while the broken line indicates that of the original sample. In comparing these two curves, the fact that the above separated grains are actually responsible for the RTRM will be understood.

It will also be seen that, along the field-cooling curve of the separated grains in the figure, there is a distinct rise of the value of normal magnetization at about 210°C below which the curve goes steeply downward. This rise, that was not distinct in the curve of the original sample, may be considered to be due to the very magnetization that exerts H_d upon *B* when the sample is cooled through the Curie point of *B*. The curve will, then, suggest that the Curie point of the *A*

phase responsible for the appearance of RTRM is about 320°C and not as high as that of the Ti-poor Ti-Mt, as was presumed to be the case in the previous study. Thus a new constituent was found which more adequately explains the RTRM than the Ti-poor Ti-Mt constituent, in the two-constituent model. In order to distinguish these constituents, the new one will be called A'. Therefore the grains obtained by the above stated separation will be called $A'B$-grains. As for the phase of this A'-constituent, there are two possibilities: a Ti-rich Ti-Mt phase, or an Il-Ht solid solution, like the B-constituent, but with a higher Curie point than the latter. An X-ray analysis of the $A'B$-grain offered some indication that the second possibility should be regarded as the more probable, as will be stated in § 4.

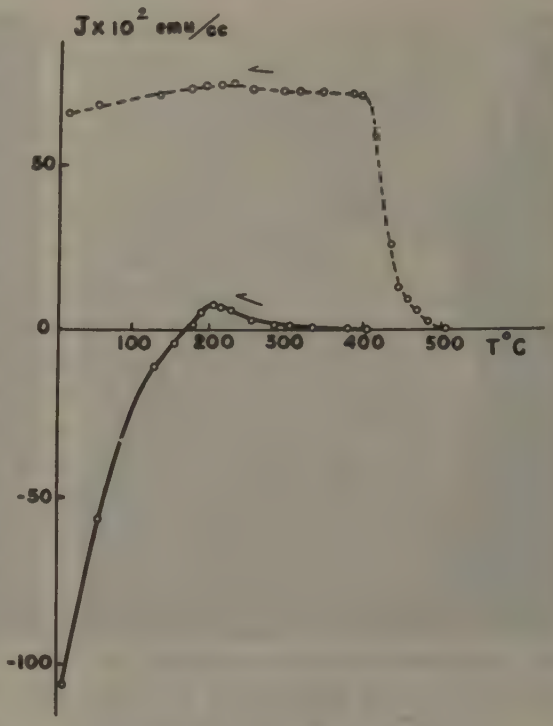

Fig. 2. Development of total TRM: $J(T)=\kappa(T)\times H_{ex}+J^{T_c}_{T_c,H_{ex}}(T)$, where $H_{ex}=2.0$ *Oe*. Full line: $A'B$-grains. Broken line: original ferromagnetic mineral grains.

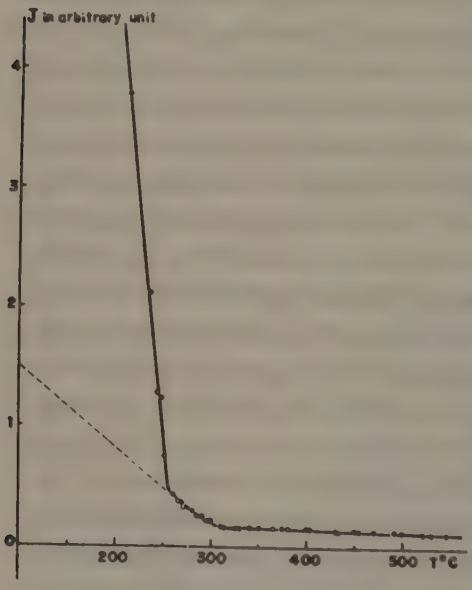

Fig. 3. a. Thermo-magnetic curve of $A'B$-grains. The broken line indicates the estimated thermo-magnetic curve of A'-constituent. $H_{ex}=3000Oe$.

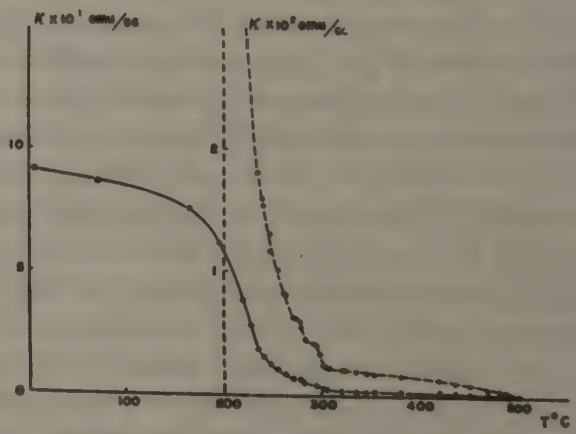

Fig. 3, b. Thermal change of magnetic susceptibility of $A'B$-grains. The curve near the Curie point is shown also in larger scale by broken line. $H_{ex}=22.0Oe$.

The results of a careful measurement of the temperature change of spontaneous magnetization and of susceptibility, namely the $J_s(T)$ and the $\kappa(T)$ of the $A'B$-grains are shown in Figs. 3, a and 3, b, where the curve for the latter is plotted also in larger scale near the Curie point. The kink at about 260°C, though not very distinct, may have been caused by the included A'. If the above argument that the relevant A-constituent is a ferromagnetic material with Curie point at about 320°C, or A', is correct, the fact that RTRM takes place most remarkably during the field-cooling in the limited temperature interval of 300°C and 250°C in the original specimen can be explained very plausibly, since this temperature interval is supposed to include the domain-fixing temperature of A'. In the previous paper [1-4], where the Curie point of the relevant A-constituent was supposed to be about 500°C, this characteristic was explained by the assumption that the reversible part of the magnetization of the Ti-poor Ti-Mt would be primarily responsible for H_{cl}

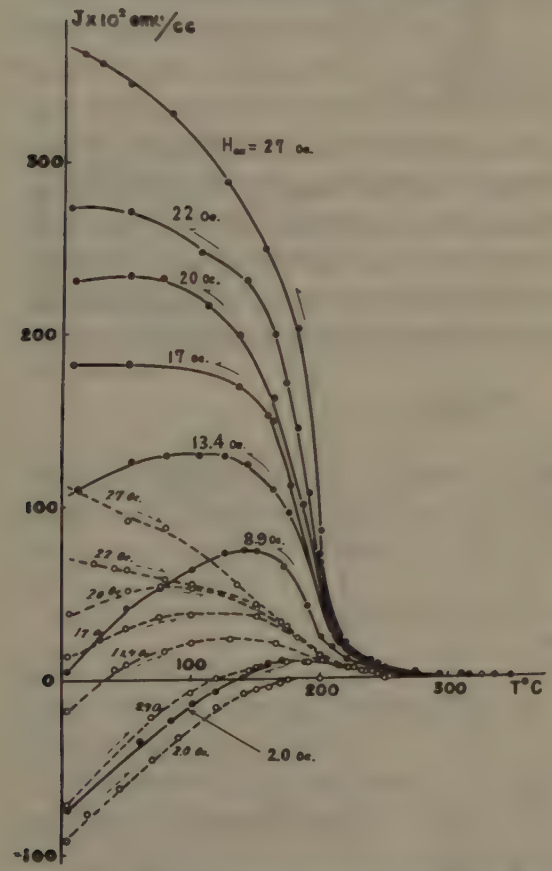

Fig. 4,a. Modes of development of total TRM and its decay by heating in non-magnetic space, for various intensities of H_{ex}. ($A'B$-rgains) Full lines: modes of development: $J(T) = \kappa(T) \times H_{ex} + J^{T_0}_{T_c, H_{ex}}(T)$. Broken lines: modes of decay of fixed magnetization: $J(T) = J^{T_0}_{T_c, H_{ex}}(T)$.

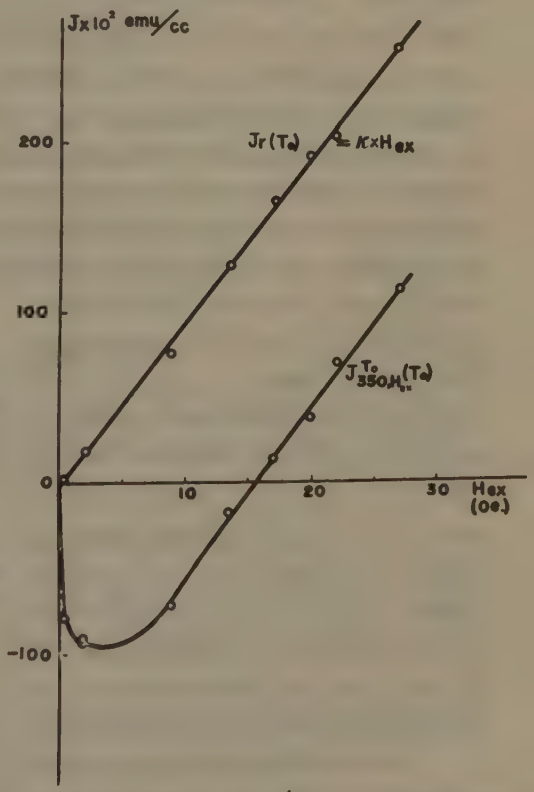

Fig. 4, b. Field dependence of $Jr(T_0) = \kappa(T_0) \times H_{ex}$ and of total TRM $J^{T_0}_{350, H_{ex}}(T_0)$. ($A'B$-grains).

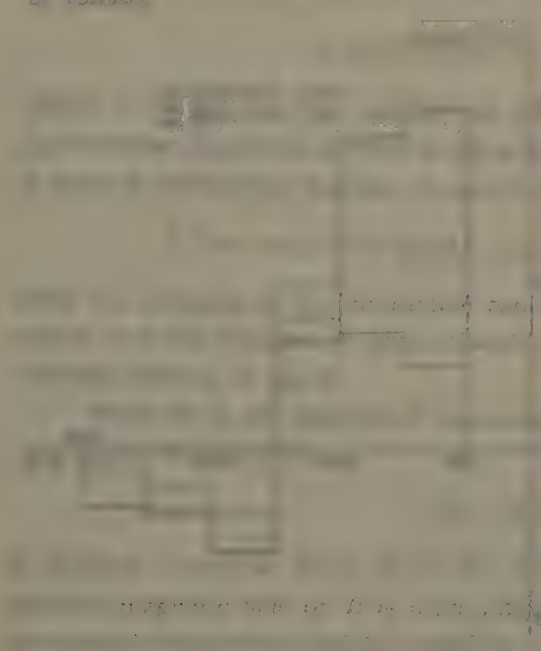

exerting on B.

The A'-constituent, being supposed to be intergrown in the host of B, may be considered to have been generated by an exsolution process. Consequently, the chemical composition of both A' and B may depend on the local density of the exsolution in the host. This means that the Curie points of A' and B may vary over a certain temperature interval. The Curie points of A' and B estimated from the above expriments would, then, be the mean values.

The modes of development of total TRM and its demagnetization by heating in a non-magnetic space for various field intensities are shown in Fig. 4, a, and the $\kappa(T_0)\times H_{ex}$ and the $J^{T_0}_{350,H_{ex}}(T_0)$ curves deduced from the data in Fig. 4, a are shown in Fig. 4, b. The manner in which RTRM ceases to occur as the intensity of H_{ex} is increased will be observed in these figures. The disappearance of RTRM by the increase of H_{ex} was interpreted to be caused by the fact that the effective magnetic field becomes positive when the intensity of H_{ex} reaches some $20\,Oe.$ This value is remarkably smaller than that which was estimated in the previous paper (See Fig. 2 in [2-1], where the fact that the reversal of the magnetization of B was still occuring under H_{ex} with an intensity as high as $40\,Oe.$ in partial TRM $J^{250}_{300,H_{ex}}$ was regarded as evidence indicating that $H_d>40\,Oe.$). At that stage of study, the fixing of magnetization of B was supposed to complete during the time when H_{ex} is acting, namely at a temperature between 300°C and 250°C. But the data shown in Fig. 4,a suggest that such an assumption may not be correct: i.e. fixing of magnetization of B mainly takes place below 200°C. This relation is well illustrated in Fig. 5 which shows the partial TRM characteristics of $A'B$-grains in strong fields. The partial TRM $J^{T}_{T+50,H_{ex}}(T_0)$, $T>250$°C is reversed even when H_{ex} amounts to $1000\,Oe.$ while the partial TRM $J^{T}_{T+50,H_{ex}}(T_0)$, $T<200$°C is normal. This figure suggests that H_d which magnetizes B in the reverse direction in $J^{T}_{T+50,H_{ex}}$, $T>250$°C, is due to the *fixed part* of magnetization of A', and that the domain-fixing of B takes place after H_{ex} is suppressed.

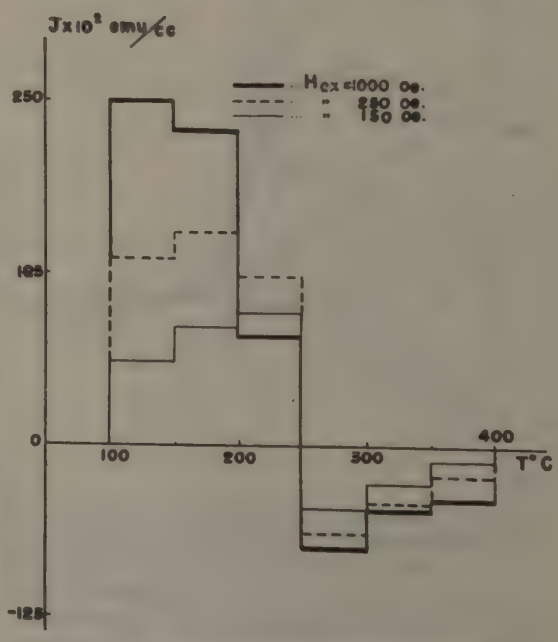

Fig. 5. Partial TRM, $J^{T}_{T+50,H_{ex}}(T_0)$, of $A'B$-grains in strong magnetic fields.

In concluding this section, facts revealed at the present stage may be summarized as follows: (i) the magnetic interaction between A' and B, responsible for RTRM, takes place within each grain of which the main constituent is B: (ii) A, in the

separated A-grains and in the state of coarse attachment to B in AB-grains, has no essential meaning with respect to RTRM, and should be excluded from the study on its mechanism: (iii) A' in $A'B$-grains is in a state of minute exsolution and its mean Curie point should be estimated to be about 320°C: (iv) the effective H_d working on B in $A'B$-grains at the time of the fixing of magnetization of B is of the order of $10\,Oe$.

§ 3. Magnetic Interaction in a System Composed of Two Ferromagnetic Materials with Different Curie Points

It can be shown that the presence of two ferromagnetic constituents with different Curie points does not always produce a magnetically anti-parallel coupling between them. Therefore, it is presumed that the mutual relation of the two constituents in the case of RTRM must be of some particular configuration favourable for an anti-parallel coupling.

In general, the total magnetization of a two-constituent system at a temperature T, $J(T)$, can be expressed as

$$J(T)=c_A\cdot J_A(T)+c_B\cdot J_B(T), \tag{1}$$

where c is the volume concentration, and the subscripts A and B refer to the quantities of the two constituents A and B. Let us consider what will happen when this system undergoes a cooling from a temperature higher than the Curie point of A, θ_{cA}, assuming $\theta_{cA}>\theta_{cB}$, in a weak magnetic field kept constant throughout the whole process of cooling. Assuming that in a weak magnetic field the magnetization is proportional to H_{ex} and J_s, $J(T)$ at $\theta_{cA}>T>\theta_{cB}$ is expressed as follows,

$$J(T)=c_A\cdot J_A(T)=c_A\cdot\lambda_A(T)\cdot J_{sA}(T)\cdot H_{ex}, \tag{2}$$

where $\lambda_A(T)$ denotes the constant of proportionality. For the sake of simplicity, $J_A(T)$ will be considered as fixed in the process of further cooling. Then, at $T<\theta_{cB}$, if there is interaction between A and B, $J(T)$ will be,

$$J(T)=c_A\cdot\lambda_A(T)\cdot J_{sA}(T)\cdot H_{ex}+c_B\cdot\lambda_B(T)\cdot J_{sB}(T)\{H_{ex}-N\cdot J_A(T)\}, \tag{3}$$

since the intensity of the interaction can be presumed to be proportional to $J_A(T)$, where N is the constant of proportionality determined by the nature of the spatial relation between A and B.

When $N>0$, the interaction is *negative* and the magnetization of B will be reversed if the condition

$$H_{ex}<N\cdot J_A(T) \tag{4}$$

is fulfilled; whereas when $N<0$, the interaction is *positive*, and therefore the effective magnetic field on B is more intense than H_{ex}. Then the present problem of magnetic interaction reduces itself to the evaluation of N for a given configuration of the two constituents.

Fig. 6. Model of co-existence of A_1 and B_{1g}

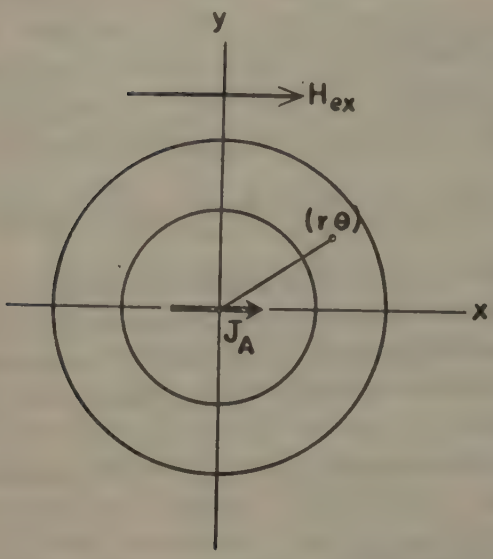

Fig. 6. Model of co-existence of A- and B-constituents in concentric spheres.

Let us consider some simple ideal cases.

Case 1. Concentric spheres: when A is included in a concentric sphere of B, (Fig. 6) and J_A is produced in the direction of H_{ex} that is oriented to the x-axis, the x-component of H_d due to J_A at (r, θ), provided that J_A is uniform, can be expressed by

$$H_{dx}=J_A \cdot v_A \cdot \frac{2\cos^2\theta-\sin^2\theta}{r^3}, \quad (5)$$

where v_A denotes the volume of A. The average value of H_{dx} over the volume of B, v_B, is given by

$$\bar{H}_{dx}=\frac{1}{v_B}\cdot\int_{v_B} H_{dx}dv. \quad (6)$$

It can be readily shown that the integral of the right-hand vanishes. There is, in such a case, no mutual magnetic interaction of significance for the present problem.

Cases 2. Uniform mixing of A and B units: when a large number of minute units of A and B are mixed at random as in Fig. 7, the magnetic interaction may be approximately treated as being similar with the case of local electric field in dielectrics. In the course of field cooling, the effective magnetic field, H_{eff}, which acts on B at the temperature where B is magnetized, can be divided into four components as

$$H_{eff}=H_{ex}+H_1+H_2+H_3, \quad (7)$$

where H_1 is the H_d resulting from the magnetic poles produced by J_A on the outer surface of the specimen, H_2 is the field by the magnetic poles on the inner surface of the fictive spherical cavity and H_3 is the sum of the magnetic field by all the units of A contained in the cavity. (See for example, p. 92 [14].) Though the units in the present case are utterly different from those in dielectrics, it may be presumed that

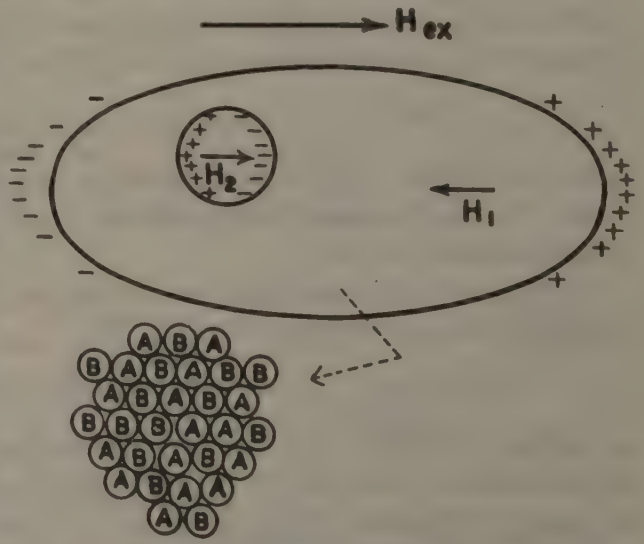

Fig. 7. Model of co-existence of A and B-units in a state of random mixing.

the calculation of H_2 may be treated in parallel manner with the case of the latter, provided that each A-unit can be approximated by a magnetic dipole oriented in the direction of H_{ex} and the number of the units is sufficiently large. Then H_{eff} can be expressed by

$$H_{eff}=H_{ex}-\left(D-\frac{4}{3}\pi\right)c_A\cdot J_A, \tag{8}$$

where D is the demagnetizing factor of the whole specimen in the direction of H_{ex}. When D is small, as in the case of a long rod specimen, it is evident that H_{eff} becomes,

$$H_{eff}\cong H_{ex}+\frac{4}{3}\pi\cdot c_A J_A > H_{ex}.$$

Therefore, in such a case, it may be expected that the interaction will be positive and that J_B will be produced in the direction of H_{ex} even in partial TRM $J_{T_1}^{T_2}{}_{,H_{ex}}$, where $T_1 < \Theta_A$ $T_2 > \Theta_B$: namely even when $H_{ex}=0$ at the temperature where the magnetization of B appears. An experiment by the author showed that in a mixture of the grains of magnetite and nickel the latter grains are magnetically coupled by positive interaction with the former ones.

In Néel's model [4], the configuration is considered to be composed of ellipsoidal B-grains embedded in a spherical specimen containing the A-grains homogeneously. In his model, H_{eff} on B is expressed by, (Fig. 8),

$$H_{eff}=H_{ex}-\left(\frac{4}{3}\pi-D\right)c_A\cdot J_A,$$

where D is the demagnetizing factor of the ellipsoid of B in the direction of H_{ex}. When the specimen is not spherical but of a long-rod shape, as is in usual experimental conditions, the interaction will become positive in this case, too.

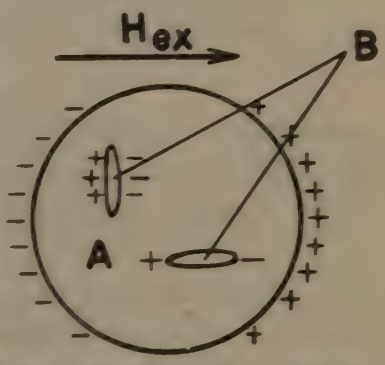

Fig. 8. Néel's model of co-existence of A- and B-constituents.

Case 3. Parallel strips model: as seen in the above examples, it is by no means self-evident that the co-existence of two different magnetic constituents can results in the production of self-reversal of TRM. Although many other kinds of configurations of A and B can be considered, the evaluation of H_{eff} in the case of parallel strips with alternate constiutents will be especially considered here, since the minute assemblages of minerals in rocks frequently take the form of intergrowth in parallel strips, like the Widmannstätten structure. In fact, the electron-microscopic ovservations described in the next section offered some evidence supporting the hypothesis that the present case is of a parallel strips structure.

The model we consider is of parallel strips with alternate constituents as shown in Fig. 9: the plane of the strips is in the (yz)-plane and the z-axis is in the upward direction vertically. The width of the strips and the height of the system are denoted by d and L. When such a system is cooled from a temperature

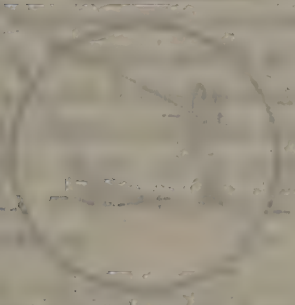

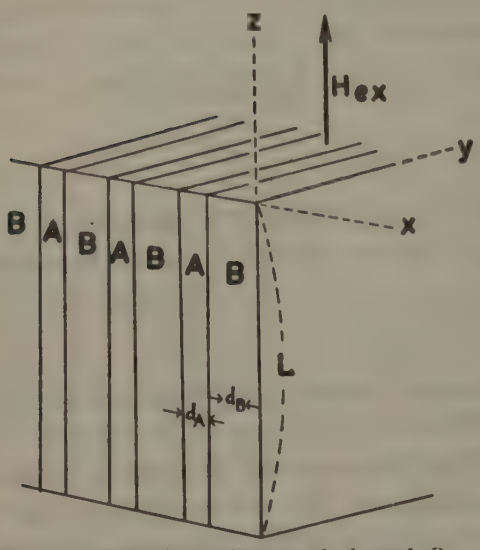

Fig. 9. Model of co-existence of A- and B-constituents in parallel strips of alternate constituents.

higher than θ_{cA} in a magnetic field, H_{ex}, applied in the z-direction, to a temperature T, where $\theta_{cA}>T>\theta_{cB}$, the A-strips are magnetically fixed in the z-direction. For the present, let us assume for the convenience of calculation that the magnetization of all the A-strips is fixed in the z-direction. The direction of the magnetization of the B-strips, in the process of further cooling down to $T<\theta_{cB}$, is determined by the local H_{eff} which is the sum of H_{ex} and H_d due to $J_A(T)$. Let us consider the cases, where J_B is oriented parallel (p-case) and where J_B is oriented antiparallel (a-case) to J_A, and compare the magnetic energy in both cases. The necessary condition for the reversal of J_B is reduced to,

$$E_a<E_p, \tag{9}$$

where E stands for the total magnetic energy and the subscripts a and p designate the a-case and the p-case as defined above. Generally, the total magnetic energy of such a system can be represented to be

$$\begin{aligned} E &= E_{\text{self}}+E_{\text{field}}, \\ E_{\text{self}} &= E_{A,\text{self}}+E_{B,\text{self}}+E_{AB}, \\ E_{\text{field}} &= E_{A,\text{field}}+E_{B,\text{field}}, \end{aligned} \tag{10}$$

where E_{self}, E_{field} and E_{AB} stand for the self energy, the interaction energy with H_{ex} and the mutual interaction energy between J_A and J_B, respectively. E_{field} and E_{self} are calculated by

$$E_{\text{field}} = -\int J\cdot H_{ex}\,dx\,dy\,dz, \tag{11}$$

$$E_{\text{self}} = -\frac{1}{2}\int J\cdot H_d\,dx\,dy\,dz. \tag{12}$$

Now, since J_A is assumed to be always fixed in the z-direction, $E_{A,\text{field}}$ can be dropped out of calculation. From Eq. (11), $E_{B,\text{field}}$ for the unit area of the (xy)-plane is given by

$$E_{B,\text{field}} = -H_{ex}\cdot\left\{\mp J_B\frac{d_B}{d_A+d_B}\right\}\cdot L, \tag{13}$$

where the signs $(-)$ and $(+)$ refer to the a-case and the p-case. The magnetic self energy of the system E_{self} is calculated approximately by a similar method as shown by Kittel [15]. In the a-case, the z-component of the magnetic field just

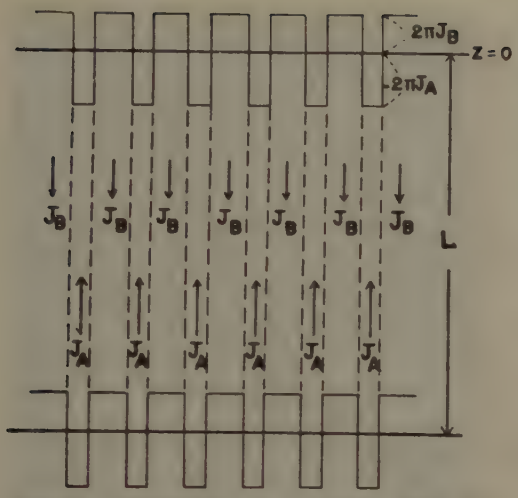

Fig. 10. Distribution of magnetic field just bellow the surface in parallel strip model. (*a*-case.)

bellow the surface due to the free poles on the surface is illustrated by Fig. 10. Expressing this distribution by the Fourier expansion, the approximate solution for the Laplace equation is given by, provided $L \gg d_A+d_B$,

$$H_z=\sum_0^\infty a_n \cdot \cos nkx \cdot e^{nkz}, \qquad (14)$$

where $k=\dfrac{2\pi}{d_A+d_B}$ and a_n are the Fourier coefficients namely,

$$a_0=\frac{2\pi}{d_A+d_B}\cdot[J_B\cdot d_B-J_A\cdot d_A],$$

$$a_n=\frac{4}{n}(J_A+J_B)\sin\frac{n\pi d_B}{d_A+d_B}. \qquad (15)$$

Putting (14) and (15) into (12), we can obtain E_{self} as

$$E_{self}=\frac{\pi L}{(d_A+d_B)^2}\cdot\{J_A\cdot d_{A(\mp)}J_B\cdot d_B\}+4(J_{A(\pm)}J_B)\sum_1^n\frac{1}{n}\left(\sin\frac{n\pi d_B}{d_A+d_B}\right)\cdot\int_{-\infty}^0 e^{nkz}dz$$

$$\times\left\{<\cos nkx>_0^{d_B/2}+<\cos nkx>_{d_B/2}^{d_A/2+d_B/2}\right\},$$

$$<\cos nkx>_0^{d_B/2}=\frac{1}{n\pi}\frac{d_A+d_B}{d_B}\cdot\sin\frac{n\pi d_B}{d_A+d_B},$$

$$<\cos nkx>_{d_B/2}^{d_A/2+d_B/2}=\frac{-1}{n\pi}\frac{d_A+d_B}{d_A}\cdot\sin\frac{n\pi d_B}{d_A+d_B}. \qquad (16)$$

where, since $L\gg d_A+d_B$, the integration with regard to z is carried out from $-\infty$ to 0 for all the terms except the first, and doubled to account for the effect from both of the top and bottom surfaces. That the signs in parenthesis in the above formula refer to the p-case can be shown in a similar manner. The final result for the condition of the reversal of J_B, from Eqs. (9), (10), (13) and (16), becomes

$$H_{ex}<2J_A\cdot\left\{\frac{\pi}{1+c}-\frac{1+c}{c}\cdot\frac{2}{A\pi^2}\sum\frac{1}{n^3}\sin^2 n\pi\frac{c}{1+c}\right\},$$

where $$A=\frac{L}{d_A+d_B}, \text{ and } c=\frac{d_B}{d_A}. \qquad (17)$$

This relationship is illustrated in Fig. 11. It is assumed in the present model, as has already been remarked, that the magnetization of all the A-strips is fixed in the direction of H_{ex}. However, unless the A-strips are magnetized to saturation, such an assumption is not warranted. Therefore, in order to utilize the condition (17) for the actual case, some statistical consideration on the arrangement of the magnetic moment of the A-strips will be necessary. It will be unnecessary to account for the case when H_{ex} is applied in the direction perpendicular to the (yz)-plane, because it can be expected that the thin strips will hardly be magnetized in the x-direction (Fig. 9).

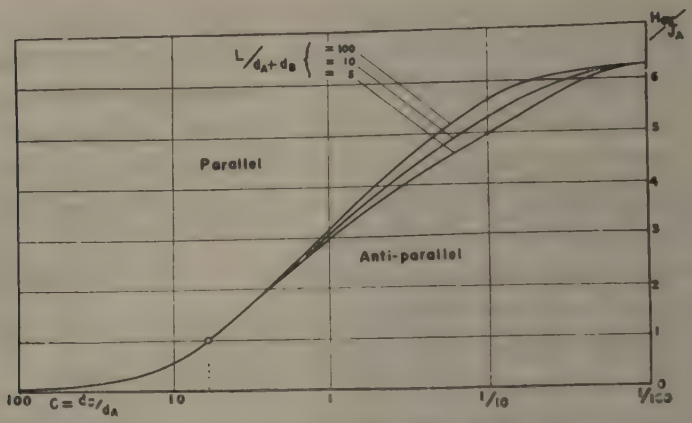

Fig. 11. Plot of Eq. (17). Bellow the curves the anti-parallel arrangement of J_A and J_B is energetically more favourable; above the curves the parallel arrangement is more favourable.

An experimental study on the model somewhat similar to the present case has recently been reported by Grabovsky and Pushkov [16]. They showed, by direct measurement of the local magnetic field, that the relation H_d H_{rr} can be fulfilled in the limited region near the plate-like specimens of magnetite when they acquired TRM in the earth's magnetic field. The dimension of their specimens were of the order of 10cm.

§ 4. Electron-Microscopic Observations on the Intergrowth of the Two Constituents, and Estimation of the Phase of the A'-constituent.

According to the calculations described in the preceding section, it may be expected that the parallel strips model can be responsible for the self-reversal of TRM under appropriate conditions. It will be reported in this section that such a structure was actually observed in the RTRM-producing grains ($A'B$-grains) of the Haruna rock with the aid of the electron-microscope. Figs. 12, a. and b. are the electron-micrographs of etched surfaces of $A'B$-grains in the Haruna rock. The observations were carried out by the methyl-metacryl alminium replica method. The strips seen in the figures were produced on the polished surfaces by etching with HCl for about 15 minutes or with HF for 1~2 minutes. The width of the strips is approximately 0.2μ, while the length ranges apparently between 1μ and 5μ. This scale may be fine enough to be comparable with that of one or several elementary magnetic domains. It seems likely that these strips are more or less chained to one another along specified directions to form fairly long and narrow strips. We may, therefore, presume that this structure consists of the intergrowth of the two constituents which makes these grains acquire the RTRM characteristics.

As for the phase of these strips, so long as we assume them to be A', there are, as has been stated in § 2., two possibilities of identification: namely the Ti-rich Ti-Mt and the Il-Ht solid solution. Judging from the known fact that reagents like

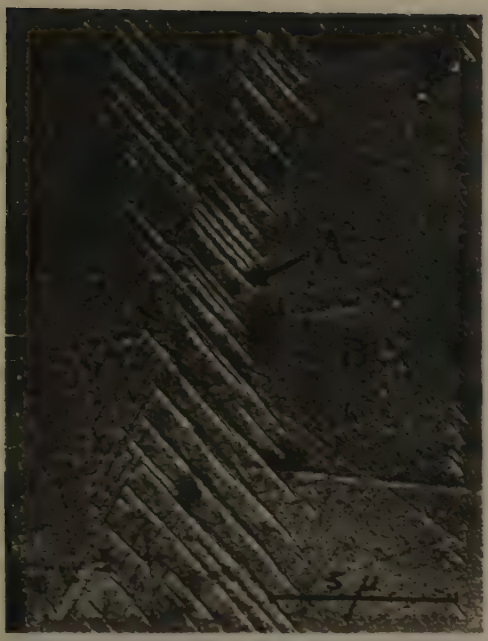

Fig. 12, a.

Fig. 12, b.

Fig. 12. Electron micrographs of polished surfaces of $A'B$-grain of Haruna ferromagnetic mineral, after etching with HCl for 15 min., showing intergrowth of A' in echelon into B.

HCl and HF etch the Ti-Mt more effectively than the Il-Ht phase, it was at first inferred that the phase of the strips should be the Ti-rich Ti-Mt [17]. But such an approach may be not so reliable as other methods like the crystallographic one. A powder method X-ray analysis, with the aid of NORELCO spectrometer, of $A'B$-grains showed no trace of the Ti-Mt phase. However, an X-ray analysis on a single crystal of $A'B$-grain showed that, in the oscillation photograph, the Debye-Scherrer rings of the Il-Ht phase could also be observed, together with the intense spots by the single crystal. Fig. 13 is an example of the oscillation photographs taken by using Mo K-radiation. The Debye-Scherrer rings, though faint, have non-uniform intensity. This fact may indicate that, in a single crystal of $A'B$-grain, some parts of the Il-Ht phase exist in a state that can cause the powder-like diffraction with a certain degree of orientation. Although the A'-constituent originating the RTRM, the strips observed by the electron-microscope, and the constituent originating the Debye-Scherrer rings in the single crystal have not been completely identified to be the same by any direct method, it would be most plausible, in order to explain

Fig. 13. Oscillation photograph of $A'B$-grain of Haruna ferromagnetic mineral, using unfiltered Mo K-radiation, 30 Kv. 20 mA. oscillation angle 18°. 10 hrs. exposure.

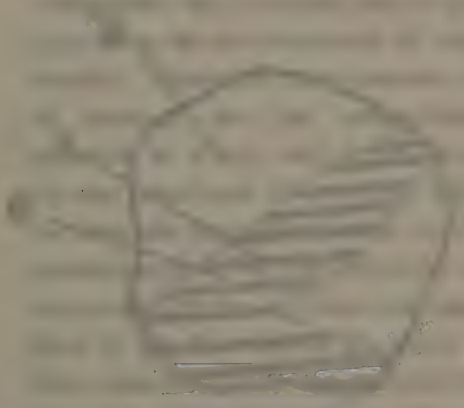

the various data obtained for the $A'B$-grains, to consider these to be the same. Therefore it will be concluded that the phase of the A'-constituent is Il-Ht, with the Curie point higher than that of B.

§ 5. Application of the Parallel Strip Model to the Self-Reversal of TRM of the Haruna-Type

A theoretical consideration of the mechanism of RTRM of the Haruna-type will be discussed, in this section, in terms of the parallel strip model treated in § 3. As it was verified that the ferromagnetic grains responsible for the production of RTRM of the present case are the $A'B$-grains, it would be sufficient to explain the RTRM characteristics which are summarized in Figs. 4, a. and 4, b. The rest of the ferromagnetic minerals present in the original Haruna rock, namely the A-constituent, may be considered as being non-essential with respect to the RTRM phenomenon. The principal features of the hereby proposed model are as follows.

The host mineral in the $A'B$-grains is B, a ferromagnetic Il-Ht solid solution whose Curie point Θ_{cB} is about 230 C, and there are fine strips of A' whose Curie point $\Theta_{cA'}$ ranging around 320 C. In the process of cooling in a weak magnetic field, H_{cr}, the TRM of the A' strips is produced at a certain temperature just bellow $\Theta_{cA'}$, so that there would appear the parallel-strips effect which was examined in § 3. In other words, the magnetization of the A'-strips would exert a reversely oriented magnetic field H_d upon the part of B which is between the A'-strips. The parallel-strips effect on the part of B which is not between the A'-strips may be, in the first approximation, considered to be weak enough to be neglected. In order to distinguish these two parts of B, the latter will be called B' (Fig. 14). If H_d is stronger than H_{cr}, the TRM of B will be produced in the reverse direction when the $A'B$-grains are cooled through Θ_{cB}, and if this reverse TRM of B is stronger than the normal TRM of A' and B' at the room temperature, the TRM of the whole $A'B$-grains is reversed.

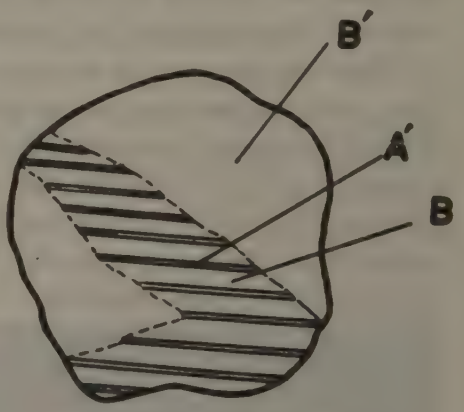

Fig. 14. Structure of $A'B$-grain.

It may be possible that the B-constituent which is between the A'-strips has the properties of *fine grains* as the A'-strips, since it is finely divided by the A'-strips. As for the nature of these two parts of the B-constituent, therefore, we may presume the following characteristics: their structure insensitive properties such as the Curie point and the spontaneous magnetization are identical but their structure sensitive properties such as the coercive force, the magnetic susceptibility and the TRM characteristics are different. Then basic assumptions on the nature of each constituent in the present discussion will be:

i) A' and B have the typical TRM characteristics, such as the large Q-value

and the saturation phenomenon of TRM in the magnetic field as weak as the order of 10 *Oe*. [18], [19]. Because the size of these constituents may be as sufficiently small as to become the case of the single-domain model of TRM by Néel [20], which could very well explain the typical TRM characteristics such as mentioned above.

ii) B' has not the typical TRM characteristics, because the size of this constituent is fairly large. Its Q-value is small, say less than unity, and there is no saturation phenomenon in TRM within the magnetic field of the order of 10 *Oe*.

At a temperature T, the fixed part of the magnetization of the $A'B$-grains can be written as

$$\begin{aligned} &J_{\text{fixed}}(T)=c_{A'}\cdot J_{A',\text{fixed}}(T)+c_B\cdot J_{B,\text{fixed}}(T)+c_{B'}\cdot J_{B',\text{fixed}}(T), \qquad (18)\\ &J_{A',\text{fixed}}(T)=s_{bA'}\cdot J_{sA'}(T)\cdot H_{ex},\\ &J_{B,\text{fixed}}(T)=s_{bB}\cdot J_{sB}(T)\cdot\{H_{ex}-\overline{H_d}\},\\ &J_{B',\text{fixed}}(T)=s_{bB'}\cdot J_{sB}(T)\cdot H_{ex}, \end{aligned}$$

where $\overline{H_d}$ is the mean value of H_d due to $J_{A'}$ and s_b denotes the domain fixing ratio defined generally by,

$$J_{\text{fixed}}(T)=s_b\cdot J_s(T)\cdot H. \qquad (19)$$

Now, the direction of the plane of the strips are supposed to be equally distributed in the (xy), (yz) and (zx)-planes (Fig. 15). As stated in § 3, when H_{ex} is applied in the z-direction, the A'-strips and B lying in the (xy)-plane do not contribute to the magnetization. Therefore, the amounts of A' and B relevant for the magnetization are reduced to $2/3\cdot c_{A'}$ and $2/3\cdot c_B$ respectively. As also mentioned at the end of § 3, in order to estimate the actual value of H_d by the parallel strip medel, the effects due to the fact that not all of the A'-strips are magnetically fixed in the direction of H_{ex} must be taken into account. Since the concentration of the A'-strips lying in the (yz) and (zx)-planes is presumed as being $2/3\cdot c_{A'}$, the fraction of the A'-strips of which magnetic moment is fixed in the direction of H_{ex} may be estimated to be $\dfrac{J_{A'}}{2/3\cdot J_{sA'}}$, where $J_{A'}$ is the intensity of magnetization of A' as a whole fixed in the direction of H_{ex}. The magnetic moment of the remaining fraction $\left(1-\dfrac{J_{A'}}{2/3\cdot J_{sA'}}\right)$ of the A'-strips should be considered to be equally distributed in z- and $-z$-directions. Then, in the first approximation, the amount of B which is under the influence of the parallel-strips effet may be regarded as reduced to $\dfrac{2}{3}c_B\times\dfrac{J_{A'}}{2/3\cdot J_{sA'}}$, and the rest of B, namely $\dfrac{2}{3}c_B\left(1-\dfrac{J_{A'}}{2/3\cdot J_{sA'}}\right)$ may be regarded to be under the effect of H_{ex} only. Since the average value of the ratio $d_B/d_{A'}$ is approximately estimated to be *five* from Fig. 12, the intensity of H_d in the present case may be estimated as being

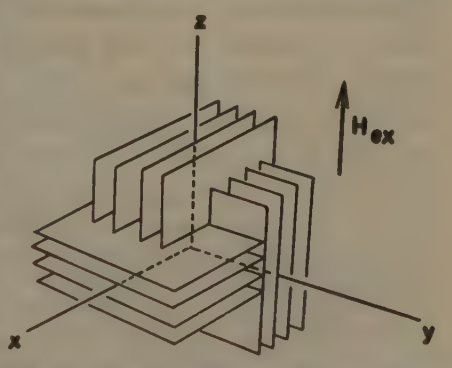

Fig. 15. Equal distribution of parallel strips in (xy), (yz) and (zx)-planes.

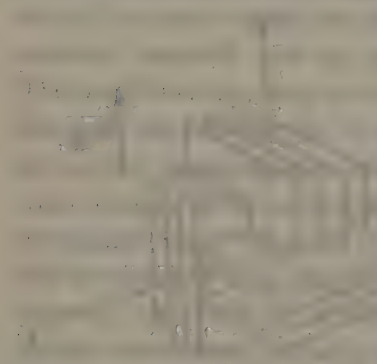

nearly equal to $J_{sA'}$, according to the curve in Fig. 11, provided that the magnetic moment of the A' is of the order of spontaneous magnetization.

Then, the average value of the effective field, H_{eff}, over all the B-constituent which can contribute to the magnetization of the $A'B$-grain may be obtained as

$$H_{eff}=(H_{ex}-J_{sA'})\frac{J_{A'}}{2/3\cdot J_{sA'}}+H_{ex}\cdot\left(1-\frac{J_{A'}}{2/3\cdot J_{sA'}}\right)=H_{ex}-\frac{3}{2}J_{A'}. \tag{20}$$

The reversible part of the magnetization of the $A'B$-grains at the room temperature T_0 is, on the other hand, expressed by

$$J_{\text{reversible}}(T_0)=\lambda_{B'}(T_0)\cdot c_{B'}\cdot J_{sB}(T_0)\cdot H_{ex}, \tag{21}$$

provided that the contribution from A' and B can be neglected by the assumption i).

From Eqs. (18), (20) and (21), the Q-value of the $A'B$-grains at the room temperature T_0 will be written as

$$Q(H_{ex})=\frac{c_B\cdot s_{bB}\cdot J_{sB}(T_0)\left\{H_{ex}-\frac{3}{2}J_{A'}(T_{bB})\right\}+c_{A'}\cdot H_{ex}\cdot s_{bA'}\cdot J_{sA'}(T_0)+c_{B'}\cdot H_{ex}\cdot s_{cB'}\cdot J_{sB}(T_0)}{c_{B'}\cdot\lambda_{B'}(T_0)\cdot J_{sB}(T_0)\cdot H_{ex}} \tag{22}$$

where $J_{A'}(T_{bB})=s_{bA'}\cdot J_{sA'}(T_{bB})\cdot H_{ex}$ and T_{bB} denotes the domain fixing temperature of B. Although it is expected that $J_{sA'}(T_0)$ is larger than $J_{sB}(T_0)$, since $\theta_{cA'}>\theta_{cB}$ [21], the difference in J_s expected from the difference in the Curie points may be small. Therefore, we may put, in the present approximation, $J_{sA'}(T_0)\cong J_{sB}(T_0)$ in Eq. (22). We may also put $s_{bB'}\cong\lambda_{B'}(T_0)/2$ by the assumption ii). The value of $\lambda_B(T)$ can be obtained as $\frac{1}{c_{B'}\times 800}$ by the definition of λ (Eq. (2) rewritten for B'.) and the data in Fig. 4, b. The value of $J_{sA'}(T_{bB})$ will be about 40 emu/cc, provided that A' is a ferromagnetic Il-Ht of which $J_s(T)$ curve is known to be linear, and $J_{sA'}(T_0)$ is nearly equal to $J_{sh}(T_0)$ which has been determined to be about 120 emu/cc previously [3].

Putting the above relations and values, together with another relation $5c_{A'}=c_B$ (Fig. 12), into Eq. (22), we can obtain

$$Q(H_{ex})\cong 4\times 10^3\cdot c_{A'}\cdot s_{bB}(1-60\cdot s_{bA'})+8\times 10^2\cdot c_{A'}\cdot s_{bA'}+1/2. \tag{23}$$

In the next place, the saturation effect of the TRM of A' and B (assumption i)) will be expressed approximately by

$$\frac{J_{\text{fixed}}(H)}{J_s}=M(1-e^{-H/h}), \tag{24}$$

where M and h are the saturation value of TRM divided by J_s and the intensity of the magnetic field in which the TRM attains the $(1-1/e)$ of its saturation value. From Eqs. (19) and (24), $s_{bA'}$ and s_{bB} will be expressed by

$$\begin{aligned} s_{bA'}&=\frac{M_{A'}}{H_{ex}}(1-e^{-H_{ex}/h_{A'}}),\\ s_{bB}&=\frac{M_B}{|H_{eff}|}(1-e^{-|H_{eff}|/h_B}), \end{aligned} \tag{25}$$

where the absolute value must be used for H_{eff} since it can be negative. Then,

the final expression for the Q-value becomes

$$Q(H_{ex}) \simeq 4\times 10^3 \cdot c_{A'} \cdot M_B \frac{1-e^{-H_{eff}/h_B}}{H_{ex}} \cdot \frac{H_{eff}}{H_{eff}} + 8\times 10^2 \cdot c_{A'} \cdot M_{A'} \frac{1-e^{-H_{ex}/h_{A'}}}{H_{ex}} + 1/2, \quad \text{where} \quad H_{eff} = H_{ex} - 60 \cdot M_{A'}(1-e^{-H_{ex}/h_{A'}}). \tag{26}$$

In Eq. (26), the value of $c_{A'}$ may be put as 0.1 from Fig. 3, a. The values of the parameters $M_{A'}$, M_B, $h_{A'}$ and h_B are inaccessible at present. The saturation value of TRM was experimentally studied by Melle. Roquet [22]. According to the result of her study, M value may be estimated to be about 1/8 for magnetite. As for the value of h, Nagata [19] and Thellier [18] have reported that some natural magnetite shows the non-linearity between the amount of TRM and the intensity of H_{ex} when H_{ex} is of the order of $1Oe$. Since the ferromagnetic materials in the present case are the ferromagnetic Il-Ht solid solutions, there seems to be no experimental data available for the estimation of these parameters. The $Q(H_{ex})$ curve in Fig. 16 has been calculated from Eq. (26) by putting, for instance,

$$M_{A'}=1/3, \quad h_{A'}=2,$$
$$M_B=1/5, \quad h_B=10.$$

In Fig. 16, the experimental $Q(H_{ex})$ values for the $A'B$-grains of Haruna sample, obtained from the data in Fig. 4, b are also plotted for comparison.

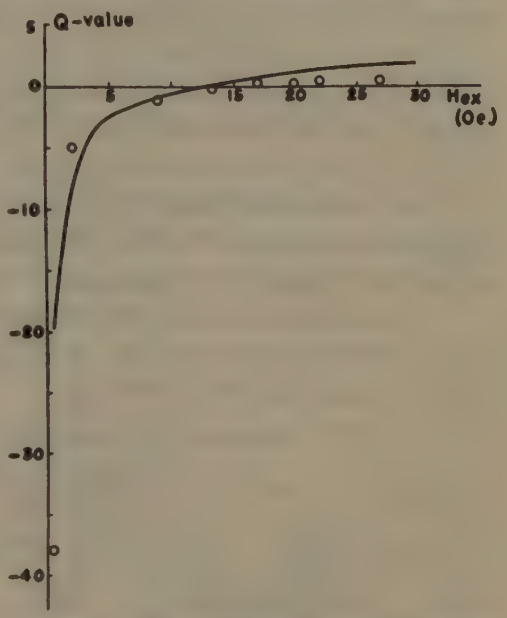

Fig. 16. Field dependence of Q-value, calculated from Eq. (26) by putting $M_{A'}=1/3$, $M_B=1/5$, $h_{A'}=2$, and $h_B=10$. Circles: experimental Q-values. $A'B$-grains.

§ 6. Other Rocks Having the Similar Composition of Ferromagnetic Material as the Haruna Pumice

There have been found, so far, 10 other rocks which contain the ferromagnetic Il-Ht solid solution together with Ti-Mt as in the Haruna pumice. The summary of the general characteristics of some of these examples reported in the recent paper by Akimoto [21] is reproduced in Table 1 with the permission of the author. Some tentative results of the examinations conducted on these samples with regard to the magnetic interaction in the process of the development of TRM will be described in this section. The examinations consisted of the following procedures, which had already been applied to the Haruna sample.

1) The thermal change of susceptibility $\kappa(T)$ and the modes of development of the total TRM in weak magnetic field and its decay by heating in a non-magnetic space. By a study of these processes, the fundamental characteristics of the sample with regard to TRM may by clarified to some extent.

intensity of H_0, when H_0 is of the order

2) The mode of the development of the partial TRM $J^{T_1}_{\Theta_{c,A},H_{r,r}}(T)$, where $T_1 > \Theta_{c,B}$. This process was conducted in order to determine the sense of the magnetic interaction between A and B, if it exists. In this process, no magnetic field but H_{β} due to J_A works on B at the domain-fixing temperature of B.

3) Thermo-magnetic separation : by this operation, it was tested whether or not grains mainly consisting of the B-phase as in the Haruna rock could be found.

4) The $\kappa(T)$ and the modes of the development and the thermal decay of total TRM of the thermo-magnetically separated B-grains, which correspond to the $A'B$-grains in the Haruna sample. The magnetic interaction within the B-grains, if such exists, should be observed, in this process more effectively than in 1), because the effect of the non-essential A-constituent is eliminated. (See, for example, Fig. 2.) The TRM characteristics, such as the Q-value, of the ferromagnetic Il-Ht phase are also obtained by this process.

5) Electron-microscopic observations on the polished surfaces of the thermo-magnetically separated B-grains. In these observations the Triahol-alminium-replica method was applied on the surfaces of the samples etched with HF for 1 minute.

The results of these examinations obtained on each sample is summarized bellow. For reference, the case of the Haruna rock, as has already been stated, will be summarized first as follows.

Table I. Properties of Ferromagnetic Ilmenite-Hematite Solid Solutions. [21]

Locality	Rock	Chemical composition* Fe_2O_3	FeO	TiO_2	Crystal parameters a_{rh}	α_{rh}	Θ_c	$I_s(T_0)$
Haruna	dacite pumice	26.9	33.2	39.9	5.480 Å	55°08′	250°	25 e.m.u./gr.
Asio	dacite pitchstone				5.483 Å	55°02′	230°	~21 ,,
Sokota	iron sand				5.483 Å	55°01′	190°	
Towada	hyp. horn. dacite pumice	19.63	38.37	42.00	5.491 Å	54°59′	100°	24 ,,
Okuboziawa Asama, volc.	dacite obsidian	20.34	40.88	38.78	5.495 Å	54 58′	110°	21 ,,
Asama	dacite pumice	16.97	40.66	42.37	5.498 Å	54 56′	100	18 ,,
Himesima	horn. mica andesite	20.70	35.53	43.77	5.489 Å	54 56′	190°	29 ,,

* in mol. %

Haruna Rock :

1) The magnetization of B is produced in a reverse direction, during the cooling process in a weak magnetic field, and the total TRM is also reversed at the room temperature. (See Fig. 20, [1-4].) In the thermal decay curve of the TRM, the anomalous increase of TRM was observed at about 450°C. (p. 161, [Rock-Magnetism])

2) The modes of the various partial TRM are shown in Figs. (11), (12), (13), (14), (15), (16), (17) and (18) in [1-4]. It is quite evident that the magnetization of B is reversed in some of the partial TRM.

3) The $A'B$-grains were separated out by the thermo-magnetic separation [2], [3].

4) The mode of the development of the total TRM for the $A'B$-grains is shown in Fig. 2. The reverse TRM of the B-constituent was about 30 times more intense than that of the original sample.

5) The well developed A'-strips were observed. (Fig. 12)

Asio Rock:

No examination has been newly made, since the sample was used up in the experiments reported in the previous paper [3]. The locality where this rock is exposed is said to have sunk under an artificial lake constructed for power development. The results reported in the previous paper are summarized as:

1) The total TRM of the original sample was normal, but it was verified through a study of TRM of the single grains that the magnetization of B is reversed within the total TRM.

2) The partial TRM $J^{200}_{20,\,H_{ex}}(T_0)$, $H_{ex}<3.5\,Oe.$ was proved to be reversed.

3) The results of thermo-magnetic separation is quite similar to that of the Haruna case [3-2]. Most of the grains with the thermo-magnetic separation temperature below 250°C showed perfect RTRM characteristics.

Sokota Iron Sand:

The self-reversal of TRM of the Asio-type of the iron sand at the Sokota-mines was, as mentioned already, discovered by Saito [13].

1) The experiments for the total TRM were carried out by the above author, according to whom the reversal of TRM of B, which is not large enough to overcome the normal TRM of A was verified. The anomalous increase at about 500°C in the heating curve was also observed.

2) The modes of the various partial TRM were also studied by the above author and it was proved that the characteristics are quite same as the Haruna and Asio cases.

3) The thermo-magnetic separation conducted by the present author at 250°C, on the sample obtained by courtesy of Mr. Saito, showed that B-grains, or $A'B$-grains are present.

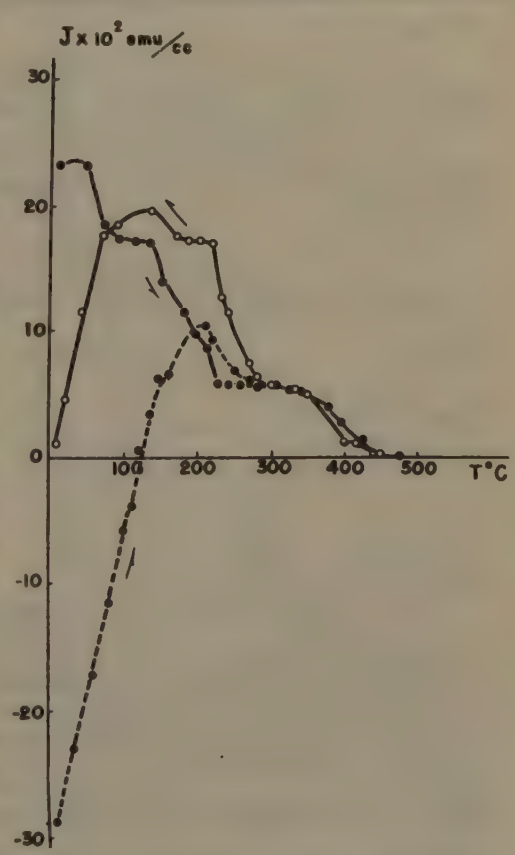

Fig. 17. Characteristics of thermo-magnetically separated B-grains of Sokota iron sand, in $H_{ex}=2.0\,Oe.$
Full circles: $\kappa(T)\times H_{ex}$ curve,
Hollow circles: development of total TRM.
Broken line: thermal decay of total TRM.

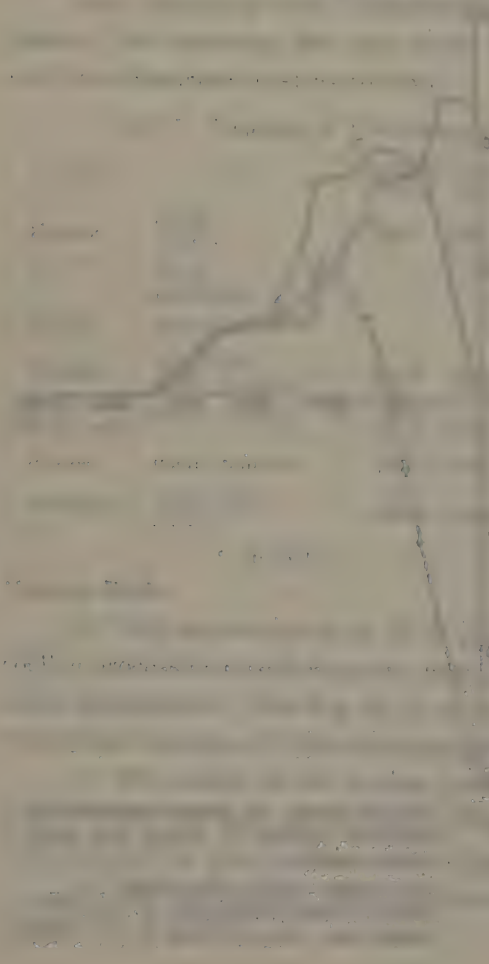

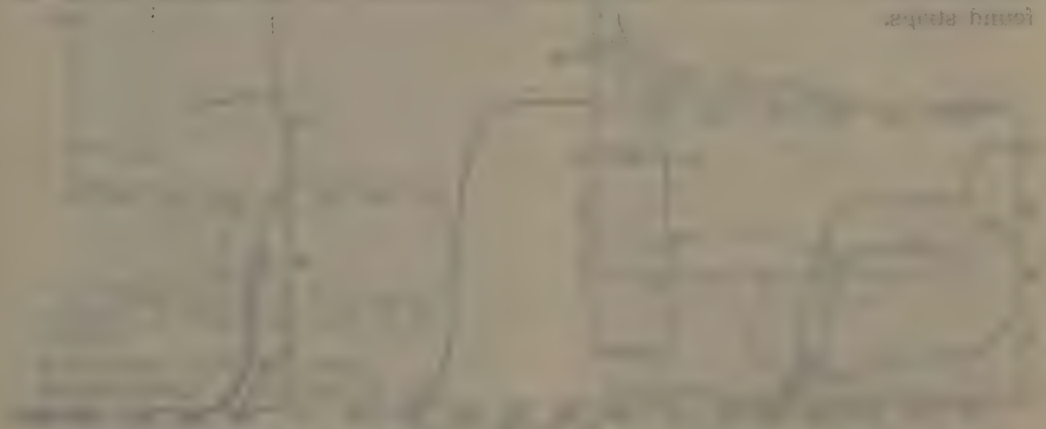

4) The mode of the development of the total TRM of the thermo-magnetically separated *B*-grains shows that they are mainly responsible for the RTRM characteristics of the Sokota iron sand. (Fig. 17)

5) In Fig. 22,a the well developed strips can be observed.

Towada Rock :

1) As seen in Fig. 18,a, the TRM of *B* is produced in the normal direction by the process of total field cooling. This type of mode of development of TRM will be called the Towada-type [10]. The anomalous increase in the heating curve was observed at about 430°C.

2) In the process of the development of the partial TRM $J^{140}_{500,8.00e}(T)$ shown in Fig. 18,b, the intensity of the remanent magnetization was observed to decrease as the specimen was cooled through $\Theta_{,B}$. The results of 1) and 2) may be interpreted as showing that the magnetic coupling in the Towada sample works anti-parallelly, but that it is so weak that its effect does not appear in the process of total field-cooling.

3) The presence of *B*-grains was affirmed by the thermo-magnetic separation at about 150°C.

4) The experiments on the *B*-grains are shown in Fig. 18,c, in which the normally oriented magnetization of *B* will be seen.

5) Very scarce traces of the strips were observed. (Fig. 22,b) Therefore, the weak interaction assumed above might be explained by the effect of the rarely found strips.

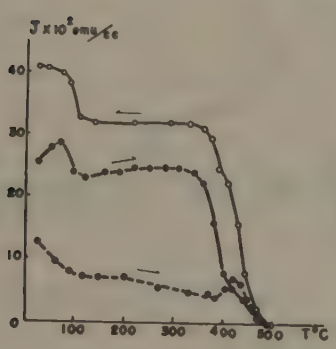

Fig. 18, a.

Characteristics of ferromagnetic minerals of Towada rock in $H_{ex}=2.0Oe$.
Full circles: $\kappa(T)\times H_{ex}$ curve,
Hollow circles: development of total TRM.
Broken line: thermal decay of total TRM.

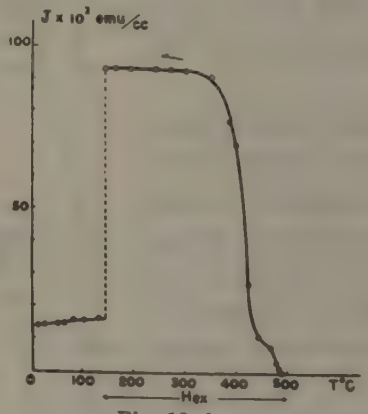

Fig. 18, b.

Development of partial TRM $J^{140}_{500,8.00e}(T)$ of Towada ferromagnetic minerals.

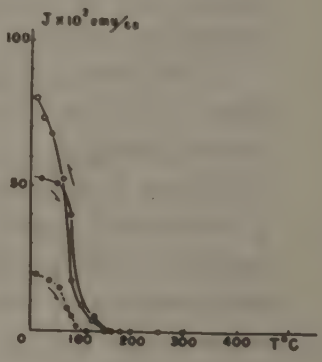

Fig. 18, c.

Characteristics of thermo-magnetically separated *B*-grains of Towada ferromagnetic minerals, in $H_{ex}=4.0Oe$.
Full circles: $\kappa(T)\times H_{ex}$ curve.
Hollow circles: development of total TRM.
Broken line: thermal decay of total TRM.

Okubosawa Rock :

1) The mode is the Towada-type. (Fig. 19,a)

2) The mode for the partial TRM $J^{150}_{500,8.00e}(T)$ is shown in Fig. 19, b. The

remanent magnetization increases as the temperature decreases. It was not possible to determine whether this increase in TRM is due to the production of the normally oriented J_B by the positive interaction with J_A, or due only to the increase of the spontaneous magetization of A.

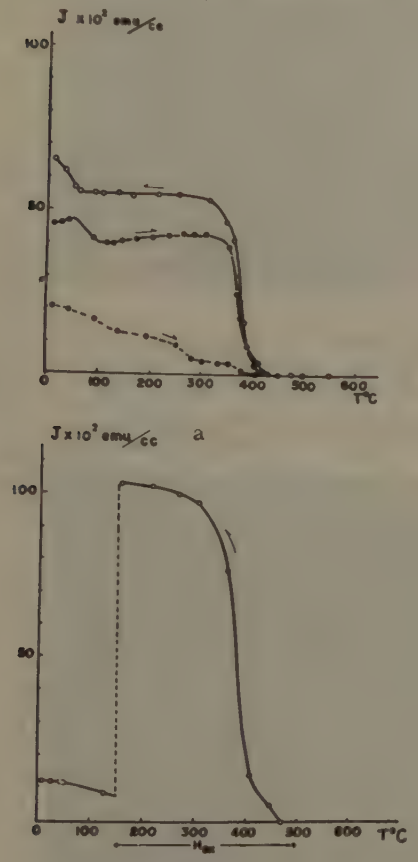

Fig. 19,
a. Characteristics of ferromagnetic minerals of Okubosawa rock in $H_{ex}=4.0Oe$.
Full circles: $\kappa(T)\times H_{ex}$ curve.
Hollow circles: development of total TRM.
Broken line: thermal decay of total TRM.
b. Development of partial TRM, $J^{150}_{500,8.0Oe.}(T)$, of Okubosawa ferromagnetic minerals.

5) The comparatively rare occurence of obscure strips was observed by electron-microscopic observations. (Fig. 22, c)

Asama Rock:

1) Although the intensity of magnetization is weak, the comparatively intense normal TRM of B will be seen in Fig. 20,a. This mode may be classified with the Towada-type.

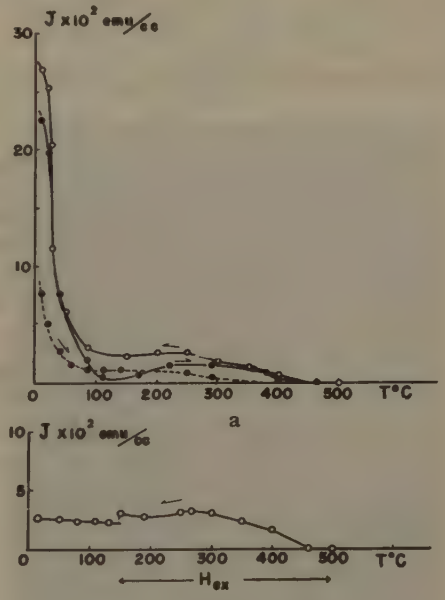

Fig. 20.
a. Characteristics of ferromagnetic minerals of Asama rock in $H_{ex}=4.0Oe$.
Full circles: $\kappa(T)\times H_{ex}$ curve.
Hollow circles: developmedt of total TRM.
Broken line: thermal decay of total TRM.
b. Development of partial TRM $J^{150}_{500,8.0Oe.}(T)$ of Asama ferromagnetic minerals.

2) No effect of the magnetic interaction was observed (Fig. 20,a) in this case, since the partial TRM $J^{150}_{500,8.0Oe.}(T)$ showed only a very slight increase below 150°C.

3) B-grains were separated out by the thermo-magnetic separation at about 150°C: more than 90% consisted of the B-grains. It will be of a petrological interest that the major constituent of this sample is Il-Ht, instead of Ti-Mt.

4) No distinct strip-shaped intergrowth was observed. In Fig. 22,d, some etched spots will be observed.

Himesima Rock :

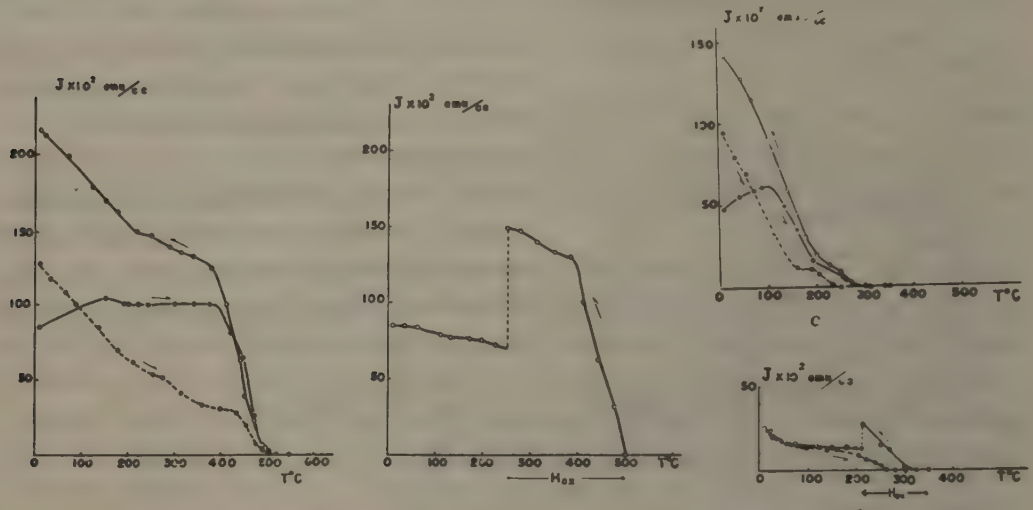

Fig. 21.

a. Characteristics of ferromagnetic minerals of Himesima rock in $H_{ex}=4.0\ Oe$.
Full circles : $\kappa(T)\times H_{ex}$ curve. Hollow circles : development of total TRM.
Broken line : thermal decay of total TRM.

b. Development of partial TRM $J^{250}_{500,4.0Oe.}(T)$ of Himesima ferromagnetic minerals.

c. Characteristics of thermo-magnetically separated *B*-grains of Himesima ferromagnetic minerals in $H_{ex}=4.0\ Oe$.
Full circles : $\kappa(T)\times H_{ex}$ curve.
Hollow circles : development of total TRM.
Broken line : thermal decay of total TRM.

d. Development and thermal decay of partial TRM, $J^{210}_{350,8.0Oe.}(T)$ of thermo-magnetically separated *B*-grains of Himesima ferromagnetic minerals.

Fig. 22. a.
Electron micrograph of polished surface of thermo-magnetically separated *B*-grain of Sokota iron sand, after etching with HF for 1 minute, showing well developed exsolution lamellae.

Fig. 22, b.
Electron micrograph of polished surface of thermo-magnetically separated *B*-grain of Towada ferromagnetic minerals, after etching with HF for 1 minute, showing scarce exsolution lamellae.

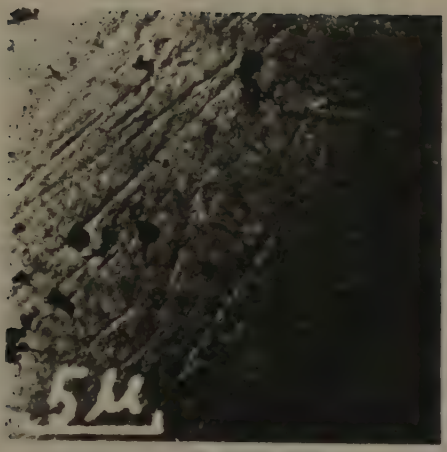

Fig. 22, c.

Electron micrograph of polished surface of thermo-magnetically separated *B*-grain of Okubosawa ferromagnetic minerals, after etching with HF for 1 minute, showing obscure exsolution lamellae.

Fig. 22, d.

Electron micrograph of polished surface of thermo-magnetizally separated *B*-grain of Asama ferromagnetic minerals, after etching with HF for 1 minute, showing undeveloped exsolutions.

Fig. 22, e.

Electron micrograph of polished surface of thermo-magnetically separated *B*-grain of Himesima ferromagnetic minerals, after etching with HF for 1 minute, showing well developed exsolution lamellae.

Fig. 22, f.

Electron micrograph of polished surface of ferromagnetic grain of Adirondack rock No. 21, after etching with HF for 1 minute, showing well developed exsolution lamellae.

1) The mode obviously belongs to the Towada-type. (Fig. 21,a)

2) The partial TRM, $J^{250}_{500,4.00e.}(T)$, increases as the sample is cooled after the suppression of H_{ex}. (Fig. 21,b)

3) *B*-grains were separated out by thermo-magnetic separation at about 250°C.

4) The TRM of *B* was in the direction of H_{ex}. (Fig. 21,c). For the *B*-grains of this sample, the mode of development of partial TRM $J^{210}_{350,8.00e.}(T)$, was also measured. (Fig. 21,d). In this process, an anomalous increase in the remanent magnetism after the suppression of H_{ex} was observed bellow 100°C. Whether or not

this increase is caused by the positive magnetic interaction between the constituent with lower Curie point and the constituent which acquired TRM before the suppression of H_{rr} is not clear at the present stage. However, the possibility of the occurence of such an effect seems to well deserve further examination.

5) It may be of interest that the patterns of the strips observed (Fig. 22,e) are similar with those in the cases of RTRM. In order to clarify the mechanism of the magnetic interaction in this case it would be desirable to study the nature of the strips; their phase, their Curie point, etc.

Finally, the ferromagnetic mineral-grains extracted from the **Adirondack** rock, which was offered by Dr. Balsley to Prof. Nagata, were examined by means of the electron-microscope. (Fig. 22,f) The rock-sample was No. 21 which was reported to have reverse natural remanent magnetism [11]. According to Balsley and Buddington, this reverse natural remanent magnetism is caused by the self-reversal of TRM, though the chemical composition of the participating ferromagnetic constituents differs from that of the Haruna case. Judging from the chemical composition reported by the above authors and the results of the X-ray analysis conducted in our laboratory, the host in Fig. 22,f may be presumed to be a titanhematite and the strips to be another titanhematite containnig less Ti than the former.

§ 7. Conclusions and the Further Problems

When more than two ferromagnetic materials are present in rocks, it is generally expected that there exists some magnetic interaction between them, especially during the process of development of thermo-remanent magnetism. The characteristics, such as the sense and the intensity, of the interaction should naturally depend on their state of co-existence. It seems, therefore, quite probable that such presence generates various phenomena in thermo-remanent magnetism, which would otherwise hardly occur.

In the Haruna rock, which is known to have the self-reversal characteristics of thermo-remanent magnetism, the titanomagnetites and the ferromagnetic solid solutions between ilmenite and hematite are contained as co-existing ferromagnetic ingredients. In the present paper, a detailed study was made, from the above mentioned viewpoint, on the actual mechanism of the magnetic interaction responsible for the particular character of the reverse thermo-remanent magnetism in this rock. The various data obtained by magnetic, crystallographic and electron-microscopic examinations on the $A'B$-grains, which were proved to be responsible for the phenomenon, demonstrated that the magnetic interaction should be assumed as being between two different ferromagnetic ilmenite-hematite solid solutions and that the titanomagnetites should be assumed as having little effect. A theoretical consideration also showed that the reverse thermo-remanent magnetism of the Haruna rock may be explained by the magnetic interaction between the two constituents intergrown in such a state as observed through the electron-microscope, provided that the fine strips of the ilmenite-hematite phases can acquire

a very strong thermo-remanent magnetism in weak fields.

Examinations were conducted on several other rocks having similar assemblages of ferromagnetic minerals as in the Haruna rock. It was shown, through these examinations, that there actually exist various degrees of magnetic interaction in natural ferromagnetic substances.

Though the studies in the present paper were confined to the rocks containing the ferromagnetic ilmenite-hematite phases, it would be highly desirable to study the nature of the magnetic interactions which take place between titanomagnetite phases, since it is known that the latter phases are of much greater importance than the former from the viewpoint of rock-magnetism as a whole [21]. In fact, several cases where magnetic interactions between titanomagnetite phases are expected to be playing an essential role have been reported. For example, Kawai et al. [23] have reported the occurence of an interesting phenomenon where the natural remanent-magnetism of some rocks changes its sign when heated in a non-magnetic space. The anomalous increase of thermo-remanent magnetism during its thermal decay process which was found in the ferromagnetic minerals from Niisima (p. 161. [Rock-Magnetism]) and in the A-constituent of the Haruna [1-4], Sokota and Towada rocks has also been interpreted as caused by an anti-parallel coupling between titanomagnetites. In order to utilize the natural remanent magnetism of rocks for palaeomagnetic purposes, it was proposed [10] that the natural remanent magnetism should be proved as having the *very* normal characteristics of thermo-remanent magnetism and as being free from any anomalous phenomena like those mentioned above. Therefore a more thorough clarification of the nature of magnetic interactions in natural ferromagnetic substances will be of great significance from the viewpoint of palaeomagnetism.

Acknowledgements

In concluding this paper, the writer would like to express his deep gratitude to Prof. T. Nagata who has kindly rendered the most pertinent directions and encouragements to the writer throughout the course of this study. His thanks are due to Prof. H. Kuno for his various valuable suggestions from the geological standpoint. The writer is especially indebted to Mr. K. Akashi, the president of Akashi Seisakusho, for his kindness in allowing the writer to use the Akashi Electron-Microscope in his factory, and to Messrs. T. Masuda, T. Umeda and other members of Akashi Seisakusho for their practical assistance in the writer's electron-microscopic observations. He also gratefully acknowledges the useful discussions and practical assistance in the microscopic study rendered by Messrs. H. Mukaiyama, S. Aramaki and A. Tono, Dept. of Geology, Tokyo Univ. As for the crystallographic examinations, the writer cordially thanks Dr. R. Sadanaga, Dept. of Mineralogy, Tokyo Univ., for his painstaking instructions and Dr. G. Honjo, Dept. of Physics, Tokyo Institute of Technology, for his kind discussions.

[16] Kato, Y., Tahegi, A. and Kato, I. Journ. Geomag. Geoelec. 6, No. 4, 206 (1955)

[18] Thellier, E., Thèses, Fac. Sc., Paris (1938)

[19] Nagata, T., Bull. Earthq. Res. Inst., 21, 1 (1943)

Finally, the writer sincerely acknowledges the numberless practical suggestions given by his senior colleague Mr. S. Akimoto and Mr. J. Ossaka, Earthquake Reseach Institute, Tokyo Univ..

References

Nagata, T.: Rock-Magnetism, Maruzen Co. Ltd., Tokyo 1953.....for general references.

[1] [1-1] Nagata, T., Akimoto, S. and Uyeda, S., Proc. Japan Acad., **27**, No. 10, 643 (1951)

[1-2] Nagata, T., Akimoto, S. and Uyeda, S., Proc. Japan Acad., **28**, No. 6, 277 (1952)

[1-3] Nagata, T., Nature, **169**, 704 (1952)

[1-4] Nagata, T., Uyeda, S. and Akimoto, S., Journ. Geomag. Geoelec., **4**, 22 (1952)

[2] [2-1] Nagata, T., Uyeda, S., Akimoto, S. and Kawai, N., Journ. Geomag. Geoelec., **4**, 102 (1952)

[2-2] Nagata, T., Akimoto, S. and Uyeda, S., Nature, **172**, 630 (1953)

[3] [3-1] Nagata, T., Nature, **172**, 850 (1953)

[3-2] Nagata, T., Akimoto, S. and Uyeda, S., Journ. Geomag. Geoelec., **5**, 168 (1953)

[4] [4-1] Néel, L., Ann. de Géophys., **7**, 90 (1951)

[4-2] Néel, L., C.R. Acad. Sc., **234**, 1991 (1952)

[5] Vincenz, S.A., M. N. R. A. S. Geophys, Supple., **6**, No. 9, 590 (1954)

[6] Hospers, J., Koninkl. Nederl. Akad. van Wetenschapper-Amsterdam, B **56**, 467 (1953): 477 (1953)

[7] Roche, A., C.R. Acad. Sc., **236**, 207 (1953)

[8] Asami, E., Proc. Japan Acad., **30**, No. 2, 102 (1954)

[9] Kato, Y., Takagi, A, and Kato, I., Journ. Geomag. Geoelec. **6**, No. 4, 206 (1955)

[10] Nagata, T., Akimoto, S., Uyeda, S., Momose, K. and Asami, E., Journ. Geomag. Geoelec., **6**, No. 4, 182 (1955)

[11] Balsley, J.R. and Buddington, A.F., Journ. Geomag. Geoelec., **6**, No. 4, 176 (1955)

[12] Graham, J.W., Journ. Geophys. Res., **58**, 243 (1953)

[13] Saito, T., Private communication.

[14] Kittel, C., Introduction to Solid State Physics, John Wiley and sons, Inc., New York (1953)

[15] Kittel, C., Rev. Mod. Phys., **21**, 541 (1949)

[16] Grabovsy, M.A. and Pushkov, A.H., Izvest. Akad. Nauk. SSSR. ser. Geofiz., (1954) No. 4, 320.

[17] Nagata, T. and Uyeda, S., Nature, **175**, 35 (1955)

[18] Thellier, E., Thèse, Fac. Sc., Paris (1938)

[19] Nagata, T., Bull. Earthq. Res. Inst., **21**, 1 (1943)

[20] Néel, L., Ann. de Géophys., **5**, 99 (1949)
[21] Akimoto, S., Japanese Journ. Geophys., **1**, No. 2, 1 (1955)
[22] Roquet, J., Ann. de Géophys., **10**, 226 (1954)
[23] Kawai, N., Kume, S. and Sasajima, S., Proc. Japan Acad., **30**, No. 9, 854 (1954)

Note added August 16, 1955—Since this manuscript was first submitted, Néel published an extensive paper on Some Theoretical Aspects of Rock-Magnetism [Adv. Phys. **4**, No. 14, 191 (1955)], in which he states that TRM is possible in multi-domain grains, too. In his theory, the intensity of TRM is shown to be proportional to the square root of the coercive force. Therefore, according to his theory, the hypothesis of the intense TRM of A' and B constituents in the author's model of $A'B$-grains may be justified by the assumption that the fine lamellae of A' and B have strong coercive force, even if the observed size of them is not considered to be sufficiently small as to give the single-domain structure. In the case of the multi-domain model, it can be readily shown that the results of the calculation described in § 5 suffer no serious alteration, as far as the contribution from the lamellae perpendicular to H_{ez} is neglected. This author, however, finally calls attention to the possibility of the dependence on temperature of the critical size for the single-domain structure: it may increase appreciably if the crystal anisotropy energy does not decrease too rapidly in comparison with the intensity of J_s as the temperature rises [(6. 1. 12), (3. 2. 7.) in [15] and J. J. Went et al., Philips. Tech. Rev. **13**,pp. 194-208. (1952)]. Hence, whether the lamellae of A' and B are of multi-domain structure or of single-domain one is to be decided by future examination.

[29] Kawai, N., Kume, S. and Sasajima, S., Proc. Japan Acad., 39, No. 3, 151 (1963)

The Thermo-Magnetic Properties and History of Some Plutonic Rocks from the Leinster Granite, Ireland

By Horace MANLEY* and David J. BURDON**

(Read Oct. 26, 1949)

Summary

The susceptibility and remanent magnetisation have been determined for seven representative samples of the granodiorite, granite and basic enclaves which form the bulk of the Arrigle Complex, lying at the south-west termination of the Leinster Granite. The determinations were made on the rocks in their natural state and again after they had been heated to 600°C and cooled in the earth's magnetic field in London. From these have been calculated X, the ratio of the susceptibility after and before heating; S, the ratio of the thermo-remanent magnetisation to the remanent magnetisation; and Z, the ratio of Q to T.

For the granodiorites, X averages about 30 and S about 50; this indicates that new magnetic minerals were developed by heating and suggests that the granodiorites, as now constituted, have not cooled through their Curie point. For the granites, X averages 1.3 and S about 32; this indicates that no new magnetic minerals have been developed by heating, but that the remanent magnetisation of existing magnetic minerals has been greatly increased. This proves that the magnetic minerals of the granite have formed below their Curie point; the petrography indicates that magnetite has formed or reformed along with other deuteritic changes, the most important of which is the change of hornblende to a biotite-quartz symplectite. Of the basic enclaves, the gabbroes show X equal to 1.6 and S equal to 2.7; this proves that the gabbroes have crystallised and cooled from above their Curie point in the normal manner of igneous rocks. Another enclave, supposedly a porphyretic dolerite, shows X equal to 3.9 and S equal to 21; either the dolerite has suffered much low-temperature metamorphism of its magnetic, or potentially magnetic, minerals, or it is a metamorphic rock closely resembling a dolerite.

Thermo-magnetic investigations, combined with petrography, along the lines outlined in this paper should prove of great assistance in the elucidation of the thermal history of many metamorphic-plutonic-igneous rocks.

Contents

* 124, Brondesbury Villas, Kilburn, London, N.W. 6.
** P.O. Box 256, Damascus, Syria.

4. Magnetic properties.
5. Thermo-magnetic properties.
6. Discussion:
   - 6.-1. Magnetic properties.
   - 6.-2. Thermo-magnetic properties.
   - 6.-3. Thermal history of the rocks.
7. Acknowledgements and Bibliography.

1. Geological Setting

The Caledonian granites of the Leinster chain form a continuous outcrop extending south-south-west for some 70 miles from Dublin to the village of Inistioge in Co. Kilkenny, Fig. 1, A. There is then a gap of some six miles between the end of the main granite outcrop and the present cover of unconformable Upper Old Red Sandstone on the west. Within this gap there are five outcrops of granitic rock. Four of these resemble closely the granite or granodiorite of the main Leinster chain: but the most westerly outcrop, in part covered by the Old Red Sandstone, consists of several different rock-types Fig. 1, B. It has been named 'The Arrigle Complex' from the small river which flows over it; the rocks described in this paper all come from the Arrigle Complex.

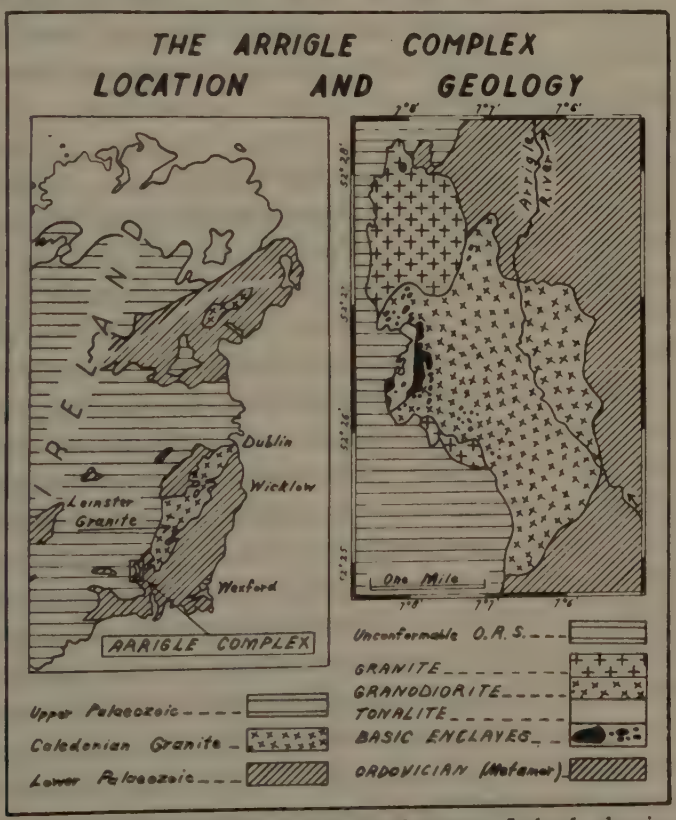

Fig. 1. Generalised geological map of eastern Ireland, showing the relationship of the Arrigle Complex to the Leinster Granite. Details of the geology are shown on the second map.

The Arrigle Complex consists of five major rock-types:—

(1) Basic Enclaves, gabbroidal to doleritic in texture.

(2) Tonalites, ranging from true Tonalites through Monzotonalits to Adamelites; these are not described in this paper.

(3) Granodiorites, with varying amounts of skialiths of sedimentary origin.

(4) Coarse granophyric Granite.

(5) Fine-grained granophyric Granite, probably a marginal phase of No. 4; it is not described in this paper.

In addition, there are the usual dyke associates of a plutonic complex, including granophyric porphyry dykes. A full description of the Arrigle Complex is to be published elsewhere, (by D.J.B.)

Exposures are poor, for there is a cover of light bog and some glacial drift over much of the valley. A magnetic survey was carried out to assist in mapping the basic enclaves, and also to trace their extension beneath the Old Red Sandstone. The interpretation of the magnetic survey necessitated a study of the magnetic properties of the rock-types forming the Arrigle Complex. This was carried out by H.M., who expanded the investigation to cover the thermo-magnetic properties of the rocks. It is considered by the joint authors that from these investigations several important facts concerning the thermo-magnetic, and hence geological, history of the rocks may be deducted.

2. Petrology of Specimens

Seven specimens were selected for examination:

4. Basic Enclaves.....Specimens Nos. 765, 768, 769, and 770.
1. Granophyric Granite.....Specimen No. 180.
2. Granodiorites .....Specimens Nos. 134 and 136.

Thin slices for petrographic examination were cut at the time the rock cubes were made. After the heated cubes had had their magnetic properties determined, further slices were cut from the actual cubes. Both sets of slices were examined to see if any petrographic changes could be seen in their constituent minerals, particularily in those with known or suspected thermo-magnetic properties. Due to the rather heterogenous nature of most of the rocks, and consequent changes from slice to slice, the latter investigation has not yielded any striking results.

Basic Enclave No. 765. This is a normal medium-coarse gabbro, composed of labradorite, augite and amphibole, with magnetite-ilmenite; the ferro-magnesian minerals are uralitised and chloritised with seperation of rare epidote, while the felspars are locally saussuritised. The labradorite is euhedral, in laths up to 10 mm long, zoned and twinned. The augite is interstitial to sub-ophitic, and is much changed to green hornblende and chlorite with granular epidote and fibrous actinolite. Some brown hornblende is probably primary. There are some chlorite areas composed of chrysotile laths forming a regular pattern but lacking any lime mineral. The iron ore forms about 3% of the rock. It is mainly in laths of ilmenite up to 1 mm long, occuring mainly in the ferro-magnesian minerals. A

little fine-grained magnetite is seen in some of the uralite areas, while skeleton magnetite occurs in the primary bown hornlende. No leucoxene was seen. Pyrite is present in small amounts, simulating magnetite in its mode of occurrence and possibly forming mixed crystals.

Basic Enclave No. 768. This is a coarse gabbro, with basic labradorite and sub-ophitic augite partially uralitised. There is some primary brown hornblende and some green hornblende which may also be primary. The former presence of bronzite is shown by bastite pseudomorphs; it is even possible that the rock once contained primary olivine. Rods of haematite may be seen in some of the felspar. In general the magnetite occurs in patches, up to 0.5mm long, but there is one large area of magnetite in the slide which is 2.5mm across. There is also a a sprinkling of fine secondary magnetite formed during the uralitisation and chloritisation of the original ferro-magnesian minerals. Pyrite is common, often in quite large crystals.

This specimen was oriented in the field, and so the cubes cut from it have also been oriented.

Basic Enclave No. 769. This coarse gabbro closely resembles No. 769, but for the fact that there is a great increase in the number of haematite rods in the labradorite; such heamatite is an exsolution phenomenon and is not unusual in labradorite. The total iron ore content of the rock lies between 4% and 5%. Around some of the magnetite patches, some deuteritic biotite has developed from the ferro-magnesian minerals: in part, it must replace some of the magnetite. Pyrite is common, but in small grains or agglomerations of grains, not in large crystals as in No. 768.

This specimen was oriented in the field, and so the cubes cut from it have also been oriented.

Basic Enclave No. 770. This is a porphyretic dolerite, with a scattering of large plagioclase crystal set in a fine-grained base with a somewhat gabbroidal texture. The large felspars are altered to tremolite-actinolite and zoisite: if it were originally labradorite, it contained no haematite rods. The augite of the base has followed the usual augite-to-hornblende and hornblende-to-chlorite changes. The total iron ore present is but 2%, much less than in the other basic enclaves. Skeletal octahedra of magnetite are seen, and there is ilmenite in rods up to 0.7mm long. There is a very little pyrite present.

Granophyric Granite, No. 180. This is a representative of the late cross-cutting granites which are the most homogeneous rocks of the Arrigle Complex. It is a leuco-granite, with quartz, orthoclase and albite forming 97.3% of the rock. The albite is subhedral and comparatively fresh. The orthoclase tends to be poekilitic; it is fresh but some areas are clouded with a dusting of fine haematite, apparently introduced from the Old Red Sandstone which till recently covered the outcrop. The quartz is strikingly granophyric; intergrowths are mainly with the orthoclase, but occasionally the albite is involved, suggesting a

ternary eutectic (see Nockolds, 1947). Green biotite forms 2% of the rock. It is strongly pleochroic, with *X* a pale buff and *Y* and *Z* a clear dark green; it is almost uniaxial and the birefringnence is low for a mica. It varies in size from well-formed flakes up to 2mm long to clots of numerous small flakes; the centre of such clots is usually sieved with quartz granules in a symplectite growth with the biotite. This suggests that it is secondary after a silica-richer ferro-magnesian such as hornblende or amphibole. The lime released in such a change now appears as epidote, grading towards clinozoisite and into allanite. Zoned epidote is seen, and pleochroic haloes occur in the biotite around the epidote/allanite. No zircon was seen. There is a little reddish-brown and grey sphene: in small grains such sphene is almost indistinguishable from allanite. In a few places, alteration of the biotite to chlorite has resulted in the formation of sagenitic rutile. There is a little pyrite present, pseudomorphed by goethite/lepidocrocite. There is a very little magnetite in the biotite, but the total iron ore content of the granite does not exceed 0.5%.

After heating, the granophyric quartz remain unchanged. The pink colour of the orthoclase, and the haematite dust, have been emphasised. But the amount of ore in the felspar has not increased, nor has the haematite changed to magnetite. The albite is clouded; sericite, sometimes stained yellow, has developed and also clinozoisite/zoisite, but no chlorite or epidote are seen in the altered plagioclase. The yellow staining may be goethite or lepidocrocite, and this would involve changes in the iron present. Of all the minerals, the mica shows the most marked changes. It is now red-brown in colour, pleochroic from brownish yellow to dark foxy red. The epidote appears darker in colour. Magnetite may be seen in the mica; it appears to be greater than that noted before heating, but the difference is not greater than might be expected from one slice to another. The haematite in the felspar has not changed to magnetite, and there is no reason why the haematite in the mica should behave differently. No change was observed in the small amounts of allanite and sphene.

Granodiorite No. 134. This specimen represents a comparatively homogeneous portion of the granodiorite, but in it 'skialiths' ('shadowstones,' Goodspeed, 1948, p. 67) may still be recognised; these consist of biotite hornfels and patches of granular quartz. In the body of the rock, the dominant mineral is oligoclase, usually heavily sericitised. The perthitic orthoclase is pockiloblastic and comperatively fresh. Biotite forms about 5% of the rock and shows a very patchy distribution. Small poekilolithic biotites may be seen in the skialiths while clots of coarser biotite occur throughout the more homogenised body of the rock. Where enclosed on orthoclase, the biotite is fresh; elsewhere it is much altered to chlorite, in which some granular epidote and sphene occur. Zircon and apatite are minor accessories. There is almost no magnetite visible in the slices cut for examination.

Granodiorite No. 136. This is a representative of skialith-rich granodiorite,

and in the hand-specimen slivers of biotite hornfels and quartz blebs are visible. The slices show the quartz blebs to consist of aggregates of rounded grains cemented by a thin coating of limonite. The hornfels consist of small biotites in a base of quartz and clouded oligoclase. There is some poekiloblastic orthoclase in the body of the rock, which closely resembles that of No. 134. The biotite is much altered to chlorite, in which sagenitic rutile is common; one small crystal of goethite was seen with the rutile. The amount of magnetite is extremely small, but there are a few specks of pyrite, with a goethite/limonite rim. The rock is so heterogeneous that each slice will vary considerably from the average for the rock.

3. Laboratory Procedure

In order to make the magnetic observations, the specimens had to be cut into cubes with sides 2cm long. This was done by means of a specially designed rock-cutting machine designed by H. M. in co-operation with Dr. Bruckshaw. It consists of a diamond-impregnated copper disk spun at 3,000 rpm by an electric motor. Where oriented cubes were required, the initial cut was made parallel to the paint-marks on the field specimen, the operator holding the rock in his hands. Thereafter the remaining five faces were cut with the aid of a jig, and a true cube obtained from the randomly-shaped specimen; if the latter had been oriented in the field, the resulting cube or cubes were also oriented. In all 25 cubes were cut from the 7 field samples examined.

The method of making the magnetic observations and calculations has been fully described by Bruckshaw and Robertson (1948); the same apparatus and procedure were used in this investigation. The direction and intensity of the remanent magnetisation was determined for each cube in three perpendicular directions. From this the amount and direction (for oriented specimens), of the remanent magnetisation were determined. The susceptibility was also found for each cube by measuring its behavior as 'an alternating magnet under the action of the changing energizing field'.

These observations were made on the cubes before and after they had been heated to above 600°C in a furnace. The results are tabulated in Tables 1 and 2.

No attempt was made to determine the Curie point directly. By heating samples of Nos. 134 and 180 to 300°, 500°, and 600°C successively, it was determined that the Curie point for these rocks was higher than 500°C, and probably close to 600°C; see Chevallier et Piere, 1932. Specimen No. 134 showed an appreciable increase in susceptibility (13) and a large increase in remanent magnetisation (32) after heating to 600°C; whatever mineral altered to magnetite, or another magnetic mineral (?), did so close to the Curie point of magnetite, which lies around 570°C for pure magnetite. Specimen 180 showed almost nil (1.3) increase in susceptibility but a marked increase (45) in remanent magnetisation; whatever mineral already in the rock took-on its latent residual magnetisation on cooling around 600°C, did so close to the Curie point of magnetite. Similar results were obtained by Michel-

Levy et Grenat, (1929), Grenat (1930), Nagata (1943) and others in similar investigations into rocks. It is concluded that the magnetic constituent is magnetite.

Due to the low concentration of the magnetite in the natural rocks and to its low susceptibility, no attempt was made to extract the amount required for an X-ray powder analysis.

4. Magnetic Properties

The following magnetic properties were determined for the rocks in their natural state:—The susceptibility (k_n) and the remanent magnetisation (R) for all specimens and also the angle and direction of magnetic dip for the oriented specimens. With its remanent magnetisation, a rock possesses an induced magnetisation due to the earth's magnetic field (H); the value of this induced magnetisation, k_nH, is readily obtained by multiplying the susceptibility by the intensity of the earth's local magnetic field. In the laboratory, H equals 0.545 oersted. The ratio of R to k_nH is called 'T,' and is a measure of the magnitude of the remanent/induced magnetisation.

Table 1 shows the results obtained. At least two cubes had been cut from each rock specimen, and in all 25 cubes were investigated. Where approximately the same figures were obtained on two or more cubes cut from the same rock, the values are not repeated in Table 1, but suffixes 'a,' 'b,' etc. have been added to indicate the number of cubes measured.

Table 1. Magnetic properties of natural rocks prior to heating. The general accuracy equals 10×10^{-6} c.g.s. units. Susceptibility and Remanent Magnetisation are expressed in 10^{-6} c.g.s. units. N.D. means 'not determind'.

Rock Type and Specimen No.	Susceptibility k_n	Remanent Mag. R	Ratio R/k_nH T	Dip	Declin.
Basic Enclaves					
765, a, b	105	120	2.0	—	—
768, a	N.D.	370	N.D.	−33°	E. 148°
768, b	N.D.	260	N.D.	−25°	E. 162°
768, c	270	270	1.8	—	—
769, a	375	810	4.0	−38°	E. 115°
769, b	155	525	6.2	−30°	E. 115°
770, a, b, c	90	40	0.8	—	—
Granites					
180, a, b, c, d	125	<10	<0.15	—	—
Granodiorites					
134, a, b, c, d	20	<10	<0.9	—	—
136, a, b, c, d, e, f, g	Nil	Nil	—	—	—

5. Thermo-Magnetic Properties

When the foregoing measurements had been completed, the cubes were heated to 600°C in a furnace and then allowed to cool slowly to room temperature in the earth's magnetic field. In so cooling through its Curie Point (which could not be greater than 580°C), each cube acquired new magnetic properties.

These new magnetic properties were measured in exactly the same manner as that used on the unheated-treated rocks. Table 2 shows the results obtained. The new susceptibility is indicated by 'k' and the new remanent magnetisation by 'P'; this may be described as the thermo-remanent magnetisation of the specimen. The ratio of P to k_tH is indicated by 'Q'. This ratio is of considerable interest and diagnostic use. It was first introduced by Koenigsberger (1933, 1938); Thellier (1938) and Nagata (1941, 1943) have shown that it is a magnetic characteristic of rocks, independant of the field strength for small field intensities.

Table 2. Magnetic properties of the rocks after they had been heated to 600°C, and allowed to cool in the earth's magnetic field. Susceptibility and Remanent Magnetism are expressed in 10^{-6} c.g.s. units.

Rock Type and Specimen No.	Susceptibility k_t	Remanent Mag. P	Ratio P/k_tH Q	Dip
Basic Enclaves				
765, a	165	320	3.5	61°
765, b	165	330	2.8	59°
768, a	350	1,225	6.5	—
768, b	270	540	4.3	—
768, c	290	1,520	9.7	64°
769, b	285	1,150	7.4	64°
770, a	390	1,025	4.8	68°
770, b	310	680	4.0	65°
770, c	345	840	4.5	69°
Granites				
180, a	230	420	3.4	65°
180, b	135	235	3.2	68°
180, c	155	290	3.5	67°
Granodiorites.				
134, a	330	570	3.2	68°
134, b	115	200	3.2	67°
134, c	335	570	3.1	63°
136, a	400	830	3.8	67°
136, b	375	735	3.6	64°
136, c	275	620	4.1	68°
136, d	250	470	3.5	67°
136, e	275	600	4.0	70°
136, f	330	685	3.8	69°

It will be noticed that the heated cubes take on the magnetic dip approximating to that measured for the laboratory, (65°); the mean value for the cubes is 66°, and the range extends from 59° to 70°. Sample 769, a completely disintegrated during heating, and 769, b was severely fractured. This phenomenon is rare and may be due to the expulsion of volatiles or to the release of strain at moderately high temperature.

The ratios of the three sets of values given in Tables 1 and 2 have been

calculated and are given in Table 3. The ratio of the susceptibility after heating to the susceptibility bofore heating is called 'X'; any departure of this ratio from unity may be taken as implying a formation or destruction of magnetic constituents in the rock by and during the heat treatment process. The ratio of the thermo-remanent magnetism after heating to the remanent magnetism of the natural rock is called 'S'; its interpretation is by no means simple. Finally, the ratio of Q to T is called 'Z'; this Z ratio is the S ratio corrected for changes of susceptibility produced by the heat treatment.

Table 3. Ratios between the Susceptibilities, Remanent-Induced Magnetisation and Remanent Magnetisation after and before heating to 600°C.

Rock Type and Specimen No.	Ratio k_i/k_n X	Ratio P/R S	Ratio Q/T Z
Basic Enclaves			
765, a	1.6	2.7	1.7
765, b	1.6	2.8	1.8
768, a	N.D.	3.3	N.D.
768, b	N.D.	2.1	N.D.
768, c	1.1	3.6	5.4
769, b	1.8	2.0	1.2
770, a	4.3	26.	6.0
770, b	3.5	17.	5.0
770, c	3.8	21.	5.6
Granites			
180, a	1.7	40.	23.
180, b	1.1	25.	16.
180, c	1.2	30.	23.
Granodiorites			
134, a	16.	55.	3.5
134, b	6.	20.	3.5
134, c	17.	55.	3.5
136, a	40.	large	—
136, b	40.	large	—
136, c	30.	large	—
136, d	25.	large	—
136, e	30.	large	—
136, f	35.	large	—

6. Discussion 6.-1. Magnetic Properties

The figures for remanent magnetisation given in Table 1 indicate a sharp division of the rocks into two groups; a similar, but less sharp, division may be made on the figures for susceptibility. The basic enclaves show appreciable susceptibility and remanent magnetisation; the granite and granodiorites are markedbly low susceptibility and almost no remanent magnetisation. This general grouping of the rocks investigated corresponds to the known geological facts: basic rocks are normally more magnetic than those at the acid end of the series.

Considering the basic enclaves as a group, it is seen that the three gabbroes (Nos. 765, 768 and 769) are very similar. Susceptibilities range from 375 to 105, remanent magnetisation from 810 to 120, and T values run from 6.2 to 1.8. The magnetic properties of the fourth enclave, No. 770, are very different, and the rock is a porphyretic dolerite. Susceptibility is 90, the remanent magnetisation is but 40, while T is 0.8. Other workers in this field have tentatively established the criterion that rocks with T values above 3, and possibly above 2, have crystallised and cooled through their Curie point, (Nagata, 1943). This criterion would establish the high-temperature origin of the gabbroes and at the same time suggest that the porphyretic dolerite was of low-temperature origin.

The granophyric granite shows appreciable susceptibility, and a very little magnetite was seen in the slices. Hence the extremely low remanent magnetisation indicates that the rock has not cooled from above its Curie point, or that new low-temperature magnetic minerals have been added after cooling, or that the rock has an abnormally low coercivity. The last explaination is rejected, for magnetic rocks in general have a high coercivity. The thermo-magnetic properties will permit the elimination of one of the two remaining explanations.

The granodiorites have low to nil susceptibility and remanent magnetisation. Virtually no magnetite was seen in the slices. The lack of susceptibility also indicates that no magnetic minerals are now present; hence little can be learnt of the thermal or geological history of the rock from an investigation confined to its magnetic properties.

Information regarding the absolute direction and sign of the dip of the basic enclaves is based on two oriented specimens obtained from in situ outcrops; from these oriented cubes were cut. The error lies within 5°. Table 1 shows that the dip is around 30°, and that there was a reversal of magnetism. The declination for one specimen was 155°, and for the other 115°. These results do not necessarily indicate a reversal of the earth's magnetic field towards the close of the Caledonian orogeny. The basic enclaves were presumably free to move and rotate within the fluid granodiorite, whether the latter is considered as a magmatic or metasomatic product. Clearly this line of investigation would enable the amount of relative movement undergone by different enclaves to be determined, but only significantly if a great number of in situ enclaves could thus be investigated.

6. Discussion 6.-2. Thermo-magnetic Properties

Basic Enclaves. The 765 samples have increased their susceptibility by 60% and their remanent magnetisation by a factor of 2.7, giving a Z ratio of 1.7. This Z value implies that the rock has lost 40% of its remanent magnetism if the earth's magnetic field was then of the same strength as it is today, or that the minimum field in which the rock cooled was 0.31 gauss. The 769 b sample increased susceptibility by 80% and doubled its remanent magnetisation, giving a Z ratio of 1.2. This Z value implies that the rock has lost 17% of its remanent

magnetisation if the earth's magnetic field was then of the same strength as it is today, or that the minimum field in which the rock cooled was 0.46 gauss. The differences in the estimates of the minimum terrestrial field some 400 million years ago may be due to different coercivities in the two rocks, or to the fact that only minimum values can be estimated.

Only incomplete results are available for sample 768. The high Z ratio would suggest that the rock has not passed through its Curie point, but this is not supported by other evidence.

The 770 specimens have increased susceptibility by 290%, and their remanent magnetisation by a factor of 21, giving a Z ratio of 5.5. The increase in susceptibility is sufficiently large to indicate that some mineral which can thermally change to magnetite has been deposited in the rock after cooling, or that the rock has never before been heated above its Curie point. The high Z ratio also implies that this rock has never before been above its Curie point, for there are no reasons to believe that it has demagnetised more rapidly than the other rocks of the group.

Granite. The 180 samples have increased their susceptibility by the low factor of 30%, but their remanent magnetisation by the extremely large factor of 32, giving a Z ratio of 21. Even allowing for the fact that the initial remanent magnetisation may have been in error by 50%, since it was so low, this change is far greater than that found for other rocks in this present investigation, or in the literature on this subject. Likewise the Z ratio is the highest encountered, but the Q ratio is very close to the average for all the rocks from the Arrigle Complex.

Granodiorites. The 134 samples have increased their susceptibility by a mean factor of 13 and their remanent magnetisation by 36; the resultant Q and Z ratios are quite normal at 3.2 and 3.5 respectively. The 136 samples have behaved in a similar manner, though the increased susceptibility shows a factor of 33 and the remanent magnetisation factor is of the order of 50; however the Q ratio is quite normal at 3.8, and the indeterminate S ratio may also be normal. The heat treatment has therefore brought about the formation of new magnetic minerals in the rock, as witnessed by the high X values. As the rock cooled, these new magnetic minerals passed through their Curie point, and the great increase in the thermo-remanent magnetisation is shown by the high S values. The new magnetic mineral is taken as magnetite.

6. Discussion 6.-3. Thermal and Geological History of the Rocks

The magnetic changes produced by heating a rock above its Curie point and allowing it to cool in a magnetic field whose strength is close to that of the earth's may be considered under two heads:—

(i) The heating may alter the magnetic properties of the magnetic mineral already present in the rock.

(ii) The heating may cause new magnetic minerals to form from the pre-

existing minerals presesent in the rock.

The effect of (i) should be to alter the remanent magnetisation yet leave the susceptibility unchanged or very little changed. The effect of (ii) should cause the susceptibility to increase, and since new magnetic minerals will have been formed, the remanent magnetisation will also increase. Of course the two effects may be produced in the same rock undertreatment, while other rocks will contain no magnetic minerals before or after the heat-treatment. Such peculiar effects as the destruction of magnetic minerals by the heat-treatment, or the imparting of 'latent magnetic properties' to pre-existing minerals are not considered. And it is assumed that the rocks will have the normal high coercivity.

Table 4. Utalisation of the natural magnetic and the thermo-magnetic ratios of rocks to assist in the diagnosis of their thermal history.

Remanent Magnetisation	Susceptibility	
	Unchanged by Heating	Increased by Heating
Unchanged by Heating	Case A. Gives a valid indication that the rock has previously cooled through its Curie point.	Case B. Impossible.
Increased by Heating	Case C. Gives a valid indication that the rock has not previously cooled through its Curie point.	Case D. This is not disagnostic. It suggests that the rock has not previously cooled through its Curie point.

It may be accepted that magnetite is the magnetic mineral with which this investigation is dealing. It has been indicated (Herroun and Hallimond, 1943, p. 220) that the only satisfactory explanation for the remanent magnetisation found in many natural rocks is that the magnetite took on its permanent remanent magnetisation in cooling through its Curie point. The Curie point for pure magnetite has been determined as lying between 580° and 570°C; impurities lower this temperature, (Chevallier et Piere, 1932). The Curie point for the rocks from the Arrigle Complex has been fixed roughly as around 550° to 580°C (see Section 3 above).

Some temperatures at which silicate minerals crystallise are of interest for comparison. The albite-oligoclase plagioclase felspars commence to crystallise around 1400°C. The eutectic for quartz-orthoclase is 800°C and the hypertectic is 680°C. Quartz-orthoclase-hornblende has a ternary eutectic point at 680°C. Primary magnetite in such rocks is usually considered to be one of the first minerals to crystallise; it should do so at temperatures high above its Curie point, and under such circumstances should take-up a strong remanent magnetisation. When it does not do so, the theory that it has cooled from a high-temperature 'magma' falls under suspicion.

The application of these arguements to the basic enclaves show that the three gabbroes (Nos. 765, 768 and 769) are normal igneous rock which cooled from above the Curie point of their magnetic constituents. They fall into Case A of Table 4. This is in harmony with the petrography and presumed geological

history of these rocks.

The porphyretic dolerite (No. 770) occurs as a basic enclave in the granodiorite, but appears to have a very different thermal history from the gabbroes; it falls into Case D of Table 4. Magnetite is developed on heating to above the Curie point, and all the indications are that the rock as at present constituted has not previously passed through its Curie point. There are two possible geological explanations of the phenomenon in this case. After the dolerite had cooled through its Curie point, low-temperature metamorphic changes may have destroyed all the magnetic minerals; these reformed when the rock was again heated in this investigation; the metamorphic changes may have occurred when the dolerite was engulphed by the granodiorite. It is not easy to see why the same changes did not affect the gabbroes. On the other hand, the dolerite might be a metamorphic rock, derived say from volcanic ash, passing through a hornfels stage into a pseudo-dolerite. The porphyries rather favour this theory, but otherwise the petrography denies it. The investigation has focussed attention on the uncertainty of the origin of what would otherwise be taken for a normal igneous dolerites.

The granophyric granite (No. 180) falls into Case B of Table 4; the susceptibility has barely increased while the remanent magnetisation has increased enormously. This indicates that the rock, as at present constituted, has not previously passed through its Curie point. At first sight, this appears as a startling result, for the geological evidence points to the granophyric granite as a late cross-cutting intrusive granite, while the petrography indicated that it has crystallised from a molten silicate smelt. The iron ore introduced from the Old Red Sandstone (or even from some other source) does not affect the question. It is seen to be haematite before heating and to remain haematite after heating. However, the petrographic examination of the slices indicated that there had been late-stage deuteritic alteration of hornblende into biotite with exsolution of silica as quartz blebs. At the same time, the magnetite seen in small quantities in the biotite may have formed; such magnetite would be low-temperature magnetite and would have low or nil remanent magnetisation. On heating in the laboratory, the existing magnetite would pass through its Curie point and then obtain its remanent (or thermo-remanent) magnetisation. This is considered to be the correct explanation. The main body of the rock crystallised at high temperature; the magnetite is deuteritic, but its idioblastic habit makes it liable to be identified as primary idiomorphic magnetite.

Both the granodiorites (Nos. 134 and 136) fall into Case D of Table 4; thus they resemble the porphyretic dolerite No. 770). New magnetite appears to have been created; it could form from low-temperature minerals belonging to the skialithic portion of the granodiorite, or from low-temperature or decomposed high-temperature minerals belonging to the body of the granodiorite. From this it is clear that the magnetic, or potentially magnetite forming, minerals of the granodiorite as found in the field, are low-temperature minerals, whether or not

they originated from high-temperature minerals. The examination did not reveal what minerals were changed into magnetite on heating; Michel-Levy (1929) considered that sphene decomposed on heating, but it could hardly form appreciable amounts of magnetite.

It is concluded that the relation between the magnetic and the thermomagnetic properties of rocks yields much information as to the thermal and geological history of the rocks, but that this information must be used with caution and must be governed by the history of the rock as revealed by its petrography and other geological features.

7. Acknowledgements and Bibliography

This investigation formed part of seperate theses submitted for the Ph. D degree from the University of London. The author's thanks and acknowledgements are due to Professor H.H. Read and to Dr. J. Mc G. Bruckshaw for advice and encouragement in the carrying out of this work, and to the Anglo-Iranian Oil Company for funds from which the rock-cutting and testing equipment were purchased.

J. Mc G. Bruckshaw, and E.I. Robertson, "The Measurement of Magnetic Properties of Rocks." Jour. Sci. Instr. and Phy. Indust., Vol. 25, pp. 444-446 (1948).

R. Chevallier et J. Piére., "Thermo-Magnetic Properties of Rocks." Ann. Physique, V, 18, pp. 383-477. (1932).

G.E. Goodspeed, "Origin of Granites," Mem. No. 28, Geol. Soc. of Amer. pp. 55-78. (1948).

G. Grenat, "Sur les propriétés magnétiques des roches." Ann. Physique, Tome XIII, pp. 263-348. (1930).

E. Herroun, and A.F. Hallimond, "Laboratory Experiments on the Magnetism of Rocks." Proc. Phys. Soc., Vol. LV, pp. 214-221. (1943).

J.G. Koenigsberger, "Residual Magnetism and the Measerement of Geologic Time." XVI Inter. Geol. Congress, Vol. I, pp. 225-231. (1933).

J.G. Koenigsberger, "Natural Residual Magnetism of Eruptive Rocks." Terr. Mag. Atmos. Elect., Vol. 43, pp. 119-130 and 299-320. (1938).

H. Manley, "An Estimate of the Time taken for a Dyke to Cool through its Curie Point." Geofis. Pura Appli., Milan. Vol. 27, pp. 105-109. (1954).

A. Michel-Lévy, et G. Grenat, "Relations entre l'augmentation de la susceptibilité magnétique de certaines roches chauffées et les modifications de leur mineraux constituents" Compt. Rendu., Tome 188. (1929).

T. Nagata, Bull. Earth. Res. Inst., XIX, pp. 579-596. (1941).

T. Nagata, "The Natural Remanent Magnetism of Volcanic Rocks and its Relation to Geomgnetic Phenomena." Bull. Earthquake Inst. Tokyo Imper. Univ., XXI, pp. 1-196. (1943).

S.R. Nockolds, "The Granite Cotectic Curve." Geol. Mag., Vol LXXXIV, pp. 19-28. (1947).

E. Thellier, Thesis, Paris (1938).

The Diurnal Variation of Cosmic Rays

By Kazuo NAGASHIMA
Earth Science, Kyoto University

Abstract

An attempt is made to examine the energy gain or loss of the primary cosmic ray produced by an electro-magnetic field of solar stream, and then to explain the diurnal variation of cosmic rays at the time of the magnetic storm by this energy variation of cosmic rays.

The amplitudes and the times of the maximum intensity of the diurnal variations are calculated at various altitudes and latitudes by using the above mentioned electric field.

Whether the diurnal variation of cosmic rays averaged over all days can be explained or not from the standpoint of the electric field hypothesis is also discussed.

1. Energy variation of Cosmic Rays in an Electro-magnetic Field Produced by a Solar Stream

It has been supposed that the occurences of the magnetic storm and aurora were due to the solar stream which was composed of neutrally ionized particles, emitted from the active region of the sun, with a mean velocity of about $2 \cdot 10^8$ cm/sec., [1 and 2]. Although the outbreak mechanism of the stream from the sun is still obscure, it is sufficient to quote the experiments of Meinel [3] and Gartlein [4] in order to show its existence. Such a stream will be polarized electrically by the solar magnetic dipole field, and moreover if the electrical conductivity of the stream is very good, the magnetic field in the vicinity of the sun will be frozen in the stream and pushed forward with it [5]. Although the influence of the electro-magnetic field of the stream upon the diurnal variation of cosmic ray intensity was pointed out by several authors [6, 7, 8, 9 and 10], its quantitative discussion is not yet given. As the electrical influence of the stream, polarized electrically by the solar magnetic dipole field, upon the diurnal variation of cosmic rays is of the same character as that of the stream, freezing the magnetic field in itself, so hereafter only the latter case is considered. Strictly speaking, the magnetic field frozen in the stream is not uniform but, in order to simplify the analysis and to obtain the essential feature of the influence of the stream upon the diurnal variation, the uniform magnetic field is assumed to be frozen in. First, we will consider the following case.

A stream of Equatorial type—This denotes the one which is bounded by the two parallel infinite planes, perpendicular to the solar equatorial plane. The magnetic field H frozen in it is parallel to the boundary planes and moves with a velocity v. On the other hand, it is assumed for simplicity that the magnetic field outside the stream is zero. Such a situation is shown in Fig. 1. As seen from the coordinate system (x, y, z) fixed to the earth (hereafter refered to as the rest system), an electric field is observed besides the magnetic one, and then the cosmic rays change their energies by this electric field when they encounter the stream. In order to examine the cosmic ray orbit and its energy variation in such an electro-magnetic field, it is useful to introduce another coordinate system (x', y', z') fixed to the stream (hereafter refered to as the moving system), because there exists only the magnetic field in this system. When a cosmic ray, having its initial velocity $\boldsymbol{u}_0$ and its initial total energy W_0 as seen from the rest system, reaches the boundary surface on the left hand side (cf. Fig. 1), we make the rest system transform into the moving one by the Lorentz transformation as follows,

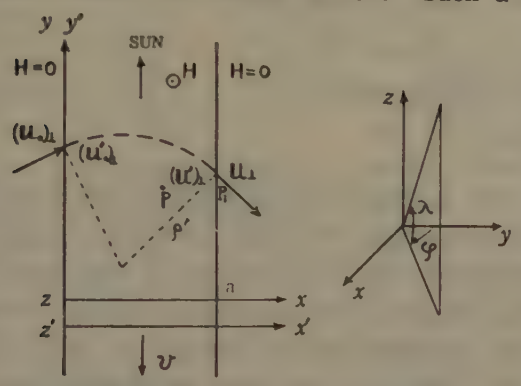

Fig. 1. A stream of Equatorial type.

$$(\boldsymbol{u}_0')_x=\frac{(\boldsymbol{u}_0)_x\sqrt{1-\beta^2}}{1+\beta\frac{(\boldsymbol{u}_0)_y}{c}},\quad (\boldsymbol{u}'_0)_y=\frac{(\boldsymbol{u}_0)_y+v}{1+\beta\frac{(\boldsymbol{u}_0)_y}{c}},\quad (\boldsymbol{u}'_0)_z=\frac{(\boldsymbol{u}_0)_z\sqrt{1-\beta^2}}{1+\beta\frac{(\boldsymbol{u}_0)_y}{c}}, \tag{11}$$

where $$\beta=\frac{v}{c},$$

and a prime indicates the quantity measured in the moving system. In this system, the cosmic ray is subjected to only the magnetic deflection and reaches another boundary surface with a velocity $\boldsymbol{u}'$. The relation between $\boldsymbol{u}'$ and $\boldsymbol{u}'_0$ is given by the following equation,

$$\left.\begin{aligned}\cos\varphi'&=\cos\varphi'_0-\frac{a}{\rho'},\\ \rho'&=\frac{mc(\boldsymbol{u}_0')_\perp}{eH'}.\end{aligned}\right\} \tag{1.2}$$

As for the notations in Eq. (1.2) confer Fig. 1. Here again we make the Lorentz transformation and obtain the final velocity $\boldsymbol{u}$ and the final total energy W of the cosmic ray in the rest system.

$$\boldsymbol{u}_x=\frac{\boldsymbol{u}'_x\sqrt{1-\beta^2}}{1-\beta\frac{\boldsymbol{u}'_y}{c}},\qquad \boldsymbol{u}_y=\frac{\boldsymbol{u}'_y-v}{1-\beta\frac{\boldsymbol{u}'_y}{c}},\qquad \boldsymbol{u}_z=\frac{\boldsymbol{u}'_z\sqrt{1-\beta^2}}{1-\beta\frac{\boldsymbol{u}'_y}{c}}. \tag{1.3}$$

The relations of the final quantities to the initial ones in the rest system are

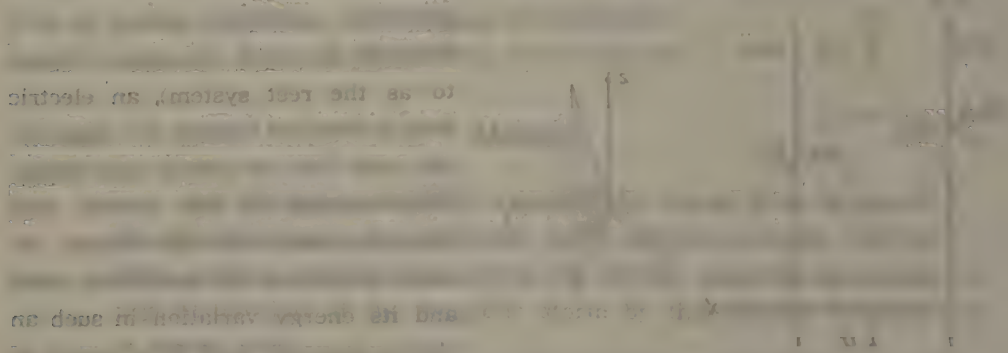

(I.3)

and a is the width of the stream. ΔW_c in Eq. (I.1) is the energy gap of cosmic ray, after traversing the stream from the left to the right, and is the same for ability of passing through. On the other hand, the particle passing through

obtained from Eqs. (1.1), (1.2) and (1.3), and the results are as follows,

$$\Delta W_a = W - W_0 = \beta e a H, \tag{1.4}$$

$$\cos\lambda\cos\varphi = \frac{\left(\frac{u_0}{c}\right)\cos\lambda_0\cos\varphi_0 - \frac{\Delta W_a}{\beta W_0}}{\sqrt{\left(\frac{u_0}{c}\right)^2 + 2\frac{\Delta W_a}{W_0} + \left(\frac{\Delta W_a}{W_0}\right)^2}}, \tag{1.5}$$

$$\sin\lambda = \frac{\sqrt{W_0^2 - (m_0c^2)^2}}{\sqrt{(W_0 + \Delta W_a)^2 - (m_0c^2)^2}}\sin\lambda_0, \tag{1.6}$$

in which $u_0 = u_0$

and a is the width of the stream. ΔW_a in Eq. (1.4) is the energy gain of cosmic ray, after traversing the stream from the left to the right, and is the same for all particles regardless of their energies and velocity directions, if they have the ability of passing through. On the other hand, the particles, passing through from the right to the left, lose their energies by the amount of ΔW_a. The minimum energy $W_a^m(\lambda)$ of the particle, which has the ability of passing through the stream and the final velocity of which is directed towards λ, is approximately given by the following formula,

$$W_a^m(\lambda) \approx \frac{W_a^m}{\cos\lambda} \tag{1.7}$$

where

$$W_a^m = \frac{\Delta W_a}{2\beta}. \tag{1.8}$$

The above relations hold under the next conditions.

$$\beta \ll 1, \qquad \frac{\Delta W_a}{2\beta\cos\lambda} \gg m_0c^2. \tag{1.9}$$

W_a^m denotes the minimum energy in case that $\lambda = 0$. If we adopt W_a^m as an energy unit and represent the total energy by the next equation,

$$W = XW_a^m, \tag{1.10}$$

a dimensionless variable X can be adopted as a new measure of the energy.

As seen from Eqs. (1.5) and (1.6), the particles after traversing the stream are directed towards the given directions (λ, φ), which form a definite region in the velocity space. Next, we examine this region under the conditions of Eq. (1.9) which result also in the following relations by considering Eqs. (1.6) and (1.7),

$$\left.\begin{aligned} &\Delta W_a \ll W \text{ (or } W_0), \\ &\sin\lambda \approx \sin\lambda_0. \end{aligned}\right\} \tag{1.11}$$

Case [I] when the observer is located at a point P_1 ($x \leqq a$).

(1) $X\cos\lambda \geqq 1$

In such a case, at least some of the particles, incident upon the stream from the left with the given energies, can traverse it as seen from Eqs. (1.7), (1.8) and (1.10). By considering Eqs. (1.5), (1.6) and (1.11), their velocity directions at P_1 in the rest system are restricted by the following relation,

where
$$\pi \geq \varphi \geq (\varphi_a)_c, \qquad \text{(Accelerated Region)} \tag{1.12}$$
$$(\varphi_a)_c = \cos^{-1}\left(1 - \frac{2\sec\lambda}{X}\right). \tag{1.13}$$

This holds approximately under the conditions of Eq. (1.9) or (1.11) provided that

$$\cos\lambda \gg \beta. \tag{1.14}$$

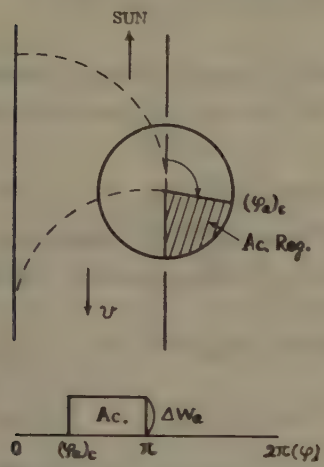

Fig. 2 a. (upper) and b. (lower) Velocity distribution, and energy variation ΔW as a function of φ, in case that $x=a$ and $X\cos\lambda \geq 1$.

Such a situation is illustrated in Fig. 2 a. The particles, their velocity directions lying in the striped region of a circle in Fig. 2 a, are those, which have passed through the stream and then gained their energies by the amount of ΔW_a. On the other hand, those, having their velocities lying in the remaining region of the circle, do not gain or lose their energies. This situation is shown in Fig. 2 b. It is the purpose to examine the diurnal variation of cosmic rays produced by such an energy variation mechanism, so that it is useful to expand ΔW_a in Fourier series regarding ΔW_a as a function of φ, (cf. Fig. 2 b).

$$\Delta W_a(\varphi) = \frac{a_0}{2} + (a_1\cos\varphi + b_1\sin\varphi) + (a_2\cos 2\varphi + b_2\sin 2\varphi) + \cdots$$
$$= \frac{a_0}{2} + A_1\cos(\varphi - \delta_1) + A_2\cos(2\varphi - \delta_2) + \cdots. \tag{1.15}$$

a_0 in the above equation contributes to the intensity variation not dependent on local time. This contribution is somewhat different from the one in the case of the static electric field [9] because a_0 is in general a function of W and λ, but is not refered to here. The diurnal variation of cosmic rays is caused by the quantities a_1 and b_1 or A_1 and δ_1 which are obtained easily from Eqs. (1.12) and (1.13) as follows,

$$\left.\begin{aligned} a_1 &= -\frac{\Delta W_a}{\pi}\sin(\varphi_a)_c = -\frac{2\Delta W_a}{\pi}\sqrt{\frac{\sec\lambda}{X}\left(1-\frac{\sec\lambda}{X}\right)}, \\ b_1 &= \frac{\Delta W_a}{\pi}\left[1+\cos(\varphi_a)_c\right] = \frac{2\Delta W_a}{\pi}\left(1-\frac{\sec\lambda}{X}\right), \end{aligned}\right\} \tag{1.16}$$

$$\left.\begin{aligned} A_1 &= \frac{\Delta W_a}{\pi}\sqrt{2[1+\cos(\varphi_a)_c]} = \frac{2\Delta W_a}{\pi}\sqrt{1-\frac{\sec\lambda}{X}}, \\ \tan\delta_1 &= -\sqrt{X\cos\lambda - 1}\,. \end{aligned}\right\} \tag{1.16}'$$

Hereafter $-a_1$, b_1 and A_1 are refered to as the 12 hour, 18 hour and resultant components of the diurnal variation of ΔW_a respectively, because the vectors $-a_1$, b_1 and A_1 point to the earth from the directions of 12, 18 and T_1 $(=2\pi-\delta_1)$ hour local times respectively. It must be emphasized here that although all the particles traversing the stream gain (or lose) their energies by the same amount of ΔW_a, A_1 depends on X and λ as seen from Eq. (1.16)′.

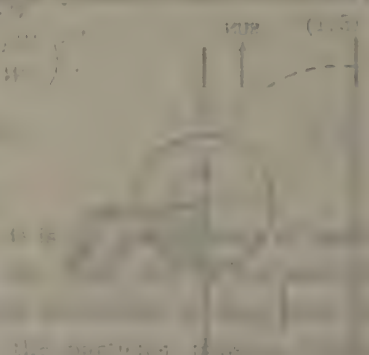

(2) $X\cos\lambda<1$.

In this case none of the particles can traverse the stream so that we are not able to observe the accelerated particles at P_1 and then a_1, b_1 and A_1 are zero.

Case [II] when the observer is located at a point P in the stream $(0<x<a)$.

(1) $X\cos\lambda\geq 1$.

Similarly as in the above case, the particles passing through the left boundary surface gain their energies at P by the amount of $\Delta W_x(=\beta exH)$ and are restricted in the velocity directions as follows,

$$[\varphi_x]_c\geq\varphi\geq(\varphi_x)_c. \qquad \text{(Accelerated Region)} \qquad (1.17)$$

On the other hand, particles, traversing from the right, lose their energies at P by the amount of ΔW_{a-x} $(=\beta e(a-x)H)$ and are restricted in the following velocity directions,

$$2\pi+(\varphi_x)_c\geq\varphi\geq[\varphi_x]_c, \qquad \text{(Decelerated Region)} \qquad (1.18)$$

where

$$(\varphi_x)_c=\cos^{-1}\left(1-\frac{x}{a}\cdot\frac{2\sec\lambda}{X}\right), \qquad (\pi>(\varphi_x)_c\geq 0) \qquad (1.19)$$

$$[\varphi_x]_c=\cos^{-1}\left(-1+\frac{a-x}{a}\cdot\frac{2\sec\lambda}{X}\right). \qquad (2\pi>[\varphi_x]_c\geq\pi) \qquad (1.20)$$

Such a situation is illustrated in Fig. 3. a_1 and b_1 or A_1 and δ_1 in Eq. (1.15) are obtained as follows,

$$\left.\begin{aligned} a_1&=\frac{\Delta W_a}{\pi}[\sin[\varphi_x]_c-\sin(\varphi_x)_c]=-\frac{2\Delta W_a}{\pi}\left[\sqrt{\frac{a-x}{a}\cdot\frac{\sec\lambda}{X}\left(1-\frac{a-x}{a}\cdot\frac{\sec\lambda}{X}\right)}\right.\\ &\qquad\left.+\sqrt{\frac{x}{a}\cdot\frac{\sec\lambda}{X}\left(1-\frac{x}{a}\cdot\frac{\sec\lambda}{X}\right)}\right],\\ b_1&=\frac{\Delta W_a}{\pi}[\cos(\varphi_x)_c-\cos[\varphi_x]_c]=\frac{2\Delta W_a}{\pi}\left(1-\frac{\sec\lambda}{X}\right),\end{aligned}\right\} \qquad (1.21)$$

$$\left.\begin{aligned} A_1&=\frac{\Delta W_a}{\pi}\sqrt{2[1-\sin[\varphi_x]_c\sin(\varphi_x)_c-\cos[\varphi_x]_c\cos(\varphi_x)_c]},\\ \tan\delta_1&=\frac{\cos(\varphi_x)_c-\cos[\varphi_x]_c}{\sin[\varphi_x]_c-\sin(\varphi_x)_c}.\end{aligned}\right\} \qquad (1.21)'$$

In particular, when the observer is located at the centre of the stream $(x=a/2)$, these quantities become as follows,

$$\left.\begin{aligned} a_1&=-\frac{2\Delta W_a}{\pi}\sqrt{\frac{\sec\lambda}{X}\left(2-\frac{\sec\lambda}{X}\right)},\\ b_1&=\frac{2\Delta W_a}{\pi}\left(1-\frac{\sec\lambda}{X}\right),\\ A_1&=\frac{2\Delta W_a}{\pi}, \qquad \delta_1=\frac{\pi}{2}+(\varphi_{\frac{a}{2}})_c.\end{aligned}\right\} \qquad (1.22)$$

It is a remarkable fact that as seen from Eq. (1.21), the 18 hour component (b_1) is independent on x and only the 12 hour component ($-a_1$) varies with the movement of the observer's position.

(2) $X\cos\lambda<1$.

In the same way as above, the velocity distribution is divided into the

following three regions,

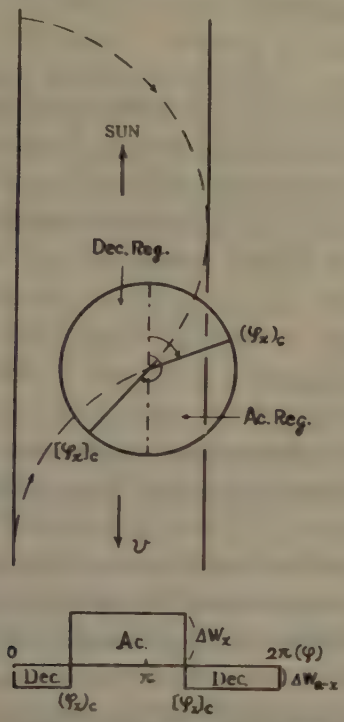

Fig. 3. a (upper) and b (lower) Velocity distribution, and energy variation ΔW as a function of φ, in case that $0<x<a$ and $X\cos\lambda \geqq 1$.

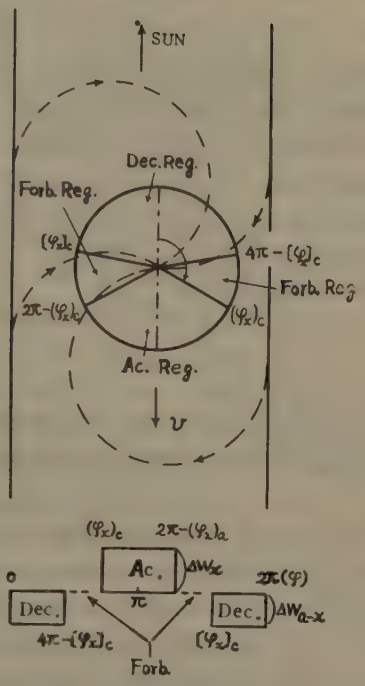

Fig. 4. a (upper) and b (lower) Velocity distribution, and energy variation ΔW as a function of φ, in case that $0<x<a$ and $X\cos\lambda \geqq 1$.

$$\left.\begin{aligned} &2\pi-(\varphi_x)_c \geqq \varphi \geqq (\varphi_x)_c, && \text{(Accelerated Region)}\\ &[\varphi_x]_c > \varphi > 2\pi-(\varphi_x)_c, && \text{(Forbidden Region)}\\ &4\pi-[\varphi_x]_c \geqq \varphi \geqq [\varphi_x]_c, && \text{(Decelerated Region)}\\ \text{and}\quad &2\pi+(\varphi_x)_c > \varphi > 4\pi-[\varphi_x]_c. && \text{(Forbidden Region)} \end{aligned}\right\} \tag{1.23}$$

where $(\varphi_x)_c$ and $[\varphi_x]_c$ are defined by Eqs. (1.19) and (1.20) respectively, (cf. Fig. 4). The Accelerated and Decelerated Regions have the same meanings as in the previous case. The Forbidden Region signifies that particles having their velocity directions lying in this region do not exist. This region is caused by the action of the magnetic field which is called the magnetic cut-off. So that in this energy region where $X\cos\lambda<1$, the contribution of the magnetic field to the diurnal variation of cosmic rays coexists with that of the electric field. It must be emphasized here that both contributions have only the 12 or 24 hour component and not the 18 or 6 hour component, because the distribution of the above three regions as a function of φ is symmetrical about the point $\varphi=\pi$ (or 2π) as seen from Eq. (1.23) or Fig. 4. The contribution of the electric field can be obtained, in the same way as in the previous cases, by assuming that ΔW is zero in the Forbidden Region.

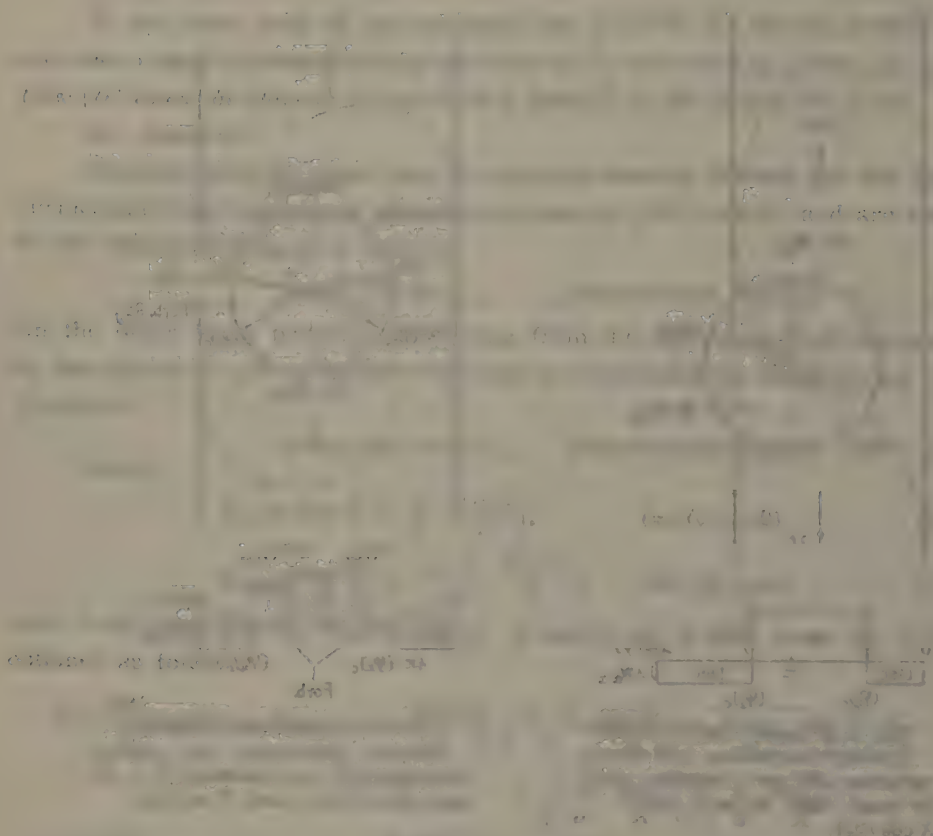

$$\left.\begin{aligned} a_1 &= \frac{2}{\pi}\{-\Delta W_x \sin(\varphi_x)_c + \Delta W_{a-x}\sin[\varphi_x]_c\} \\ b_1 &= 0 \end{aligned}\right\} \tag{1.24}$$

On the other hand, the cotribution of the magnetic field is obtainced as follows: Let $i(X)dX$ be the cosmic ray intensity in the energy interval between X and $X+dX$. If the influence of the electric field upon $i(X)$ is neglected, $i(X)$ is constant in all the regions except for the Forbidden Region in which $i(X)=0$, and is expanded in Fourier series regarding as a function of φ. The 12 hour component $-a_1{}^i$ of $i(X)$ is given by the following equation.

$$\left.\begin{aligned} a_1{}^i &= -\frac{2i(X)}{\pi}\{\sin(\varphi_x)_c + \sin[\varphi_x]_c\}, \\ b_1{}^i &= 0. \end{aligned}\right\} \tag{1.25}$$

The term $a_0{}^i/2$ produced by the action of the magnetic cut-off contributes to the cosmic ray intensity variation not dependent on local time, but is not refered to here.

As above, we have examined the influence of the solar stream of Equatorial type upon the diurnal variation of cosmic ray. It is noteworthy here that, when the observer goes into the stream from the outside, only the 12 hour component $-a_1$ (or $-a_1{}^i$) is changed in its magnitude, on the contrary the 18 hour component b_1 (or $b_1{}^i$) is always constant irrespective of the observer's position. In case that $X\cos\lambda \geq 1$, this remarkable character is illustrated by the harmonic dial in Fig. 5 in which the radii of large and small circles O and O' are $2\Delta W_a/\pi$ and $\Delta W_a/\pi$ respectively. If we choose P on the Ob_1-axis so as to satisfy the following relation $OP=2\Delta W_a(1-\sec\lambda/X)/\pi$ and draw a straight line parallel to Oa_1-axis through P then PP_1 and OP represent $-a_1$ and b_1 respectively, when the observer is located outside the stream, (cf. Eq. (1.16)). The observer entering in the stream, the 12 hour component $-a_1$ begins to increase and continues to do so until the observer reaches the centre of the stream, where $-a_1$ is represented by PP_2, as seen from Eq. (1.18) or (1.19). In case that $X\cos\lambda<1$, such a character is easily seen from Eqs. (1.24) and (1.25). It is also noteworthy that even if the magnetic field vector is directed inversely, the above character is unchanged except for the point that the 18 hour component is taken the place of by the 6 hour component.

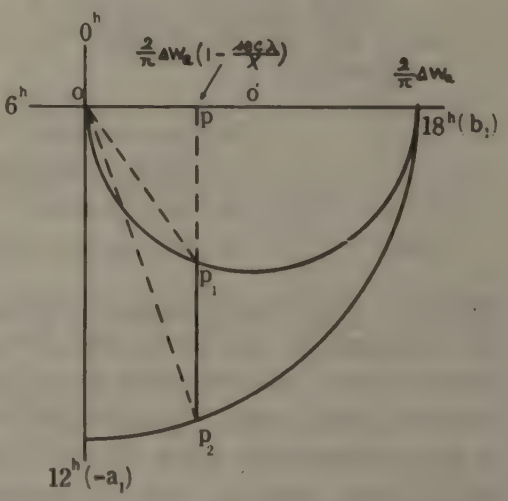

Fig. 5.

In the above discussion, the uniformity of the magnetic field is assumed in

the stream. If there would be some deviation from the uniform magnetic field, a_1 and b_1 given in the previous equations would be changed of course. But even so, this deviation from the uniform magetic field would not change essentially the above mentioned character that only the 12 hour component is changed in its magnitude when the observer goes into the stream from the outside. The deformation of the stream from the Equatorial type also changes a_1 and b_1, but would not alter decisively the above character. At any rate, it will not be meaningless to examine the influence of the deformation upon a_1 and b_1.

Fig. 6 b shows a stream with a finite cross section in xz-plane and with infinite length along oy-axis. The magnetic field is uniform inside the stream and its direction is parallel to oz-axis. At the upper and lower boundaries of the stream in Fig. 6 b, the magnetic lines of force change their directions and are parallel to oy-axis. As this magnetic field, its direction being parallel to oy-axis, does not produce any energy variation of cosmic ray because the direction of this magnetic field is parallel to that of the stream's velocity, so the influence of this field is neglected here. By the same procedure as discussed above, a calculation of the energy variation of cosmic rays is made in a case when the observer is located at the centre of the stream which has the relation $b=a$. Only the result is shown in Fig. 6 which shows some deviation of A_1 and T_1 with the increase of the latitude from those of the stream of Equatorial type given by Eq. (1.22). As discussed above the magnetic field at the upper and lower boundaries does not

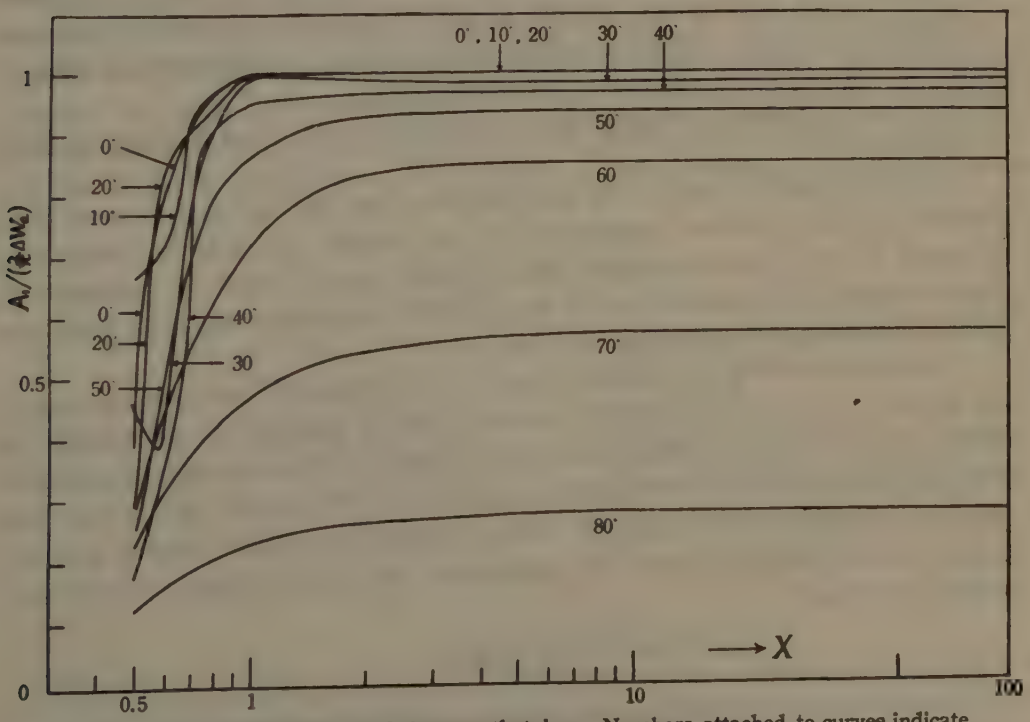

Fig. 6 a. A_1 as a function of X, in case that $b=a$. Numbers attached to curves indicate latitudes.

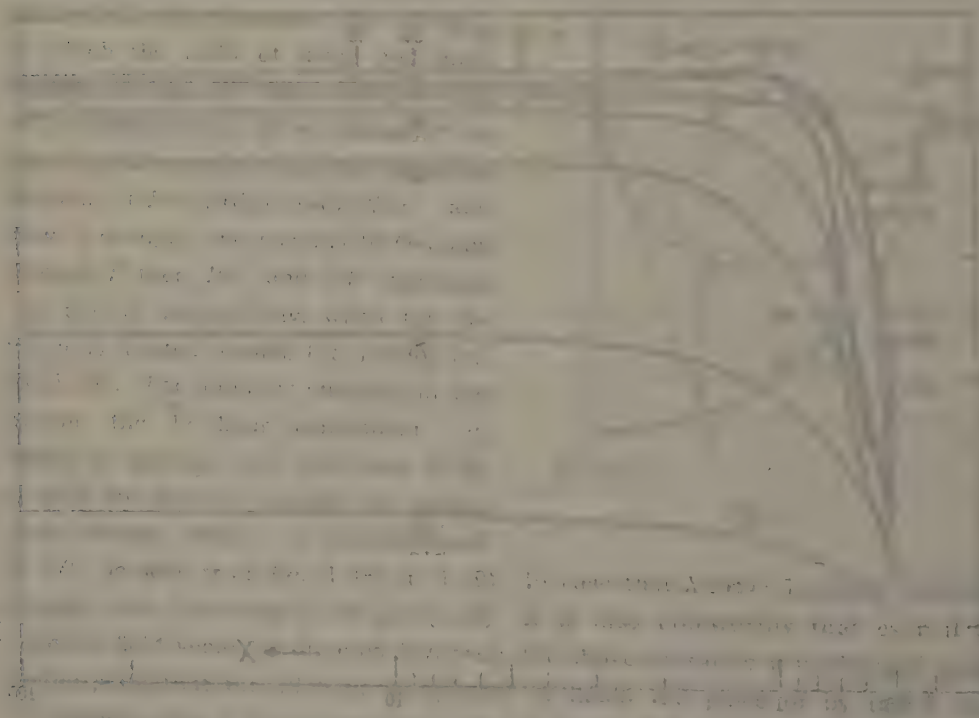

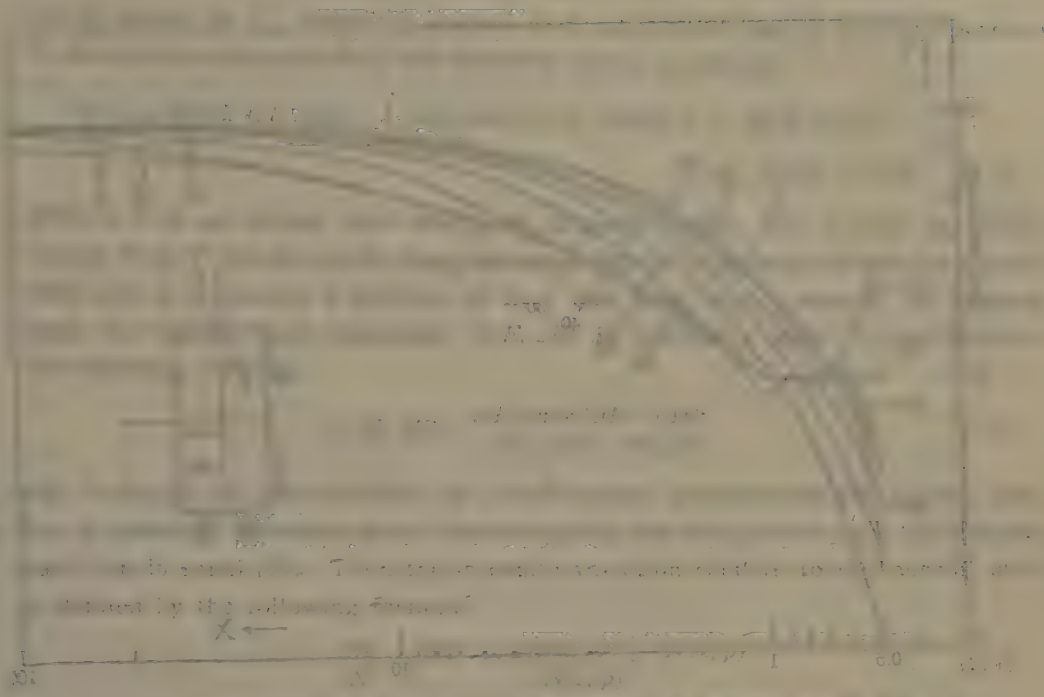

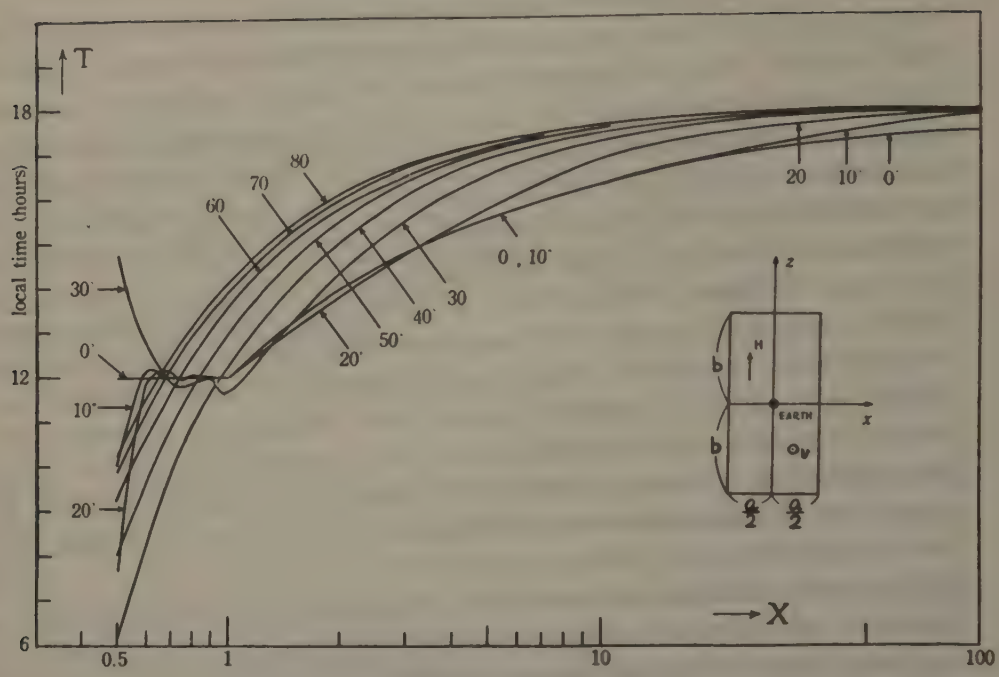

Fig. 6 b. T_1 as a function of X in case that $b=a$, where $T_1=2\pi-\delta_1$. Numbers attached to curves indicate latitudes.

cause any energy variation of cosmic rays, but produces the deflection of cosmic ray orbit, so that the neglection of this magnetic field may produce some error in T_1 at the high latitude. If b becomes very longer than a, it is sufficient to consider only the influence of the stream of Equatorial type.

2. Diurnal Variation of Cosmic Rays produced by the Electric Field of Solar Stream

In the preceding section, we have obtained the 12 hour and 18 hour components (or the resultant component) of the energy variation of cosmic ray produced by the electro-magnetic field of solar stream. Now we examine the diurnal variation of cosmic ray in the earth's atmosphere expected from the existence of such 12 and 18 hour components.

As pointed out in a previous paper [11], the intensity variation of cosmic ray caused by an electric field not derived from a potential is represented as follows: In the normal state when any disturbing field except for the earth's magnetic field does not exist, the vertical intensity of cosmic rays $N(\lambda, p)$ observed under the atmospheric depth p g/cm^2 at the geomagnetic latitude λ degree, is given by the following equation, under the assumption that all the primary cosmic rays consist of protons.

$$N(\lambda, x)=\int_{E_\lambda}^{\infty} m(E, p)i(E)dE\,. \qquad (2.1)$$

Where $m(E, p)$ and $i(E)$ are the over-all multiplicity [11 and 12] and the differential intensity spectrum of the primary cosmic rays respectively, and E_λ represents the

cut-off energy at λ°. When an electric field not derived from a potential is added to the earth's magnetic field, the intensity varies as follows,

$$N\{\lambda, p, \Delta E(E, \lambda, t), \delta E_{\lambda}\} = \int_{E_{\lambda}+\delta E_{\lambda}}^{\infty} m(E, p)[1+L\{E-\Delta E(E, \lambda, t), \Delta E(E, \lambda, t)\}] \times i\{E-\Delta E(E, \lambda, t)\}dE \quad (2.2)$$

$\Delta E(E, \lambda, t)$ is an energy gain which the primary cosmic ray, having its kinetic energy E at λ° on the earth, has undergone during its passage through the electric field, and is in general a function of E, λ and local time t because ΔE depends upon the cosmic rays trajectory. $L\{E, \Delta E\}$ is Liouville's effect [11] and given by the following formula.

$$L\{E, \Delta E\} = \frac{2(E+m_0c^2)\Delta E+(\Delta E)^2}{(E+m_0c^2)^2-(m_0c^2)^2} . \quad (2.3)$$

δE_{λ} in Eq. (2.2) is the variation of cut-off energy produced by the electric field, but is neglected hereafter under the assumption that its influence upon the intensity variation is small [13]. Then the intensity variation relative to the normal state is defined by the following formula.

$$\frac{\Delta N}{N} = \frac{N\{\lambda, p, \Delta E(E, \lambda, t)\}-N(\lambda, p)}{N(\lambda, p)} \quad (2.4)$$

In the case of the above discussed electric field of solar stream, the formula of $\Delta E(E, t)$ is determined under the following assumption that only the earth's magnetic field is considered in the region where its influence upon the motion of cosmic ray is superior to that of the solar stream, on the contrary, outside this region only the field of solar stream is taken into consideration. The deflection of cosmic ray orbit in the earth's magnetic field is obtained from the results of the model experiments of Malmfors [14] and Brunberg [15] and shown schematically in Fig. 7, where λ_N represents the latitude of the asymptotic orbit of cosmic ray

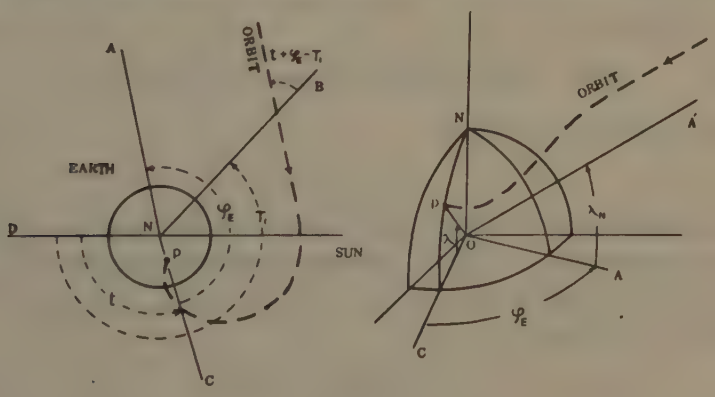

Fig. 7.

and φ_E is the difference between the longitude of the asymptotic orbit and that of the observed point. BN in Fig. 7 represents the direction from which a cosmic ray is incident into the earth's magnetic field with a maximum energy gain, and

obtained in the previous paper [11] is used.

If it is assumed that

it follows from Eq. (1.5) that

which corresponds to $Y = Y_c$. In such a case, $(\Delta^2 V)_0$ and r_{max} of the

is hereafter refered to as the direction of anisotropy. If the equatorial plane of the earth is assumed for simplicity to be paralled to that of the sun, this direction coincides with that of the vector $-a_1$, b_1 or A_1. Then $\Delta E(E, \lambda, t)$ is given by the following formula,

$$\Delta E(E, \lambda, t) = \Delta E_1(E, \lambda_N) \cos(\varphi_R + t - T_1), \tag{2.5}$$

where

$$\left.\begin{aligned} \Delta E_1(E, \lambda_N) &= \Delta W_a \cdot f(E, \lambda_N) = \begin{cases} -a_1(E, \lambda_N) = \Delta W_a \cdot f_{a_1}(E, \lambda_N) \\ b_1(E, \lambda_N) = \Delta W_a \cdot f_{b_1}(E, \lambda_N) \\ A_1(E, \lambda_N) = \Delta W_a \cdot f_{A_1}(E, \lambda_N), \end{cases} \\ T_1(E, \lambda_N) &= 2\pi - \delta_1(E, \lambda_N). \end{aligned}\right\} \tag{2.6}$$

If the resultant component A_1 is adopted as ΔE_1, T_1 in Eq. (2.5) is a function of E and λ_N as seen from Eqs. (1.16)′, (1.21)′ and (1.22) or Fig. 6. On the other hand, if the 12 hour component $-a_1$ (or the 18 hour component b_1) is adopted as ΔE_1, T_1 is independent on E and λ_N, and is equal to 2π (or $3\pi/2$). Introducing Eq. (2.5) into Eq. (2.4), we are able to obtain the diurnal variation of cosmic rays by the following method: the values of $\Delta N/N$ are calculated numerically at the twelve local times, $t = 0^h$, 2^h, 4^h, ...22^h, respectively, and then the diurnal amplitude $(\Delta N/N)_1$ and the time of the maximum intensity t_{max} are obtained respectively by the harmonic analysis of the above twelve values of $\Delta N/N$. As an example, we will calculate $(\Delta N/N)_1$ and t_{max} by adopting A_1 and T_1 in Fig. 6. In the following calculation, Neher spectrum [12 and 16] given by Eq. (2.7) is adopted as $i(E)$ and $m(E, p)$ obtained in the previous paper [11] is used.

$$\left.\begin{aligned} i(E) &= \frac{0.048}{E^{2/3}(1+0.09E^{4/3})^{3/2}}, && (E \geq 0.8 \text{ Bev.}) \\ &= 0. && (E < 0.8 \text{ Bev.}) \end{aligned}\right\} \tag{2.7}$$

If it is assumed that

$$\Delta W_a = 1.\dot{3} \cdot 10^{9} \text{ev.} \quad \text{and} \quad \beta = \frac{2}{3} \cdot 10^{-2}, \tag{2.8}$$

it follows from Eq. (1.5) that

$$W_a^m = 10^{10} \text{ ev.}, \tag{2.9}$$

which corresponds to $X = 1$. In such a case, $(\Delta N/N)_1$, and t_{max} of the ionizing and neutron components at various altitudes and latitudes are shown in Table I. If we determine an energy $\bar{E}$ by using the value of t_{max} in Table I so as to satisfy the following relation,

$$\varphi_R + t_{max} - T_1 = 0, \tag{2.10}$$

we see that the cosmic rays, whose kinetic energies are $\bar{E}$, being incident into the earth's magnetic field from the direction of anisotropy, just hit the point of the geomagnetic latitude λ degree on the earth at the local time t_{max}. We are able to define this energy $\bar{E}$ as the mean energy of the diurnal variation of cosmic rays.

Table I.

Diurnal amplitude $(\Delta N/N)_1$, time of the maximam intensity t_{max}, mean energy $\bar{E}$ and S in case of the resultant component A_1 shown in Fig. 6.

($\Delta W_a = 1.\dot{3}\cdot 10^8$ ev. and $\beta = \frac{2}{3}\cdot 10^{-2}$)

λ		ionizing component		neutron compnent
	p g/cm^2	1030	0	680
0°	$\left(\frac{\Delta N}{N}\right)_1$ %	0.30	0.78	0.59
	t_{max}	$10^h 16^m$	$6^h 56^m$	$8^h 33^m$
	$\bar{E}$ Bev.	30	19	22
	S	0.17	0.29	0.25
50°	$\left(\frac{\Delta N}{N}\right)_1$ %	0.64	2.0	1.7
	t_{max}	$11^h 14^m$	$8^h 20^m$	$8^h 42^m$
	$\bar{E}$ Bev.	21	7.0	8.2
	S	0.26	0.30	0.29
80°	$\left(\frac{\Delta N}{N}\right)_1$ %	0.36	2.8	
	t_{max}	$13^h 36^m$	$12^h 32^m$	
	$\bar{E}$ Bev.	13	9.0	
	S	0.09	0.52	

Table II.

Diurnal amplitude $(\Delta N/N)_1$, time of the maximum intensity t_{max}, mean energy $\bar{E}$ and S.

(A) denotes the case of the resultant component A_1 shown in Fig. 6.
(a) ,, the 12 hour component $-a_1$,,
(b) ,, the 18 hour component b_1 ,,

($\Delta W_a = 0.\dot{6}\cdot 10^8$ ev. and $\beta = \frac{2}{3}\cdot 10^{-2}$)

λ		(A)		(a)		(b)	
		ionizing component	neutron component	inoizing component	neutron component	ionizing component	neutron component
	p g/cm^2	1030	680	1030	680	1030	680
0°	$\left(\frac{\Delta N}{N}\right)_1$ %	0.14	0.32	0.10	0.22	0.16	0.31
	t_{max}	$11^h 16^m$	$9^h 32^m$	$5^h 41^m$	$5^h 15^m$	$13^h 37^m$	$12^h 19^m$
	$\bar{E}$ Bev.	25	22				
	S	0.14	0.27				
50°	$\left(\frac{\Delta N}{N}\right)_1$ %	0.35	1.0	0.25	0.99	0.30	0.51
	t_{max}	$12^h 31^m$	$9^h 56^m$	$8^h 49^m$	$7^h 56^m$	$15^h 26^m$	$14^h 54^m$
	$\bar{E}$ Bev.	15	7.7				
	S	0.21	0.32				
80°	$\left(\frac{\Delta N}{N}\right)_1$ %	0.22		0.094		0.20	
	t_{max}	$41^h 47^m$		$10^h 29^m$		$16^h 24^m$	
	$\bar{E}$ Bev.	11					
	S	0.098					

$\bar{E}$, thus defined, is shown in Table I, together with $(\Delta N/N)_1$ and t_{max}.

In case where

$$\Delta W_a = 0.\dot{6}\cdot 10^8 \text{ ev.}, \quad \beta = \frac{2}{3}\cdot 10^{-2} \quad \text{and} \quad W_a^m = 5\cdot 10^9 \text{ ev.}, \tag{2.11}$$

$(\Delta N/N)_1$, t_{max} and $\bar{E}$ are given in Table II. In it, the diurnal variations caused by the 12 hour component $-a_1$ and the 18 hour component b_1 in Fig. 6 are also tabulated respectively.

In order to find the relation between $(\Delta N/N)_1$ and $\bar{E}$, it is useful to simplify Eq. (2.4) as follows,

$$\frac{\Delta N}{N} = \frac{\int_{E_\lambda}^{\infty} q(E)\dfrac{\Delta E_1(E,\lambda_N)\cos(\varphi_E + t - T_1)}{E+m_0c^2}\, m(E,p)i(E)dE}{\int_{K_\lambda}^{\infty} m(E,p)i(E)dE}$$

$$= \overline{q(E)\cdot\frac{\Delta E_1(E,\lambda_N)\cos(\varphi_E + t - T_1)}{E+m_0c^2}}, \tag{2.12}$$

under the assumption that $i(E)=(E+m_0c^2)^{\alpha}$. $q(E)$ in Eq. (2.12) is given by the next equation.

$$q(E) = \frac{2}{1-1/(1+E/m_0c^2)^{\beta}} - \alpha . \tag{2.13}$$

A bar in the above equation denotes the mean value with respect to the energy. If it is supposed that the diurnal variation is produced by the primary cosmic ray, whose energy is equal to the mean energy $\bar{E}$ obtained in the above, its amplitude becomes

$$q(\bar{E})\frac{\Delta E(\bar{E},\lambda_N)}{\bar{E}+m_0c^2} = f(\bar{E},\lambda_N)\cdot q(\bar{E})\cdot\frac{\Delta W_a}{\bar{E}+m_0c^2}$$

as seen from Eq. (2.12). $(\Delta N/N)_1$ in Table I or II does not necessarily coincide with this amplitude but can be connected with this by the following relation,

$$\left(\frac{\Delta N}{N}\right)_1 = s\cdot f(\bar{E},\lambda_N)\cdot q(\bar{E})\frac{\Delta W_a}{E+m_0c^2} = S\cdot q(\bar{E})\frac{\Delta W_a}{E+m_0c^2}, \tag{2.14}$$

where ΔW_a denotes the energy gain of the cosmic rays which traverses the stream, and s is called the smoothing factor [21] which is caused by the deflection of cosmic ray in the earth's magnetic field and f is called the effiiciency factor which is caused by the influence of the stream's form upon $\Delta E(E,\lambda_N)$. If it is assumed that ΔE does not depend upon E and λ_N and is equal to ΔW_a, it follows that the cosmic ray being incident upon the earth loses its energy by the amount of ΔW_a regardless of its velocity direction and then that the field which produces such a character of ΔE must be a static electric field. In such a case, Eq. (2.14) can be written as follows [17],

$$\frac{\Delta N}{N} = q(\bar{E})\frac{\Delta W_a}{E+m_0c^2}. \tag{2.15}$$

From the above consideration, S may be interpreted as the deviation of the cosmic

ray variation, produced by an electric field not derived from potential, from the variation produced by a static electric field. By using the value of $(\Delta N/N)_1$ and $\bar{E}$ in Table I and II, S is obtained and tabulated in the same place. As seen from the comparison between Tables I and II, the values of $\bar{E}$ and S depend upon ΔW_a to a certain degree, even if the same type of the stream is adopted, but as their dependences on ΔW_a is very weak they can be regarded as nearly constant.

3. Discussion and Conclusion

1) *The electric field of solar stream.*

As seen from Tables I and II, it is necessary for the value of ΔW_a to be equal to 10^8 ev. in order to produce the diurnal variation of the vertical intensity of the ionizing component at sea level, its amplitude being about 0.2 or 0.5 percent. If it is assumed that the velocity of the stream is $2\cdot10^8$ cm/sec. and the width of the stream is $5\cdot10^{12}$ cm, the magnetic field H, which causes such an energy variation ($\Delta W_a \approx 10^8$ ev.), is obtained from Eq. (1.1) as follows,

$$H=\frac{\Delta W_a}{\beta ea}\approx 10^{-5}\,\text{gauß}.$$

The solar magnetic dipole field, its strength at the sun's surface being about 1 gauß at the equator, becomes about $1.3\cdot10^{-7}$ gauß in the vicinity of the earth's orbit and is much smaller than the above required value. Then we are not able to expect the diurnal variation from the solar magnetic dipole field. But, as already discussed in paragraph 1, if it is supposed that the magnetic field in the vicinity of the active region of the sun is frozen in the stream and pushed froward with it because of the good electrical conductivity of the stream [5], the difficulty can be avoided.

2) *The diurnal variation of cosmic rays at the time of the cosmic ray storm (D_S).*

It is a well-known phenomenon that the intensity of cosmic rays is decreased at the time of the magnetic storm (*Dst*) and the anomalous diurnal variation is observed at the same time (D_S), [18]. This phenomenon is called the cosmic ray storm [19]. D_S is defined as the difference of the diurnal variation vector of the disturbing day from that of the quiet day. Various authors [6, 7, 19 and 20] examined the D_S phenomenon and pointed out its many characteristics. Yoshida [21] analyzed D_S by using data at many stations and concluded that the direction of anisotropy which causes the observed D_S is on an average towards about 13 hour local time. As pointed out in paragraph 1, when the observer goes into the stream from the outside, only the 12 hour component $-a_1$ is increased in its magnitude and the 18 hour component b_1 remains constant, (cf. Fig. 5). If the cosmic ray storm is assumed to begin at the time when the earth just enters into the stream, then the direction of the newly added anisotrapy vector is towards 12 hour local time and its magnitude is

$$\frac{2\Delta W_a}{\pi}\left\{\sqrt{\frac{\sec\lambda}{X}}\left(2-\frac{\sec\lambda}{X}\right)-\sqrt{\frac{\sec\lambda}{X}}\left(1-\frac{\sec\lambda}{X}\right)\right\} \qquad (3.1)$$

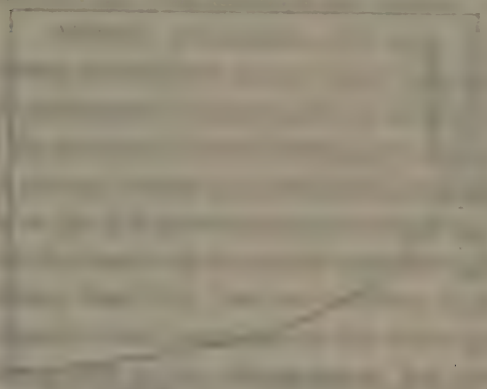

at the centre of the stream as seen from Eqs. (1.16) and (1.22), (cf. Fig. 5). This newly added 12 hour component given by Eq. (3.1) is shown in Fig. 8, as a function of $X\cos\lambda$. Such a theoretically expected direction of the newly added anisotropy vector (12 hour local time) seems to coincide with the observed one (13 hour local time) above mentioned. It must be emphasized here that as pointed out in paragraph 1, even if the magnetic field vector in the stream is directed inversely, the direction of anistropy does not change at all. Yoshida compared the energy dependence of the newly added 12 hour component shown in Fig. 8 with the one analytically obtained from various observations. This comparison seems to show that both dependences coincide with mutually in the order of magnitude [21].

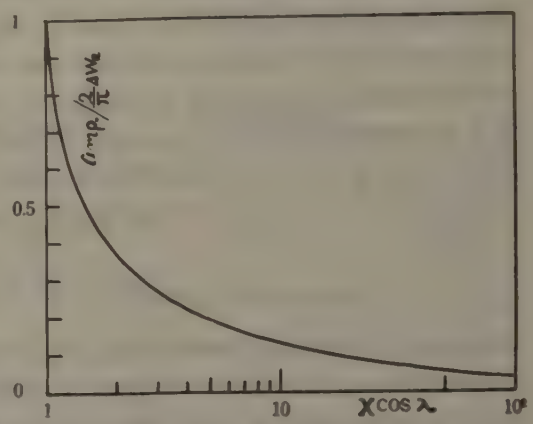

Fig. 8. The amplitude of the newly added 12 hour component as a function of $X\cos\lambda$, at the centre of the stream.

Although the main character of D_S as above seems to be explained by this mechanism, the fine structures of D_S, for example, the phase advancement of the anisotropy of the D_S vector in the course of a cosmic ray storm, etc. ...., [7, 19 and 21] cannot be explained by such a simple model of the stream. But, these problems may be explained by a suitable choice of the stream's structure.

3) *The diurnal variation of cosmic rays averaged over all days.*

Although there is enough ground for controversy as to whether this averaged diurnal variation is nothing but D_S or contains some components caused by other mechanisms quite different from that of D_S [22], what is examined here is whether the observed variation can be approximately explained or not by the following assumption: this averaged diurnal variation is caused by an electric field not derived from a potential, (hereafter refered to as the electric field hypothesis). The diurnal variations calculated in paragraph 2 are those caused by the electric field of the stream, hence it may be difficult to compare them directly with the observed averaged diurnal variations. But, as it seems that even other form of the electric field, which is different from that of the stream, does not lead to any result quite different from those obtained in Tables I and II as long as the electric field hypothesis is accepted, so it may be possible to discuss qualitatively this problem according to the results in Tables I and II. Another difficulty of making a direct comparison between the observed and theoretical diurnal variations is as follows: the theoretically calculated diurnal variations are those of vertical intensity, on the other hand the observed variations are caused by the cosmic rays, incident upon the instruments with finite apertures. Taking these difficulties into consideration, we examine the observed averaged diurnal variation from a stand-

point of the electric field hypothesis.

The energy variation ΔW_a of 10^9 ev. can produce the diurnal variation of about 0.2 or 0.5 percent at sea level as seen from the above tables, on the contrary in the case of the static electric field, the same amount of ΔW_a can produce the intensity variation of about 1 percent or more at sea level [11 and 17]. Then it may be concluded that the diurnal variation is less sensitive to ΔW_a than the intensity variation. This less sensitivity is caused by the factors f and s discussed in paragraph 2. The mean energy $\overline{E}$ in the same table agrees nearly with the observed one [23], although the former depends upon the stream's form.

Altitude dependence.--As seen from Table I, the ratio of $(\Delta N/N)_1$ of the ionizing component at the upper atmosphere to that of sea level is equal to 2.6 at the geomagnetic equator and 3.1 at the geomagnetic latitude 50°. If the amplitude of the averaged diurnal variation at sea level is assumed to be equal to about 0.2 or 0.3 percent which is a reasonable value, the expected amplitude at the upper atmosphere ($p=0$) is between 0.5 and 1 percent. This does not contradict the observed fact that the amplitude of diurnal variation is less than about 1 percent at the altitude of balloon flight [24]. On the contrary, as discussed in the previous paper [11], the magnetic field hypothesis of the diurnal variation [25] or others, in which primary cosmic rays in the comparatively low energy region play an important role in the diurnal variation, will produce a larger altitude dependence than that of the electric field hypothesis because low energy rays are apt to be absorbed in the earth's atmosphere. The underground experiment of Mac-Anuff [26] shows that at the time of the large magnetic storm when the intensity decrease became about 5 percent on the ground, the intensity of underground (60 m.w.e.) did not change, on the contrary the underground amplitude of diurnal variation increased as first pointed out by Yoshida [21]. The theoretical altitude dependence of $(\Delta N/N)_1$ is smaller than that of the intensity variation in the case of the static electric field as seen from Table I, and Fig. 7 in the previous paper [11]. So that this character of these altitude dependences can explain the above cited underground experiment, although this is a problem of Ds and must be discussed in 2). The time of the maximum intensity t_{max} also changes with altitude. At a constant latitude, t_{max} at the upper atmosphere is in general two or three hours earlier than that of sea level as shown in Tables I and II, but it happens that the former is later than the latter in special cases.

Component dependence--The observed ratio of $(\Delta N/N)_1$ of the neutron component at Climax ($\lambda \approx 50°$N) to that of the ionizing component at Freiburg ($\lambda = 50°$N) is between 3.2 and 3.8 [15]. As pointed out by Yoshida and Kamiya [27], the intensity variation of the ionizing component at Freiburg is very small compared with the ones at other stations which are located at nearly the same latitude as Freiburg. It seems to be more adequate to adopt the intensity variations at the latter stations, then the values of the observed ratio cited above become small. The theoretical ratio is equal to about 2.6 in the case of Table I or 2.9 in

the case of Table II, and then seems to be in agreement with the observed one, although the theoretical one depends more or less on the form of the electric field.

Latitude dependence—The theoretical ratio of $(\Delta N/N)_1$ of the ionizing (or neutron) component at geomagnetic latitude 50 to that of the ionizing (or neutron) component at geomagnetic equator is about twice the observed ratio of the corresponding component [28 and 29]. Such a discrepancy between the theoretical and observed values may be due to the following facts: firstly the theoretical one is that of the vertical intensity, on the contrary, the observed one is that of the omnidirectional intensity; secondly the theoretical one depends more or less upon the form of $\Delta E(E, \lambda, t)$ given by Eq. (2.5). t_{max} of the ionizing component at low latitude ($\lambda = 0°$) is one or three hours earlier than the one at high latitude ($\lambda = 50°$). This tendency is caused principally by the deflection of cosmic ray in the earth's magnetic field and seems to be in agreement with observation [29 and 30].

As above, the electric field hypothesis seems to be suitable to explain also the averaged diurnal variation except for the latitude dependence, although it is somewhat difficult to discuss quantitatively this variation on account of the above mentioned causes.

In conclusion, the diurnal variation of cosmic rays at the time of the cosmic ray storm may be explained by the energy variation mechanism of cosmic rays in the electro-magnetic field of solar stream. The fine structures of the observed D_S cannot be explained by such a simple model of the stream as discussed in paragraph 1, but may be explained by a suitable choice of the stream's ftructure.

The necessary energy variation ΔW_a is about 10^8 ev. in order to produce the diurnal variation of the ionizing component at sea level, its amplitude being about 0.2 or 0.5 percent. This requires that the magnetic field is about 10^{-5} gauß in the vicinity of the earth's orbit. Such a requirement cannot be satisfied by the solar magnetic dipole field, but may be achieved by assuming that the magnetic field in the vicinity of the active region of the sun is frozen in and pushed forward with the stream.

Some parts of the averaged diurnal variation of cosmic rays also seems to be explained by the electric field hypothesis.

Acknowledgements

The writer wishes to express his hearty thanks to Prof. M. Hasegawa, for his constant interest in and encouragement of the present research, and Profs. Y. Sekido and T. Nagata for their many valuable criticisms and discussions in relation to this work.

References

[1] S. Chapman and J. Bartels, "Geomagnetism," Oxford Univ. Press, (1940)

[2] H. Alfvén, Kungl. Sv. Vet.-Akademiens Handl. (3), **18**, No. 3, (1939)
[3] A.B. Meinel, Phys, Rev. **80**, 1096 (1950) and Ap. J. **111**, 555 (1950)
[4] C.W. Gartlein, Phys. Rev. **81**, 463 (1951)
[5] H. Alfvén, "Cosmical Electro-Dynamics," Oxford Univ. Press, (1940)
[6] D.W.N. Dolbear and H. Elliot, J. Atmos. Terr. Phys., **1**, 205 (1951)
[7] Y. Sekido, S. Yoshida and Y. Kamiya, Rep. of Ionos. Res. in Japan, **5**, 195 (1951)
[8] A. Ehmert, Z. Natureforschg., **6a**, 622 (1951)
[9] H. Alfvèn, Tellus, **6**, 232 (1954)
[10] E.Å. Brunberg and A. Dattner, Tellus, **6**, 254 (1954)
[11] K. Nagashima, J. Geomag. Geoelct., **3**, 100 (1951) and **5**, 141 (1953)
[12] H.V. Neher, "Pregress in Cosmic Ray Physics," North Holland Publishing Co. Amsterdam, pp. 241–314 (1952)
[13] This assumption is hold enough in almost all the cases. (cf. [11])
[14] K.G. Malmfors, Arkiv. f. mat., astr. o. fysik, **32A**, No. 8 (1945)
[15] E.Å. Brunberg, Tellus, **4**, 135 (1953)
[16] H.V. Neher, V.Z. Peterson and E.A. Stern, Phys, Rev., **90**, 655 (1953)
[17] W.H. Fonger, Phys. Rev., **91**, 351 (1953)
[18] Y. Sekido and S. Yoshida, Rep. Ionosphere Res. Japan, **4**, 37 (1950)
[19] Y. Sekido, Proceeding of International Conference on Theoretical Physcis of 1952, Symposium on Cosmic Rays.
Working Association of Primary Cosmic-Ray Research in Japan, Communication of the Meeting of I.A.T.M.E., at Rome, Sept. 1954.
[20] A. Ehmert and A. Sittkus, Z. Naturforschg., **6a**, 618 (1951)
[21] S. Yoshida, To be published in the near future.
[22] S. Yoshida and I. Kondo, J. Geomag. Geoelect., **6**, 15 (1954)
[23] E.Å. Brunberg, Report of Cosmic-Ray Congress Meeting at Begnere-Bigorre (1953)
[24] D.I. Dawton and H. Elliot, J. Atmos. Terr. Phys., **3**, 217 (1953)
[25] M.S. Vallart and O. Godart, Rev. Mod. Psys., **11**, 180 (1939)
[26] E.P. George, "Progress in Cosmic Ray Physics," North Holland Publishing Co. Amsterdam, pp. 395–451, (1952)
[27] S. Yoshida and Y. Kamiya, Jour. Geomag. Geoelect., **5**, 136 (1953)
[28] J. Firor, W.H. Fonger and J.A. Simpson, Phys. Rev. **94**, 1031 (1954)
[29] H. Elliot, "Progress in Cosmic Ray Physics," North Holland Publishing Co. Amsterdam, PP. 455–514 (1952)
[30] T. Thambyahpillan and H. Elliot, Nature, **171**, 918 (1953)

Meeting of the Society of Terrestrial Magnetism and Electricity :

The 16th General Meeting was held at the Nagoya University on November 3–5, 1954.

Number of the Reports read at the Meeting :

Cosmic Rays, 7 ; Atmospheric Electricity and Atmospherics, 8 ; Rock Magnetism and Electricity, 8 ; Atmospherics and Radio Meteorology, 9 ; Geomagnetism, 11 ; Ionosphere, 10.

Tanakadate Prize was awarded for the following excellent workers :

The 16th, Mr. K. Sinno, Mr. T. Obayashi and Mr. H. Kamiyama ;

Study on Ionospheric Storms with Special Reference to Disturbance-Daily-Variation.

The 17th General Meeting was held at the Tokyo University on May 6-8, 1955.

Number of the Reports read at the Meeting ;

Atmospheric Electricity, Radio Meteorology and Atmospherics, 11 ; Cosmic Rays, 13 ; Rock Magnetism and Electricity, 13 ; Geomagnetism and Earth Current, 11 ; Ionosphere, 14.

Tanakadate Prize was awarded for the following excellent worker :

The 17th, Mr. N. Kawai ;

Studies on Stability of Remanent Magnetisation of Sedimentary Rocks.

昭和30年9月25日　印刷
昭和30年9月30日　發行
第7卷　第1-2號

編輯兼
發行者　日本地球電氣磁氣學會
代表者　長谷川万吉

印刷者　京都市南區上鳥羽學校前
田中幾治郎

賣捌所　丸善株式會社京都支店
丸善株式會社 東京・大阪・名古屋・仙台・福岡

JOURNAL OF GEOMAGNETISM AND GEOELECTRICITY

Vol. VII Nos. 1–2

1955

CONTENTS

JOURNAL OF GEOMAGNETISM AND GEOELECTRICITY

Vol. VII Nos. 1-2

1955

CONTENTS